INFORMATION TO USERS

This manuscript has been reproduced from the microfilm master. UMI films the text directly from the original or copy submitted. Thus, some thesis and dissertation copies are in typewriter face, while others may be from any type of computer printer.

The quality of this reproduction is dependent upon the quality of the copy submitted. Broken or indistinct print, colored or poor quality illustrations and photographs, print bleedthrough, substandard margins, and improper alignment can adversely affect reproduction.

In the unlikely event that the author did not send UMI a complete manuscript and there are missing pages, these will be noted. Also, if unauthorized copyright material had to be removed, a note will indicate the deletion.

Oversize materials (e.g., maps, drawings, charts) are reproduced by sectioning the original, beginning at the upper left-hand corner and continuing from left to right in equal sections with small overlaps.

Photographs included in the original manuscript have been reproduced xerographically in this copy. Higher quality 6" x 9" black and white photographic prints are available for any photographs or illustrations appearing in this copy for an additional charge. Contact UMI directly to order.

ProQuest Information and Learning
300 North Zeeb Road, Ann Arbor, MI 48106-1346 USA
800-521-0600

UMI®

Modeled Sensitivities of the North American Monsoon

by

David J. Gochis

A Dissertation Submitted to the Faculty of the

DEPARTMENT OF HYDROLOGY AND WATER RESOURCES

In Partial Fulfillment of the Requirements
For the Degree of

DOCTOR OF PHILOSOPHY
WITH A MAJOR IN HYDROLOGY

In the Graduate College

THE UNIVERSTIY OF ARIZONA

2002

UMI Number: 3050346

ProQuest Information and Learning Company
300 North Zeeb Road
P.O. Box 1346
Ann Arbor, MI 48106-1346

THE UNIVERSITY OF ARIZONA ©
GRADUATE COLLEGE

As members of the Final Examination Committee, we certify that we have read the dissertation prepared by David J. Gochis

entitled Modeled Sensitivities of the North American Monsoon

and recommend that it be accepted as fulfilling the dissertation requirement for the Degree of Doctor of Philosophy

Prof. W. James Shuttleworth	Date 2/20/02
Prof. Soroosh Sorooshian	Date 2/20/02
Prof. Steven Mullen	Date 2/20/02
Prof. Robert A. Maddox	Date 02-20-02
	Date

Final approval and acceptance of this dissertation is contingent upon the candidate's submission of the final copy of the dissertation to the Graduate College.

I hereby certify that I have read this dissertation prepared under my direction and recommend that it be accepted as fulfilling the dissertation requirement.

Dissertation Director W. James Shuttleworth — Date 3/19/02

STATEMENT BY AUTHOR

This dissertation has been submitted in partial fulfillment of requirements for an advanced degree at The University of Arizona and is deposited in the University Library to be made available to borrowers under rules of the Library.

Brief quotations from this dissertation are allowable without special permission, provided that accurate acknowledgment of source is made. Requests for permission for extended quotation from or reproduction of this manuscript in whole or in part may be granted by the copyright holder.

SIGNED: 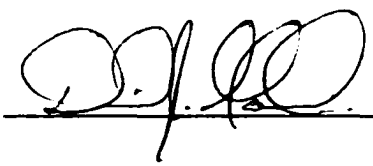

ACKNOWLEDGMENTS

Contemporary research rarely proceeds without the active participation of many talented individuals. The author wishes to acknowledge several people whose efforts and contributions made the production of this dissertation possible. First, I would like to give special thanks to my parents who always believed and encouraged me to pursue my interests, however diverse. The confidence they have instilled in me is a gift I truly value every day. Next, I wish to extend my deepest gratitude to my primary advisor, Prof. Jim Shuttleworth. Though, coincidence may have made it possible for an opportunity to study at the University of Arizona, it has been his patience, experience and talent for practical and critical analysis which has been the catalyst for the development of my most meaningful professional relationship. I hope the years to come share the same spirit of cooperative pursuit that I have experienced as his student. I would like thank Dr. Bob Maddox for providing a touchstone of reality in all work that passed across his desk. His opinions and critical suggestions were absolutely indispensable in the development of this research and I will always value the digressive conversations we've had as these lessons taught me more than any class. Special thanks also are sent to the remaining members of my doctoral committee which include Prof. Steve Mullen, Dr. Zong-Liang Yang and Prof. Soroosh Sorooshian. Each of these members, in either a large or small capacity, contributed greatly to the breadth and perspective of this research and their participation in its completion is deeply appreciated. There are many other people whose work and friendship greatly eased the burden of conducting this dissertation research. In particular, I wish to thank Jim Broerman for keeping everything running and whose door has always been open. Also I would like to extend thanks to Ray Brice and the office staff of HWR who take care of the business scientists are generally clueless about.

Finally, I would like to thank the family of friends I have which I have counted on for support in both good and bad times. These are the people who keep my world going around.

> "Your thoughts may keep you from the cold but only your friends can keep you from yourself."

And lastly,
Alicia, thank you for being with me and sharing so much of your life. Though we did not make it to the end, your support over the years has meant so much to me. I hope you find the happiness you deserve and as you always believed in me, I too will always believe in you.

DEDICATION

This work, though quantitative, is dedicated to the spirit of the universe that stirs winds, builds mountains, rains life and rests on the waves of the ocean. It is the natural world which I have sought to understand and though it is rapidly disappearing here on Earth, I hope, with all of my physical and intellectual energy that we as people can somehow learn to appreciate the continuum of the nature in which we live, that we recognize its delicate balance in a cold universe and that we act with the responsibility which puts no one form of life submissive to another.

TABLE OF CONTENTS

TABLE OF CONTENTS – Continued

TABLE OF CONTENTS – Continued

LIST OF FIGURES

LIST OF TABLES

ABSTRACT

The North American Monsoon System (NAMS) is an important climatological feature of much of southwestern North America because it is responsible for large portions of the annual rainfall in many otherwise arid and semi-arid environments. Proceeding southward from the southern Colorado Plateau into central west Mexico, monsoon rainfall become increasingly important for water resources and sustaining ecosystems. This dissertation explores issues related to numerical simulation of the North American Monsoon climate. Simulation studies using both an atmospheric general circulation model (AGCM) and a regional climate model (RCM), forced by model analyzed boundary conditions, are presented. Assessment is made of model performance when simulating many of the critical features of the NAMS. The representation of the NAMS in the AGCM and the RCM differed substantially, with the RCM yielding superior performance in many aspects.

Additional simulation studies sought to assess specific sensitivities in the model. The RCM was run for a single season with three different convective parameterization schemes for a single season to assess the sensitivity to convective representation. The main conclusions from these simulations were:

- Substantial differences in both the time-integrated thermodynamic and circulation structures of the simulated July 1999 NAM atmosphere evolve in

the simulations when different convective parameterization schemes (CPSs) are used.

- Markedly different regional circulation patterns also evolve, which are revealed in the vertical velocity and low–level divergence fields. Differences in the circulation fields contribute to markedly different fields of July average column–integrated precipitable water and surface dew point temperature.
- All simulations reproduced the maximum of precipitation along the western slope of the Sierra Madre Occidental. However, root mean squared errors and model biases in precipitation and surface climate variables were substantial, and showed strong regional dependencies between each of the simulations.
- The differing evolutions of the July precipitable water fields between model simulations appear to be related to differences in both the column–integrated moisture flux fields and the strength of the surface source or sink.
- The simulations give markedly different patterns in terms of convective and non–convective precipitation components.
- There are large differences in the monthly–total surface runoff between simulations. These differences appear to be more closely related to differences in local, precipitation intensity than to time–average or basin–average intensity. With all schemes, the generation of surface runoff is more dependent on local precipitation rates in individual events than on monthly total basin–averaged precipitation, which points to the importance of accurately representing the statistics of transient features when performing

rainfall–runoff analyses.

In the case of the AGCM, several simulations were conducted to assess the sensitivity of the NAMS to sea–surface temperature fields and also to prescribed soil moisture anomalies. The leading conclusions from these studies were:

- Many features of the North American Monsoon were poorly simulated by the AGCM used in its current configuration when using a yearly repeating cycle of sea–surface temperatures.
- In particular, the model is unable to simulate the regional patterns of monsoon circulation and rainfall. Modeled rainfall over the southwest U.S. and Mexico is much too low, while tropical precipitation is overestimated.
- Meridional streamfunction analysis indicates that the Hadley circulation in the model is much too strong thus creating excessive subsidence in the NAM region.
- The introduction of a wet soil–moisture anomaly over the NAM region generates only small increases in monsoon rainfall, suggesting that regional soil–moisture forcing may play only a minor role in the NAMS.
- Simulation of the NAMS improves when yearly–varying sea–surface temperatures are used. Anomalous sea–surface temperature forcing in the Pacific Ocean also induced model responses that resemble observed responses suggesting that sea–surface temperatures may play a modest role in establishing the monsoon circulation and hence in the generation of monsoon

rainfall.

Results from this study demonstrate that there is much remaining work in order to improve the simulation and subsequent deterministic predictability of the NAM climate system. It is also suggested that the primary issue requiring attention is improving the representation of sub–grid convection in both the AGCM and the RCM models as both models tested here have difficulty in simulating many aspects of the observed character of warm season convective rainfall over southwestern North America.

CHAPTER 1. INTRODUCTION

1.1 Nature of the problem

The term "North American Monsoon" is one that has undergone substantial evolution over recent years as enhanced diagnostic capabilities have emerged. In essence, the term is used to describe the extensive climatic evolution that occurs southwestern North America during the boreal summer. The shift is a transition from a dry subtropical regime to one of regionally increased humidity and a strong diurnal cycle of moist convection. Beginning in May and June, intense surface heating over the elevated regions in southwestern North America induces a surface thermal low–pressure system that becomes directly coupled to a divergent upper level anticyclone (Tang and Reiter, 1984; Tucker, 1998; Higgins et al., 1999). During this time, the mid–latitude jet stream migrates toward its summertime position across southern Canada, and two distinct, low–level jets over the Gulf of California and the Gulf of Mexico intensify the northward transport of moisture over continental North America (Berbery, 2001). The evolution of these large–scale circulation features coincides with the amplification of a diurnal sea breeze between the Gulf of California and mainland North America, the northward progression of diurnal, convective rainfall along the western cordillera of southern North America (Cortez, 1999), and a relative reduction in precipitation in the central plains states of the USA, in northeastern and southern Mexico and Central America (NAME, 2001; Higgins et al., 1997; 1999; Magana et al., 1999). The transition to a drier climate during the summer in the central plains and northeastern Mexico is considered to be an

integral part of the NAM circulation because this feature has been shown to be negatively correlated with monsoon precipitation in Arizona and New Mexico (Higgins et al., 1998).

The importance of monsoon precipitation is evident in many cultures past and present. Both nomadic and sedentary prehistoric communities such as the Hohokom, Patayan, Mogollon and Anasazi greatly depended upon summer rains for their subsistence (Cordell, 1984). Early inhabitants relied upon rainfed cultivars, such as maize (corn), beans, squash, and wild plants, such as mesquite pods, cactus fruits, agave, and numerous seeds for their diets (Ford, 1981). Variability in summer rains often has a great effect on crop yields, both positive and negative. Deficient summer rainfall often results in crop failures. Conversely, intense convective storms have sometimes resulted in substantial damage to crops and irrigation systems, while prolonged drought has been endemic to the monsoon region and has contributed to the abandonment of several early indigenous communities (Van Devender and Spaulding, 1979).

Contemporary communities in the southwestern U.S. and northern Mexico also directly or indirectly rely on rains attributed to the NAMS for their social well being and economic livelihood. (See, for example: Morehouse et al., 2000; or Liverman, 1996) Seasonal hydrological cycling in the NAM region is critical to plant productivity. For a site in southern Arizona, Scott et al. (2000) showed that while winter precipitation controls woody plant (e.g. mesquite) growth, summer rains drive annual grass production

which are critical to the livestock industry. The relative importance of summer precipitation on regional streamflows is evident in Figure B.1 which shows the monthly percentage of mean annual discharge for 7 river systems in the NAM region. (U.S. streamflow data in Figure B.1 comes from the USGS online historic streamflow records; USGS, 2001 and Mexican data comes from the BANDAS archive; BANDAS, 1998) It is clear that summer precipitation generates a greater portion of the annual streamflow than winter precipitation or snowmelt at the lower latitudes of Mexico.

Increasing stress on regional water supplies due to human population growth necessitates an more complete understanding of the processes and implications of the mechanisms that contribute to the regional climate of southwestern North America. Further, sustainable management of hydrological resources throughout the region depends on water users' abilities to understand the causes and effects of any extreme variations in the strength of the NAMS. Dettinger and Diaz (2000) estimate that the NAM region has variability in both precipitation and streamflow that is among the highest in the world. The increased predictive capabilities that would result from the development of comprehensive hydrometeorological prediction systems (HPSs) offers the potential to assess future vulnerability to climate shifts and variations and to take appropriate mitigating actions. One potential element of an HPS is a deterministic, numerical simulation model capable of resolving the critical features responsible for generating and sustaining the regional climate.

A recurrent finding in studies implementing such models is that simulations of convective environments are highly sensitive to the method in which unresolved, or 'sub–grid', convective processes are parameterized in the model. This dissertation directly assesses the sensitivity of a state–of–the–art regional climate model to the representation of sub–grid convection in simulations of the North American Monsoon. Additional studies using an atmospheric general circulation model (AGCM) were also undertaken to assess the response of the simulated climate to both local and remote prescribed forcing conditions (i.e. sea–surface temperatures and soil moisture).

The results of the studies just summarized are described, in detail, in a series of articles that have been submitted for publication in peer–reviewed journals (Gochis et al. 2001a, b and Yang et al. 2001a, b). These works are reproduced in Appendices A–D. Section 1.2.1 provides a brief mechanistic overview of NAM diagnostic studies, while Section 1.2.2 presents the findings of recently–published modeling studies. Section 1.2.3 introduces the concept of regional climate modeling and contrasts it with general circulation modeling and Section 1.2.4 provides an overview on the convective parameterizations tested in this dissertation.

1.2 Background

1.2.1 North American Monsoon diagnostic studies

Over the last few decades, the salient features of the North American Monsoon (NAM) have been extensively documented. Diagnostic studies by Carleton (1985), Carleton et

al. (1990), Douglas (1993), Maddox et al (1995), Schmitz and Mullen (1996), Mullen et al. (1998), Higgins et al. (1997, 1998, 1999), Barlow et al. (1998), and Berbery (2001) have consistently documented important aspects of the summertime climatological shift in the southwestern U.S. and northwestern Mexico from a dry sub-topical regime, to one with diurnal, monsoon-like convection. A variety of data sources have been used in these efforts, ranging from radiosonde archives, infra-red satellite imagery, the Bureau of Land Management lightning detection network, surface raingage networks and, more recently, model-derived data fields, such as those produced by the European Centre for Medium-range Weather Forecasting (ECMWF) and the National Center for Environmental Prediction (NCEP). Compilations of the main conclusions from many of these studies are available in the recent review by Adams and Comrie (1997) and in the North American Monsoon Experiment science plan (NAME, 2001).

Nearly all past climatological studies have emphasized the importance of the formation, persistence, and location of the North American sub-tropical high-pressure ridge at mid and upper levels. The northward and westward migration of the subtropical ridge axis over the southern U.S. supports a change in the upper-level circulation which causes mid-tropospheric winds to shift from westerly origin to south-southeasterly origin. As this transition occurs, significant amounts of moisture are transported into the arid southwestern U.S. and the northern deserts of Mexico (Maddox et al. (1995), Stensrud et al. (1995), Schmitz and Mullen (1996) and Mullen et al. (1998)). Sources of moisture for the North American Monsoon have been proposed: in early work as originating from

the Gulf of Mexico (Bryson and Lowry (1955)) and later on from the Gulf of California (Rasmussen (1967), Hales (1972)). Schmitz and Mullen (1996) support the hypothesis of Carleton (1986) that both regions are likely sources of moisture for the NAM. Douglas (1993), using data from the Southwest Area Monsoon Project (SWAMP), and Schmitz and Mullen (1996) using analyses from the ECMWF model, showed that low-level moisture entering the deserts of Northern Mexico and southern Arizona originates over the Gulf of California and, to a lesser extent, the eastern tropical Pacific, while much of the upper level moisture, above 700 mb, originates in the Gulf of Mexico.

The importance of the convective feedback processes in developing and sustaining the NAM circulation has been described in detail by Barlow et al. (1998), who, using two different re-analyzed datasets, found that residual diabatic heating attributed to deep convection was a prominent feature of the NAM. Recent work by Rodwell and Hoskins (2001) showed that the profile of diabatic heating is critical to the formation of the summertime, sub-tropical anti-cyclone governing the NAMS. A study by Mapes (2000) also showed the importance of diabatic heating due to tropical convection in generating large-scale waves. Based on these studies, it is evident that sustained, deep convection is an important element of the regional thermodynamic balance and, thus, is important to the formation of the regional climate in the NAMS.

Much research has also investigated on the seasonal-to-interannual variability of large-scale features, their teleconnective influences, and their relationship to NAM

precipitation. Early studies using atmospheric analyses focused on the relationship between the summertime 500 mb ridge pattern and NAM rainfall (e.g. Carleton et al., 1990, McCollum, 1993). These studies indicated that monsoon precipitation in Arizona was largest when the 500 mb ridge was centered over the four corners region of the southwest U.S. More recent studies using re–analyzed data sets help provide mechanistic interpretation between large–scale circulation fields and regional moisture advection patterns (e.g. Higgins et al., 1997; 1999; Higgins and Shi, 2000; and Berbery, 2001). In particular, Higgins et al. (1999) present a comprehensive analysis which combines a 26–year precipitation data set over the United States and Mexico with the NCEP/NCAR re–analysis atmospheric fields (Kalnay et al., 1996) to elucidate correlations between North American synoptic scale observations and summer rainfall patterns. Castro et al. (2000) explored teleconnective relationships and found significant correlation structures between sea–surface temperatures in the tropical and North Pacific oceans and NAM rainfall.

Another important NAM feature in regions outside the core monsoon region is the so–called "monsoon boundary", which specifies the extent of the semi–tropical precipitation regime. The northward extent of monsoon moisture, called the "Arizona monsoon boundary" by Adang and Gall (1989) is a distinct feature whose location can be readily viewed from satellite imagery. As shown by Adang and Gall, the spatial extent and perturbations to the monsoon boundary correlate well with convective activity as determined by the BLM lightning detection network. The transition to wet conditions in Arizona generally correspond to the passage of the monsoon boundary, and possibly

correlates with the transition of mid–level winds from westerly to south or southeasterly. It has been suggested that, because the monsoon boundary shows similar characteristics to frontal boundaries in the mid–latitudes, it should be expected that waves would form along this boundary, thus producing enhanced variability in regions along the boundary. More recent studies (e.g. Douglas et al. 1998, Anderson et al. 2000) have shown that the movement of westward propagating waves have a substantial impact on the northward flux of low–level moisture and, hence, the location of the monsoon boundary.

However, it has been shown that analyses at upper levels may not be completely representative of low–level features critical to the formation and sustenance of widespread convection. Douglas et al. (1993) documented the small scale feature known as the Gulf of California low–level jet, which is responsible for transporting large amounts of moisture into the western deserts of Arizona and Northern Mexico during monsoon bursts. The model results of Stensrud et al. (1995, 1997) simulated the development of the Gulf of California low level jet. Using three years of assimilation model analyses and short–term forecasts, Berbery (2001) showed marked diurnal variability in low–level wind fields across western Mexico which were not evident in higher level fields. Douglas et al. (1995) found that, in coarse–resolution analyses, lower tropospheric winds may be as much as 90° out of phase with archived soundings or experimental data. Hence, it is doubtful whether moisture flux analyses performed at relatively coarse resolutions (e.g. 2° X 2°) can adequately capture critical small scale features such as the Gulf of California low level jet and terrain induced circulations.

Research focusing strictly on hydrological aspects of the NAM are few relative to those focusing on climatological aspects. Precipitation climatologies using infra–red satellite imagery (Douglas et al., 1993), surface rain gauge networks (e.g. Higgins et al., 1996; Comrie and Glenn, 1998) and, more recently, merged precipitation products (e.g., Xie and Arkin, 1996) have documented the mean annual and mean monthly features of the warm season precipitation regime over North America. It has been shown that the "core" monsoon region, the region which that possesses the strongest monsoon signal, is along the western slope of the Sierra Madre Occidental (Douglas et al., 1993; Higgins et al., 1999) in western Mexico. A principal components analysis of precipitation regimes by Comrie and Glenn (1998) also determined a similar (but larger) region as the leading mode in the southwestern North American precipitation field, while a sub–regional analysis in this same study indicated that the region encompassing the Sierra Madre Occidental in central Mexico possess the strongest monsoon signal. It is in this same region where the largest percentages, in excess of 70%, of the annual average rainfall occur during the warm season months of July, August and September. It is also where the coefficient of variation of seasonal precipitation is relatively low compared to surrounding regions (Higgins et al., 1997; Mosino and Garcia, 1974). The temporal structure of convective precipitation remains largely undocumented, except for a few satellite–based estimates (e.g., Negri et al., 1994; Vazquez, 1999) and one modeling study that demonstrated a diurnal cycle of convection over the SMO and western Mexico. Stensrud et al. (1995), shows a diurnal cycle of convection as estimated from

satellites and a numerical weather prediction model which possesses a strong maximum in the evening and a minimum near local sunrise.

As part of a global streamflow analysis, Dettinger and Diaz (2000) estimated that the NAM region has among the highest variability in both precipitation and streamflow in the world. They found that the peak in runoff over the NAM region occurred during the months of September and October and possessed a time lag of approximately two months behind the seasonal precipitation maximum. In excess of 50% of the annual streamflow occurred during the peak month in the core monsoon region while peripheral regions showed progressively less monsoon signal. Runoff per unit area was small compared to other regions around the world, on the order of a few tens of millimeters per year, suggesting significant losses of precipitation to either evaporation or deep percolation. Correspondingly, runoff efficiency values, defined as streamflow divided by precipitation, in the core NAM region ranged between 20% and 50%. It was also found that interannual variation in annual streamflow exceeds the variation in annual precipitation over much of the NAM region by factors of eight or more. Reasons for this were not given by Dettinger and Diaz (2000), but serve to highlight the non-linear relationship between precipitation and runoff.

1.2.2 Regional Modeling Studies of the North American Monsoon

Comparatively little work has moved past the diagnostic phase of describing the NAM into the process-modeling phase. In fact Higgins et al. (1999) notes that "advance[ing]

the seasonal prediction of warm season precipitation over North America requires a better understanding of the physical processes that govern the time–dependent behavior of the monsoon system." Numerical models performing global and regional climate simulations have recently been employed (e.g. Stensrud et al., 1995; 1997) to quantify advective fluxes of moisture into typically arid regions in the SW U.S. and North West Mexico. This section briefly summarizes recent progress and the problems recently identified by numerical modeling investigations of the North American Monsoon.

Meso–scale and regional–scale simulations of the North American Monsoon are few but increasing in number. The seminal work by Stensrud et al. (1995), which used 32 consecutive 24–hr integrations and four–dimensional data assimilation (FDDA) at 25 km horizontal grid spacing, successfully characterized several meso–scale features that had been observed in field campaigns but were not detected in synoptic–scale analyses. These features include diurnal changes in the intensity of the Gulf of California low–level jet, the land–sea breeze along the coastline of mainland Mexico, low–level moisture fluxes, and the diurnal cycle of convection. Stensrud et al. found that low–level winds attributed to the low–level jet and diurnal sea–breeze contributed most of the regional moisture flux into the core monsoon region over the Sierra Madre Occidental and northward into Arizona. This finding suggests that the Gulf of California acts as a major source of moisture for monsoon convection.

A follow–up study by Stensrud et al. (1997) further addressed specific features related to

the occurrence of "gulf surge" events, which are transient, low-level, northward surges of moist air that propagate up the Gulf of California into the low deserts of Arizona. They found that their model, when running in assimilation mode (as described by Stensrud et al., 1995), accurately simulated individual surge events and that these events were, in part, caused by complementary positioning of westerly propagating midlatitude waves and easterly propagating tropical waves. Specifically, if a midlatitude trough passes through the western United States a few days prior to the passage of a tropical easterly wave, a strong surge event is likely to occur. Weak surge events appeared to occur only when tropical easterly waves were active in the region.

Using a regional climate model, Anderson et al. (2000a,b) and Anderson and Roads (2001) attempted to elucidate the structure and factors contributing to the low-level moisture flow over the Gulf of California and from the Gulf of Mexico, and the associated monsoon precipitation field. Anderson et al. (2000a) showed that many of the same features reported by Stensrud et al. (1995, 1997) were also accurately simulated by a model that was not run in an assimilation mode. Mechanistic interpretations of the low-level wind structure over the Gulf of California were provided in Anderson et al. (2000b). From their study, they concluded that the southerly component of the low-level jet is the result of a geostrophic balance between the cross-gulf pressure gradient and the Coriolis force. Offshore pressure gradients were established at night due to nocturnal cooling of the elevated slope of the Sierra Madre. The vertical wind shear structure above the nocturnal boundary layer was attributed to the horizontal temperature

gradients over the sloped orography while, within the boundary layer, frictional effects played a major role. Daytime winds exhibited a weaker jet structure and more closely resembled a direct land–sea breeze forced by diurnal heating of the slopes of the Sierra Madre to the east of the Gulf and the low deserts in western Arizona to the north.

Small (2001) also performed a regional climate simulation of the NAM in an attempt to assess the sensitivity of regional precipitation and geopotential height fields to the location of soil moisture anomalies. He found that the simulated climate was sensitive to soil moisture anomalies prescribed to as saturated for the duration of the simulation. When soil moisture anomalies were introduced over the southern Rocky Mountain region, monsoon precipitation in Arizona and New Mexico is suppressed and, conversely, when soil moisture anomalies are present over central Mexico, Arizona–New Mexico, precipitation is enhanced. The simulated sensitivity of the regional climate to soil moisture anomalies suggested that surface forcing due to soil moisture may play a significant role in modulating the NAM regional climate.

1.2.3 Global and Regional climate modeling

The emergence of regional climate modeling (RCM) about a decade ago was fostered by the need for scientific researchers and impacts analysts to obtain more spatially detailed information than was currently available from, then, state–of–the–art global circulation models (GCMs) (Giorgi and Mearns, 1999). It was also recognized that, although GCM's have the ability to properly both mean and transient synoptic scale features, they

were not capable of simulating the fine scale atmospheric phenomenon typically classified as mesoscale circulations. The need to account for the effects of mesoscale circulations and the need for high resolution predictions of climate change and climate variability for impact studies lead to the implementation of high–resolution, limited–area models for use in climate research. The following sub–sections compare and contrast GCM's and RCM's.

1.2.3.1 Definition of the Problem

The overarching goal of climate modeling is to construct a framework that allows for the realistic simulation of the statistics of the day–to–day evolution of the atmosphere. Although, the correlation between simulated and observed transient disturbances may be insignificant, a successful climate simulation should be able to reproduce or predict time– and spatial–mean circulation patterns and their associated variability in terms of variance, trend, and higher order statistics (Simmons and Bengtsson, 1988). Given this goal, climate modeling is, by definition a boundary–value problem, in the sense that the simulated atmosphere is largely a function of the non–linear interactions between the time–evolving model state at the domain boundaries and the internal processes represented by the model. As such, the effects of the initial conditions are comparatively insignificant in comparison with the influence model processes and boundary forcing. Therefore, the primary differences between GCMs and RCMs are in the definition of model boundaries and in the selection internal components that represent unresolved physical processes, the latter often being scale dependent.

1.2.3.2 Overview of Global Circulation Models

An atmospheric general circulation model (AGCM) is a numerical model which explicitly simulates the day–to–day evolution of the large–scale planetary disturbances that are an essential component of the climate system and which also includes parameterizations of important smaller–scale dynamical and physical processes, such as moist convection, turbulent mixing and radiation (Simmons and Bengtsson, 1988). For an AGCM, the modeled domain is the entire globe. Increasingly, AGCM's have become coupled to dynamic ocean circulation models which, in effect, changes the nature of the oceanic lower boundary because the sea surface is allowed to dynamically interact with the atmosphere to estimate surface temperature, salinity, roughness, and chemical and momentum exchange.

There are typically two types of AGCMs which are distinguished by their horizontal discretization; namely, the spectral and the finite difference models. The difference between these two is well described by Simmons and Bengtsson (1988) as follows:

> "In the finite difference method, variables are represented at one of a variety of grids, and solutions to the governing equations are obtained using finite difference integration techniques. In the spectral method, the predicted variables, which include vorticity and divergence, are represented in terms of truncated expansions of spherical harmonics. In

this technique, nonlinear terms (including parameterized contributions) are evaluated on an almost regular latitude–longitude grid and the spectral tendencies calculated by quadrature. "

At large scales (approximately 500–250 km) spectral methods representations yield "favorable" solutions (e.g., Manabe et al., 1979) and are computationally more efficient. At higher resolutions, the differences become less significant. The better computational efficiency of the spectral method has fostered its proliferation in the general circulation modeling community. The physical parameterizations used in an AGCM must be able to accurately account for the large–scale exchanges of heat, moisture, chemicals and momentum, while also being computationally efficient so as not to yield excessively long integration periods.

The atmosphere, and thus the climate system, is often viewed as a convective heat engine in which atmospheric motions serve to redistribute both sensible and latent heat vertically and from tropical regions towards the poles. Hence, the representation of convection in AGCMs is critical in governing the modeled general circulation. The representation of convection in AGCM's is constrained by model resolution. Factors that influence the initiation of deep convection, such as topography or heterogeneous land surface characteristics, are often smoothed out at AGCM model resolutions. Numerous methods for parameterizing deep convection in AGCMs have been developed over the past several years, as described in section 1.2.4. Many of these formulations are simpler than

parameterizations designed for use in numerical weather prediction (NWP) models because they are often required to operate at reduced spatial scales and with greater computational efficiency. They may, for instance, use simplified moist convergence/instability triggers, and/or simple profile relaxation closure methods, or have no hydrometeor representation or explicit resolution of mass fluxes and, hence, no representation of downdrafts, or transfer of momentum from the convective column to the surrounding atmosphere. As elaborated on below, the differences between convective processes in typical AGCM simulations and in typical RCM simulations is a major differences between the two modeling frameworks.

1.2.3.3 Overview of Regional Climate Models

Regional climate models are defined by Giorgi and Mearns (1999) as limited area models (LAMs) run in a climate mode. Thus, the difference between traditional numerical weather prediction using a limited area model and regional climate modeling is the duration of the simulation. In regional climate modeling the duration of the simulation exceeds the 'spin–up' time of the model, the 'spin–up' time being defined as the time taken for the lateral boundary information to pervade the model domain and generate a new dynamical equilibrium between lateral boundary forcing and the RCM physics and dynamics.

Recognizing the need for high resolution climate forecasts, Dickinson et al. (1989) developed what was to become the first RCM. In doing so, they made several

adaptations to a state–of–the–art limited area NWP model "to balance the need for realistic impacts research with available computer resources" (Dickinson et al., 1989). Existing GCM simulations produced modeled fields that were too coarse to describe the details of regional climate in areas where dynamical and/or thermodynamical forcing varied on a scale of less than a few hundred kilometers, in regions of complex topography, for example. By implementing a relatively high–resolution model they sought to resolve mesoscale circulations that are instrumental in defining the regional climate of the southwestern U.S. Such regional features include: terrain flows, rainshadows, and surface hydrological processes, all of which become locally inaccurate by the gross smoothing of topography at typical GCM resolutions.

However, to simulate the time and spatial mean and variability patterns of the climate, the model physics of the LAM were changed to better simulate the processes that become important on climate time–scales. Included were changes in the radiation code, to to give more realistic radiative heating rates, as well as implementing a land surface model that realistically simulated the exchanges of heat and moisture over the land surface. The primary conclusion of Dickinson et al. (1990) was that, even though the RCM was driven by lateral boundary conditions supplied by the GCM at domain boundaries a substantial distance away from the area of interest, the mesoscale features simulated by the RCM were more representative of the observed climate. In effect, they were able to dynamically "downscale" results from a GCM simulation, using a RCM to a resolution appropriate for impacts analysis.

Since this original study, much work has been done to assess and improve the performance of RCMs in a variety of applications and configurations. It has been found that the results obtained from an RCM simulation can be sensitive to a several things. Seth and Giorgi (1998), for example, found that location of model domain boundaries and the size of the overall model domain can have a pronounced effect on RCM simulation results. Their conclusion was that smaller nested domains simulate a climate more similar to that of the large–scale driving fields imposed at the model boundaries, while larger domains simulated climates that, in some cases, were substantially different from the driving fields. RCM results have also been found to be sensitive to both model resolution and the choice of model physical parameterizations (e.g. Giorgi and Marinucci, 1996; Giorgi and Shields, 1999). In particular, simulations by Giorgi and Shields (1999) showed a marked sensitivity to selections of convective parameterization. Similar sensitivities have also been found in GCMs. These early sensitivity studies provided motivation for the research presented in this dissertaion. Specifically, Appendices A and B address the sensitivity of the simulated regional climate to convective parameterizations. A brief overview of convective parameterizations is given in the following section.

1.2.4 Representation of cumulus convection in meso–scale models

Convective parameterizations are used in numerical simulation models to account for convective processes that occur on space and time scales smaller than those which are

resolved by the selected model grid and time step. Raymond (1993) specified four requirements of convective parameterizations, namely the ability to:

1) Calculate the vertical profile of convective mass flux

2) Calculate the vertical profile of detrained water vapor flux

3) Estimate precipitation and ice–particle detrainment

4) Estimate the convective transport of momentum

Several different kinds of convective parameterization schemes (CPSs) have been developed to meet these requirements, and Molinari (1993) has developed a system to classify CPSs into one of three different categories. These are "traditional", "fully–explicit", and "hybrid" methodologies. Traditional schemes implicitly attempt to account for the convective processes listed above at gridpoints which are convectively unstable, while the fully–explicit approach uses only explicit solutions, regardless of grid–point stability. The hybrid technique seeks to parameterize certain processes (such as convective–scale evaporation, condensation and vertical eddy fluxes) while explicitly resolving other, slowly–evolving, processes (such as heat and moisture fluxes due to detrained precipitation–sized particles falling between or downwind of convective clouds).

The selection of a particular CPS mostly depends on the scale of the simulated process as well as on the grid scale of the model. Because convective processes are continuous in

nature, it is often difficult to determine exactly which processes will dominate at a particular scale. This uncertainty has lead to the assumption of "scale separation" when attempting to implicitly simulate convective processes. According to Molinari (1993) scale separation requires the existence of a spectral gap between the scales parameterized and those resolved. This is to ensure that parameterized eddies have a time scale much smaller than grid-scale motions and their influence can be implicitly accounted for in a single time step. Assuring scale separation seeks to eliminate "double counting" of convective processes in both the implicit and explicit computations. Although no strict rules exist, Figure 1, which is from Molinari (1993), offers guidelines for selecting CPSs across a wide range of spatial scales. The question mark in Figure 1 at 4–25 km scales signals the uncertainty in justifying scale separation of convective processes for this range of length scales.

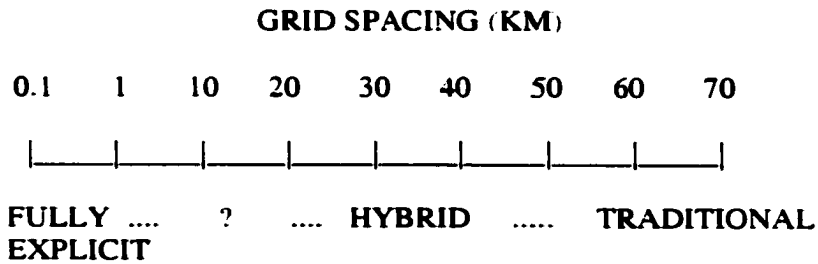

Figure 1 Proposed length scale classifications for mesoscale convective parameterizations. The question mark indicates the lack of an obvious solution. (Reproduced from Molinari, 1993)

In the NAM, many isolated, topographically-generated, convective storms have length

scales on the order of 1–4 km (Osborn et al., 1972), which is much smaller than length scales used in typical regional climate models (25–50 km). However, large organized MCC's, as defined by Maddox (1980), occur regularly in many regions of the NAM which possess length scales on the order several tens of kilometers Therefore some monsoon convection potentially violates scale separation assumptions. These factors were considered in the selection of CPSs tested under the current dissertation research. Of the contemporary schemes implemented and appropriate for use at the selected RCM simulation grid scale (30 km), three schemes were selected; the Betts–Miller–Janic (BMJ) (Janic, 1994), Kain–Fritsch (KF) (1990) or Grell (GR) (1993).

Two of these schemes, KF and GR, are, effectively, hybrid schemes with varying degrees of interaction between implicit and resolved processes. Each of these schemes possesses mass–flux formulations, meaning they exchange mass and, hence, heat and moisture, between the implicit scheme and the resolved grid. The BMJ scheme is a convective adjustment scheme in which the convective profile is relaxed towards a prescribed state. As such, it is not a mass–flux scheme and hence most closely resembles a traditional convective formulation. As can be seen from Fig. 1, both the KF and GR schemes, as hybrid schemes, should be appropriate for simulation at the 30 km grid scale. While use of the BMJ scheme extends beyond the lower limit of intended use for most traditional schemes its use was justified by the fact that this scheme is widely used in several operational numerical weather prediction models which are currently being run at grid spacings as fine as 12 km. Brief details of each of the schemes used in the convective

sensitivity studies in this dissertation are provided in Appendix A.

CHAPTER 2. PRESENT STUDY

The investigations described in subsequent chapters of this dissertation assess the performance of both a state–of–the–art regional climate model, as well as a general circulation model, for simulating the North American Monsoon (NAM). In each case the models are used in a variety of sensitivity experiments designed to isolate dominant forcing mechanisms in the manifestation of the NAM regional climate. The findings from these studies have been documented in a series of peer–reviewed journal articles which have been, or are in the process of being, published. In total, four articles have been submitted for publication. The first two focus on results obtained from a regional climate modeling study in which the model's sensitivity to convective parameterization was investigated. The second two articles describe the results of a series of sensitivity tests conducted using an AGCM. The experimental setup, data analyses, and results are discussed in detail in each of the articles, hence only a brief description of each study and its conclusions are provided in this chapter.

2.1 Sensitivity of Regional Climate Model Simulations to Convective Parameterization

Each of the prior studies reviewed in Section 1.2.4 had difficulty in simulating regional precipitation patterns. Additionally, each simulation yielded circulation patterns that differed, often significantly, from one another. The complex, non–linear nature of mesoscale simulation models makes direct intercomparisons difficult from the point of

view of isolating the causative mechanisms responsible for specific model results. Based on earlier works of Wang and Seaman (1997) and Giorgi and Shields (1999), the following hypothesis is advanced. The choice of a convective parameterization scheme (CPS) can have a significant influence on both model precipitation and circulation fields. This hypothesis was developed considering the work of Barlow et al. (1998) and Rodwell and Hoskins (2001), who both showed that regional diabatic heating due to deep convection plays a significant role in maintaining the regional thermodynamic balance. Additionally, each CPS used in the above studies has different formulations for initiating sub–grid convection, and this can result in substantial differences in the occurrence and intensity of modeled convection.

Therefore, the goal of the study described in the papers in Appendices A and B was comprehensively to document the sensitivity of the simulated regional climate to the representation of sub–grid convection in a regional climate model, in this case the Pennsylvania State University/National Center for Atmospheric Research (PSU/NCAR) Mesoscale Model (MM5) version 3.4 (Grell et al. (1994)). Three CPS's were selected for analysis; namely, the Betts–Miller–Janic (Janic, 1994), Kain–Fritsch (Kain and Fritsch, 1990), and Grell (Grell, 1993) parameterizations. Simulations were made for before and after the onset of the monsoon in the summer of 1999. All of the simulations were identical except for the selection of CPS. A secondary objective of this study was to assess the performance of the regional climate model relative to that of the atmospheric general circulation model (described in Section 2.2). The primary

conclusions emerging from this study are:

- Seasonal integrations of the RCM, when forced by analyzed boundary conditions, yield more realistic results than those of the AGCM. However, results from RCM simulations are highly sensitive to the representation of sub–grid convection.

- Substantial differences in both the time–integrated thermodynamic and circulation structures of the simulated July 1999 NAM atmosphere evolve when different convective parameterization schemes (CPSs) are used. Markedly different regional circulation patterns emerge, which are revealed in the modeled vertical velocity and low–level divergence fields.

- Differing evolutions of the July precipitable water fields between model simulations are related to differences in both the column–integrated moisture flux fields and the strength of the surface source or sink.

- All simulations reproduced a maximum of precipitation along the western slope of the Sierra Madre Occidental. However, root mean squared errors and model biases in precipitation and surface climate variables were substantial, and showed strong regional dependencies between each of the simulations.

- The simulations give markedly different patterns in terms of convective and non–convective precipitation components which contribute to large differences in the monthly–total surface runoff between simulations. With all schemes, the generation of surface runoff in the monsoon region is more dependent on local precipitation rates within individual events than on monthly–total basin–averaged precipitation.

2.2 Assessment of the Performance of the NCAR CCM3 in Simulating the North American Monsoon

2.2.1 Initial Model Assessment

The primary objective for the first study using an AGCM was to document the model's capability to simulate the salient features of the NAM and reproduce its mean characteristics. The National Center for Atmospheric Research (NCAR) Community Climate Model (CCM) version 3 was used to perform 11 yearly integrations of the general circulation using climatological, monthly–average, sea–surface temperatures. The model was run at the T42 resolution, which corresponds to a nominal grid spacing of approximately 280 km. This relatively coarse resolution resulted in marked smoothing of the topography throughout western North America and also failed to resolve the Gulf of California completely. Model results were compared against a the climatology derived from the National Center for Environmental Prediction (NCEP)/NCAR global re–analysis data product over a 30–year period from 1969–1999. Verification analyses focused on regional precipitation patterns, circulation fields and moisture flux balances

over Arizona and New Mexico. The primary conclusions of this study were:

- Simulations of the NAM using the National Center for Atmospheric Research Community Climate Model (NCAR–CCM3) exhibited many deficiencies in terms of precipitation and circulation patterns. Errors in the establishment of the large–scale circulation resulted in marked underestimation of moisture convergence, and hence rainfall, over Arizona and New Mexico.

- Excessive tropical convection in the CCM3 yielded an enhanced Hadley circulation which resulted in excessive subsidence and low estimates of convective rainfall over the NAM region.

Several sensitivity tests were conducted to evaluate the effect of different processes on the simulations. The first test was to introduce a wet soil anomaly over the entire NAM region. The anomaly prescribed soil moisture values over the NAM region to their field capacity values at May 1 of each simulation year. The soil was then allowed to dry down according to the forcing provided by the model climate. This study contrasts with that of Small (2001) in that the soil moisture field here was allowed to freely evolve after the re–initialization to field capacity each year. The conclusion of this sensitivity study was:

- Prescription of anomalously wet soil moisture over the NAM region yielded only slight changes in the simulations, these changes showing better agreement

with analyzed observations than the control simulation.

Additional simulations were also conducted to test the effects of using alternate land–surface models in the CCM3 modeling system. However, these simulations yielded only minimal changes from the initial simulation.

2.2.2 Sensitivity of the Simulated Climate to Sea–Surface Temperature Forcing

One major shortcoming of the study just described was that the sea–surface temperature (SST) field was set to its monthly climatological value. This does not allow the simulated climate to respond to changes in the observed temperature field and this eliminates teleconnective influences on the regional climate. Because it has been shown that NAM precipitation exhibits a modest correlation structure with SST's in both the tropical and North Pacific (e.g. Castro et al. 2000), we conducted several simulations which sought to assess the effect of prescribed SST's on the simulated regional climate. The first was to run the model using the observed, yearly varying, sea–surface temperature field. Additional simulations isolated specific regions in the tropical and North Pacific oceans and prescribed these regions to have SST values observed in years with anomalous conditions. In these experiments, similar assessments were made as in the initial simulations. The primary conclusions of these studies were:

- Simulation of the NAMS improves when actual yearly–varying sea–surface temperatures are used. Modest improvements in the onset and intensity of

monsoon convection were found. The structure of the subtropical anticyclones were also better than those simulated using yearly–repeating sea–surface temperatures.

- Anomalous sea–surface temperature forcing in the Pacific Ocean also induced model responses that resemble observed responses, suggesting that sea–surface temperatures may play a significant role in establishing the monsoon circulation and hence in the generation of monsoon rainfall.

- Extreme fluctuations in Pacific sea–surface temperatures generate non–linear responses in the monsoon precipitation and circulation. The teleconnective and time–delayed response of the NAM circulation to remotely prescribed sea–surface temperature fields indicates that such transient fields play an important role in contributing to the overall NAM climatology.

2.3 Statement of Work

The work contained in the following chapters was a collaborative effort among several researchers. This paragraph specifies which parts of the research were performed by the candidate. The author of this dissertation was solely responsible for pre– and post–processing of data, executing simulations, and preparing the manuscripts contained in Appendices A and B. Co–authors to these papers provided advice on design of simulations, aided with interpretation of results and, assisted with editorial comments.

For the research described in the papers given in Appendices C and D the candidate was responsible for compiling and preparing verification data, creating graphics, providing advice on the design of simulations, interpreting results, and editing the manuscript.

REFERENCES

Adams, D.K. and A.C. Comrie, 1997: The North American Monsoon. *Bull. Amer. Met. Soc.* 78 (10), 2197–2212.

Adang, T.C. and R.L. Gall, 1989: Structure and Dynamics of the Arizona Monsoon Boundary. *Mon. Wea. Rev.*, 117, 1423–1438.

Anderson B.T. and Roads J.O., 2001: Summertime moisture divergence over The southwestern US and northwestern Mexico. *Geophys. Res. Let.*, 28 (10), 1973–1976. MAY 15, 2001.

Anderson B.T., Roads J.O., and Chen S.C., 2000a: Large–scale forcing of summertime monsoon surges over the Gulf of California and the southwestern United States. *J. Geophys. Res.*, 105 (D19), 24455–24467.

Anderson, B.T., J.O. Roads, S–C. Chen, and H–M. Juang, 2000b: Regional simulation of the low–level monsoon winds over the Gulf of California and southwestern United States. *J. Geophys. Res.*, 105 (D14), 17955–17969.

BANDAS, 1998: CDROM–Bancos Nacional de Datos de Aguas Superficiales. Comission Nacional del Agua (can) y Instituto Mexicano de Tecnologia del Agua

(IMTA).

Barlow, M., S. Nigam and E.H. Berbery, 1998: Evolution of the North American Monsoon system. *J. Climate*, 11, 2238–2257.

Berbery, E.H., 2001: Mesoscale Moisture Analysis of the North American Monsoon. *J. Climate.*, 14, 121–137.

Bryson, R. A., and W. P. Lowery, 1955: Synoptic climatology of the Arizona summer precipitation singularity. *Bull. Amer. Meteor. Soc.*, 36, 329–339.

Carleton, A.M., 1985: Synoptic and satellite aspects of the southwestern United States summer monsoon. *J. Climatology*, 5, 389–402.

Carleton, A.M., 1986: Synoptic–Dynamic Character of 'Bursts' and 'Breaks' in the Southwest U.S. SummerPrecipitation Singularity. *J. Climatology*, 6, 605–623.

Carleton, A.M., D.A. Carpenter, and P.J. Webster, 1990: Mechanisms of interannual variability of the southwest United States summer rainfall maximum. *J. Climate*, 3, 999–1015.

Castro, C.L., R.A. Pielke, Sr. and G.E. Liston., 2000: The relationship and response of

the North American Monsoon to tropical and North Pacific sea surface temperatures. *Second Southwest Wea. Symp.*, Sept. 21–22, 2000, Tucson, AZ.

Comrie, A.C. and E.C. Glenn, 1998. Principal components–base regionalization of precipitation regimes across the southwest United States and northern Mexico, with an application to monsoon precipitation variability. *Climate Res.* 10(3), 201–215.

Cordell, L.S., 1984: Prehistory of the southwest. Academic Press. 409 pages.

Dettinger, M.D., and H.F. Diaz, 2000: Global characteristics of stream flow seasonality and variability. *J. Hydrometeorology*, 1, 289–310.

Dickinson, R.E., R.M. Errico, F. Giorgi and G.T. Bates, 1989. A regional climate model for the western United States. *Clim. Change*, 15, 383–422.

Douglas, M.W., R.A. Maddox, K.W. Howard and S. Reyes, 1993: The Mexican Monsoon. *J. Climate*, 6, 1665–1677.

Douglas, M.W., 1995: The summertime low–level jet over the Gulf of California. *Mon. Wea. Rev.* 123, 2334–2347.

Douglas, M.W., A. Valdex–Manzanilla, R.G. Cueto, 1998: Diurnal variation and horizontal extent of the low–level jet over the northern Gulf of California. *Mon. Wea. Rev.* 126, 2017–2025.

Ford, R., 1981: Gardening and Farming before A.D. 1000. *J. Ethnobiology* 1, 6–27.

Giorgi, F. and M.R. Marinucci, 1996: An investigation of the sensitivity of simulated precipitation to model resolution and its implications for climate studies. *Mon. Wea. Rev.* 124(1), 148–166.

Giorgi, F. and L.O. Mearns, 1999: Introduction to special section: Regional climate modeling revisited. *J. Geophys. Res.* 104(D6), 6335–6352.

Giorgi, F. and C. Shields, 1999: Tests of precipitation parameterizations available in latest version of NCAR regional climate model (RegCM) over continental United States. *J. Geophys. Res.* 104(6), 6353–6357.

Gochis, D.J., Z–L. Yang, W.J. Shuttleworth, 2002a: Sensitivity of the modeled North American Monsoon regional climate to convective parameterization. In press. *Mon. Wea. Review.*

Gochis, D.J., W.J. Shuttleworth and Z.–L. Yang 2002b: Hydrometeorological response

of the modeled North American Monsoon to convective parameterization. Submitted to, *J. Hydrometeorology*, November 2001.

Grell, G.A., 1993: Prognostic evaluation of assumptions used by cumulus parameterizations. *Mon. Wea. Rev.*, 121, 764–787.

Grell, G.A., J. Dudhia, and D.R. Stauffer, 1994: A description of the fifth generation Penn State/NCAR mesoscale model (MM5). NCAR Tech. Note NCAR/TN–380+STR, 138 pages.

Hales, J. E., Jr., 1972: Surges of maritime tropical air northward over the Gulf of California. *Mon. Wea. Rev.*, 100, 298–306.

Higgins, R. W., J. E. Janowiak, and Y. Yao, 1996: A Gridded Hourly Precipitation Data Base for the United States (1963–1993). NCEP/Climate Prediction Center Atlas 1, 47 pp.

Higgins, R.W., Y. Yao, and X–L. Wang, 1997: Influence of the North American Monsoon system on the U.S. summer precipitation regime. *J. Climate*, 10, 2600–2622.

Higgins R.W., K.C. Mo and Y. Yao, 1998: Interannual variability of the US summer

precipitation regime with emphasis on the southwestern monsoon. *J. Climate*. 11, 2582–2606.

Higgins, R.W., Y. Chen and A.V. Douglas, 1999: Interannual Variability of the North American Warm Season Precipitation Regime. *J. Climate*, 12, 653–680.

Higgins, R. W. and W. Shi, 2000: Dominant Factors Responsible for Interannual Variability of the Summer Monsoon in the Southwestern United States. *J. Climate*, 13, 759–776.

Janjic, Z.I., 1994: The step–mountain eta coordinate model: further developments of the convection, viscous sublayer, and turbulence closure schemes. *Mon. Wea. Rev.*, 122, 927–945.

Kain, J.S. and M. Fritsch, 1990: A one–dimensional entraining/detraining plume model and its application in convective parameterization. *J. Atmo. Sci.*, 47, 2784–2802.

Kalnay and Coauthors, 1996: The NCEP/NCAR reanalysis project. *Bull. Am. Met. Soc.*, 77, 437–471.

Liverman D.M. 1999: Vulnerability and Adaptation to Drought in Mexico. *Natural Resources Journal*. 39, 99–115.

Maddox, R.A., D.M. McCollum, and K.W. Howard, 1995: Large–Scale Patterns Associated with Severe Summertime Thunderstorms over Central Arizona. *Wea. and Forec.*, 10, 763–778.

Magana, V., J.A. Amador and S. Medina, 1999: The Midsummer Drought over Mexico and Central America. *J. Climate*, 12, 1577–1588.

Manabe, S., D.G. Hahn and J.L. Holloway, 1979: Climate simulations with GFDL spectral models of the atmosphere: Effect of spectral truncation. In GARP Publication Series No. 22, pp. 41–94.

Mapes, B.E., 2000: Convective Inhibition, Subgrid–Scale Triggering Energy, and Stratiform Instability in a Toy Tropical Wave Model. *J. Atmospheric Sciences*, 57, 10, 1515–1535.

McCollum, D.M., 1993: Synoptic–scale patterns associated with severe thunderstorms in Arizona during the summer monsoon. M.S. thesis, School of Meteorology, University of Oklahoma, 166 pp.

Molinari, J., 1993: An overview of cumulus parameterization in mesoscale models. In *The Representation of Cumulus Convection in Numerical Models*. K. Emmanuel

and D.J. Raymond Eds. American Meteorological Society. 246 pages.

Morehouse, B.J., R.H. Carter and T.W. Sprouse, 2000: The implications of sustained drought for transboundary water management in Nogales, Arizona and Nogales, Sonora. *Nat. Res. Journal.*, 40, 783–817.

Mosino, P. and E. Garcia, 1974. The climate of Mexico. World Survey of Climatology, Vol. 11, Climates of North America, R.A. Bryson and K.F. Hare, Eds., Elsevier, 345–404.

Mullen, S.L., J.T. Schmitz and N.O. Renno, 1998: Intraseasonal Variability of the Summer Monsoon over Southeast Arizona. *Mon. Wea. Rev.*, 126, 3016–3035.

NAME, cited–2001: North American Monsoon Experiment Science Plan. [Available online: http://yao.wwb.noaa.gov/monsoon/NAME.html].

Negri, A.N., R.F. Adler, E.J. Nelkin and G.J. Huffman, 1994. Regional rainfall climatology derived from Special Sensor Microwave Imager (SSM/I) Data. *Bull. Am. Met. Soc.*, 75(7), 1165–1182.

Osborn, H.B., L.J. Lane, J.F. Hundley, 1972: Optimum gaging of thunderstorm rainfall in southeastern Arizona. *Water Resources Research*, 8(1), 259–265.

Rasmusson, E.M., 1967: Atmospheric water vapor transport and the water balance of North America, Part 1, Characteristics of the water vapor flux field. *Mon. Wea. Rev.*, 95, 403–426.

Raymond, D.J., 1993: Observational constraints on cumulus parameterizations. In *The Representation of Cumulus Convection in Numerical Models*. K. Emmanuel and D.J. Raymond Eds. American Meteorological Society. 246 pages.

Rodwell, M.J. and Hoskins, B.J., 2001: Subtropical anticyclones and summer monsoons. *J. Climate*, 14, 15, 3192–3211.

Schmitz, J.T. and S.L. Mullen, 1996: Water vapor transport associated with the summertime North American monsoon as depicted by ECMWF analyses. *J. Climate*, 9, 1621–1634.

Seth, A. and F. Giorgi, 1998: The effects of domain choice on summer precipitation simulation and sensitivity in a regional climate model. *J. of Climate*, (11), 2698–2712.

Simmons, A.J. and L. Bengtsson, 1988: Atmospheric general circulation models: Their design and use for climate studies. In *Physically–Based Modeling and Simulation*

of Climate and Climatic Change: Part 1. Ed. M.E. Schlesinger. Kluwer Academic Publishers 624 pages.

Small, E.E., 2001: The influence of soil moisture anomalies on variability of the North American monsoon system. *Geophys. Res. Let.*, 28(1), 139–142.

Stensrud, D.J., R.L. Gall, S.L. Mullen and K.W. Howard, 1995: Model climatology of the Mexican Monsoon. *J. Climate*, 8, 1775–1794.

Tang, M. and E.R. Reiter, 1984: Plateau monsoons of the Northern Hemisphere: A comparison between North America and Tibet. *Mon. Wea. Rev.*, 112, 617–637.

Tucker, D.F., 1998: The Summer Plateau Low Pressure System of Mexico. *J. Climate*, 12, 1002–1015.

USGS, cited–2001: Digital coverage archive [Available online: http://water.usgs.gov/GIS/metadata/usgswrd/huc250k.html].

Van Devender, T. R. and W. G. Spaulding, 1979: Development of vegetation and climate in the Southwestern U.S. *Science*, 204, 701–710.

Vazquez, M.C., 1999: Marcha annual de la actividad convectiva en Mexico. *Atmosfera*,

12. 101–110.

Wang, W. and N.L. Seaman. 1997: A comparison study of convective parameterization schemes in a mesoscale model. *Mon. Wea. Rev.*, 125. 252–278.

Yang, Z–L. D.J. Gochis and W.J. Shuttleworth. 2001a: Evaluation of the simulations of the North American Monsoon in the NCAR CCM3. *Geophys. Res. Lett.*, 28(7). April 1 2001. 1211–1214.

Yang, Z–L. D.J. Gochis and W.J. Shuttleworth. 2001b: The impact of sea surface temperatures on the North American Monsoon. Tentatively accepted. *Geophys. Res. Lett.*

Xie, P. and P. Arkin. 1996: Analysis of global monthly precipitation using gage observations, satellite estimates, and numerical model predictions. *J. Climate*. 9. 840–858.

APPENDIX A.

Sensitivity of the Modeled North American Monsoon Regional Climate to Convective Parameterization

David J. Gochis[1], W. James Shuttleworth[1,2] and Zong-Liang Yang

In press. *Monthly Weather Review*, January 2001

[1] Department of Hydrology and Water Resources, University of Arizona, Tucson, AZ 85721, USA
[2] Department of Atmospheric Sciences, University of Arizona, Tucson, AZ 85721, USA

Subject: Re: Permission to use article in Thesis
Date: Mon, 28 Jan 2002 07:57:56 -0500
From: Melissa Weston <mweston@ametsoc.org>
To: Dave Gochis <gochis@hwr.arizona.edu> (by way of Tara Partlow <tpartlow@ametsoc.org>)

Dear Dave:

Through this e-mail, the American Meteorological Society grants you permission to reprint the following articles as described in your request.

Ref: MWR 2337 "Sensitivity of the Modeled North American
Monsoon Regional Climate to Convective Parameterization"
Gochis, Shuttleworth, Yang

Ref: 083-01-JHM " Hydrometeorological Response of the Modeled
North American Monsoon to Convective Parameterization"
Gochis, Shuttleworth, Yang

Full acknowledgments to AMS as the copyright holder and bibliographical details of the publication should be cited.

Best regards,
Melissa Weston

Sensitivity of the Modeled North American Monsoon Regional Climate to Convective Parameterization

Abstract

This paper documents the sensitivity of the modeled evolution of the North American Monsoon System (NAMS) to convective parameterization in terms of thermodynamic and circulation characteristics, stability profiles, and precipitation. The convective parameterization schemes (CPSs) of Betts–Miller–Janjic, Kain–Fritsch, and Grell were tested using version 3.4 of the PSU/NCAR MM5 mesoscale model running in a pseudo–climate mode. Model results for the initial phase of the 1999 NAM are compared with surface climate station observations and seven radiosonde sites in Mexico and the southwestern United States. The results show substantial differences in modeled precipitation, surface climate, and atmospheric stability occurring between the different model simulations, which are attributable to the representation of convection in the model. Moreover, large inter–simulation differences in the low–level circulation fields are found. While none of the CPSs tested gave perfect simulation of observations everywhere in the model domain, the Kain–Fritsch scheme generally gave significantly superior estimates of surface and upper air verification error statistics.

1. Introduction

The application of regional climate models (RCMs) has increased dramatically since their inception (Dickinson et al..1989; Giorgi. 1990; Giorgi and Mearns. 1999). as have studies conducted to assess the sensitivity of modeled regional climate to changes in surface forcing (e.g.. Small. 2001; Giorgi and Marinucci. 1996; Giorgi and Shields. 1999; Copeland et al.. 1996) and model physics (e.g.. Wang and Seaman. 1997; Giorgi and Marinucci. 1996). Sensitivity to physical parameterization. parameter values. grid– and domain–size (Seth and Giorgi. 1998). and boundary forcing greatly complicates the implementation of regional climate models. Model verification is therefore essential. but may well be complicated by differences between the grid used in the RCM and that of the analyzed fields of observational data used for verification. and by the fact that re–analyzed data sets may contain similar physical parameterizations (and biases) as the model being evaluated. Conversely. re–analyzed data sets may contain disparaging biases associated with totally different physical parameterizations.

The adequate representation of convective processes is particularly important in RCMs. but there is no universally accepted framework for representing convection in numerical simulation models operating with grid scales that prohibit fully explicit representation. In fact. the representation of convection is strongly scale–dependent (Molinari and Dudek. 1990). and several different CPSs have been developed that implicitly account for the associated sub grid exchanges of mass. heat. and moisture. The differences in these formulations have a pronounced influence on numerical modeling results (e.g.. Wang and

Seaman, 1997; Giorgi and Shields, 1999; Zhang and McFarlane, 1995; Giorgi and Marinucci, 1996) and vary with the convective environment being simulated. To date, there has been no comprehensive assessment of CPS performance in simulating deep convection over the southwest U.S. and Mexico.

The Pennsylvania State University (PSU)/National Center for Atmospheric Research (NCAR) MM5 model (and similar modeling systems) is being increasingly recognized as critical in operational hydrometeorological prediction systems. However, there have been no definitive publications offering guidance on the relative performance of CPSs in MM5 over the North American Monsoon (NAM) region, although a preliminary study by Gochis et al. (2000) suggested that substantial differences were likely (for a thorough description of the NAM, see Douglas et al., 1993., Adams and Comrie, 1997, or Higgins et al., 1997). Basic convective research (e.g., Kain and Fritsch, 1990), indicates that differing representations of sub grid convection yields not only different amounts of precipitation but also differing degrees of atmospheric heating due to parameterized latent heat exchanges. With regard to the NAM system (NAMS), Barlow et al. (1998) concluded that residually derived, mid– and upper–tropospheric diabatic heating attributed to convection plays a significant role in developing the NAM circulation. Thus, the primary goal of this study was to provide quantitative assessment of three CPSs available in the MM5 model (Grell et al., 1994) and to document through verification and sensitivity analyses the relative performance of these CPSs when simulating the North American Monsoon System (NAMS). In this paper, we refine the previous study

by Gochis et al. (2000) by (a) extending the internal nested domain used in MM5 to approximately 120°W; (b) allowing sea–surface temperature to vary, these being updated every six hours along with the lateral boundary conditions; and (c) including a third convective parameterization, the Betts–Miller–Janic (BMJ) scheme, in the comparison along with the Kain–Fritsch (KF) and Grell (GR) schemes.

Section 2 briefly describes the model configuration and simulation and verification procedures, while Appendix A provides a brief description of each of the three CPSs. The results are presented in Section 3 and discussed in Section 4. Section 5 gives concluding comments.

2. Model and Analysis Methods

2.1 The MM5 Model

The PSU/NCAR MM5 mesoscale model version 3.4 (Grell et al., 1994) consists of a nonhydrostatic dynamic core and a suite of optional physical parameterizations integrated on a terrain–following, sigma, vertical coordinate system. A two–way interacting nested configuration (90 km and 30 km) was used in this study, with the coarse domain covering approximately 125°W–85°W and 10°N–45°N and the fine domain covering most of Mexico and the southwestern United States (see Figure 1). The model was integrated continuously from 00 UTC 16 May through 00 UTC 2 August 1999, while the lateral boundary forcing for the coarse domain was one–way and was provided by the NCEP/NCAR re–analysis data set (Kalnay et al., 1996). Model sea–surface temperatures

(SSTs) taken from the weekly dataset of Reynolds and Smith (1994) were linearly interpolated to six–hourly values and used as lower boundary conditions. The model output was saved every three hours for analysis. Because only the results for the month of July were compared, the spin–up period for the simulations is on the order of six weeks. As suggested by Giorgi and Mearns (1999), this should be more than adequate for thorough propagation of lateral boundary conditions, but may not be adequate for a full spin–up of certain land–surface conditions such as soil moisture, hence our use of the phrase "pseudo regional climate simulations" to describe our *modus operandi*. Other significant model options used in this study are listed in Table 1.

The three different CPSs selected for study in this sensitivity experiment were the schemes of Betts–Miller (Betts, 1986; Betts and Miller, 1986) as implemented by Janjic (1994), hereafter referred to as BMJ, of Grell (Grell, 1993; Grell et al., 1994), hereafter referred to as GR, and of Kain–Fritsch (Kain and Fritsch, 1990), hereafter referred to as KF. These schemes vary in their representation of physical processes (Appendix A), ranging from the relatively simple profile adjustment scheme of BMJ to the entraining–detraining mass flux scheme of KF. The schemes also vary in their formulation of convective initiation ("trigger function") as well as their criteria for convective termination ("relaxation"). All of the CPSs have been implemented and tested in the MM5 modeling framework and have shown success in simulating convection at the 20–40 km grid resolution (Giorgi and Shields, 1999; Janjic, 1994; Kain and Fritsch, 1990) in climates such as the North American Great Plains. A brief description of each CPS is

given in Appendix A, but readers are referred to the articles given above for more thorough descriptions of the individual schemes.

Assumptions in the GR and KF formulations preclude their application at the coarse domain grid of 90–km. Consequently, the BMJ scheme, which does not possess the same scale–limiting assumptions as the GR and KF schemes, was always used for the intermediate 90–km grid. Thus, the only difference between the simulations was that convective processes were represented by the BMJ, GR, and KF schemes within the internal 30–km domain. In each case, the default parameters for each CPS were used. As discussed later, this may impact the results of the sensitivity study. Although the model was integrated from mid–May through July, only the results for July are presented here because convective activity is much more prevalent throughout the NAM region in July than it is during June, and the intersimulation differences for June were not definitive.

2.2 Evaluation of Upper Level Climate

The differences in the monthly mean profiles of temperature, specific humidity, equivalent potential temperature, and wind at specified levels were calculated between the model and five sounding observations in Mexico, specifically at Chihuahua (MCV), Guaymas (GYM), Mazatlan (MZT), Manzanillo (MAN), and Guadalajara (GUD), and at two sounding observations in the U.S., specifically at Tucson, AZ (TUS) and Del Rio, TX (DRT). Observational soundings were obtained from the online archive maintained by the NOAA Forecast Systems Laboratory. These observations undergo extensive gross

error and hydrostatic consistency checks prior to being archived. No spatial averaging was performed on these upper air variables. Bias is expressed as the July mean model minus July mean observed soundings, the modeled values having been selected to correspond to the time of the sounding, i.e., 12 UTC for GYM, MAN, and DRT, and TUS, and 00 UTC for MCV and MZT. Although both 00 UTC and 12 UTC observations were available for TUS and DRT, the 12 UTC sounding was selected for use in the analysis because it is suspected to be less contaminated by afternoon convection. In addition to the station verification, spatial plots of pressure–integrated wind and divergence, column–integrated precipitable water, and monthly total precipitation were also constructed to aid discussion of the differences between the model simulations. (Note: detailed analyses of moisture transport features and hydrologic fluxes are the subject of a forthcoming paper).

2.3 Evaluation of Surface Climate

The model–calculated, near–surface, daily average air temperature, T_{av}, and dew–point temperatures, T_d, at 2 m above ground level were compared to surface station observations obtained from the National Climatic Data Center's (NCDC) Global Surface Summary of Day historical archive. These data are quality controlled by the United States Air Force through a variety of automated routines. No correction was made for the differences between grid and station elevation, which may introduce systematic bias into the error estimates, as discussed in Section 3. However, we believe this does not change our overall conclusions on the relative merits of the schemes considered in this

study. Paired samples of modeled and observed air and dew–point temperatures were constructed for each station location by spatially averaging all of the available station and gridpoint values within one–degree radius of each station and the center of each corresponding model grid cell. Errors calculated as model values minus observed values for each station were then averaged for the entire month of July. Precipitation statistics were calculated in the same way, except that monthly total station rainfalls were used rather than daily values. The rainfall data were daily total rainfall observations from Mexico and from the NCDC U.S. Surface Summary of Day historical archive. Data from NCDC undergo internal quality control prior to archiving as provided above. Mexican rainfall data are screened for missing and erroneous data values by the Servicio Meteorology Nacional (SMN). The exact methods used by SMN in their quality control procedures were not known at the time of this writing, and as such error analyses over Mexico are subject to greater uncertainty than those over the U.S. Mexican and United States rain–gauge locations are indicated by the small numbers in Figure 1. From Figure 1 it is evident that extensive regions exist (e.g., northern Mexico) where gauge density is very low. Verification analyses in such regions are subsequently subject to more uncertainty than analyses in regions with higher gauge densities.

Monthly statistics in the form of regional mean bias (BIAS) and regional root mean square error (RMSE) were calculated over the physiographically similar regions shown in Figure 1. Statistical significance at the 95% level in the intersimulation differences in regional mean biases was assessed using the nonparametric Mann–Whitney test as

described in von Storch and Zwiers (1999). The regions correspond roughly to those used by Schmitz and Mullen (1996) in their analysis of water vapor transport over the NAM region. Region 0 corresponds to the entire modeled domain, Region 1 to Arizona and New Mexico, Region 2 to the Southern Great Plains, Region 3 to the Sierra Madre Occidental and western coastal plain, Region 4 to the Central Plateau, Region 5 to the Sierra Madre Oriental and eastern coastal plain, and Region 6 to the Balsas Basin Complex. This allowed regional assessment of the model error in surface climate variables.

3. Results

3.1 Evaluation Relative to Upper Level Soundings

Figure 2 shows the difference between monthly average profiles of modeled and observed temperature, specific humidity, and equivalent potential temperature at the seven sounding stations. The RMSE and mean bias statistics for these three variables evaluated over all stations and at all levels are given in Table 2. Statistically significant differences between mean biases, at the 95% level, are denoted by the superscript text next to each simulation title. Significance in the upper air variable differences was tested using a Students t–test adjusted for unequal variances as described in von Storch and Zwiers (1999).

There are substantial differences as well as some common features between each station shown in Figure 2. As reported by Gochis et al. (2000), the model run using the GR

scheme consistently produces atmospheric structures that are cooler and drier than observed, especially at midlevels and at northernmost stations (e.g., TUS, DRT, GYM, and MCV). This is reflected by the overall negative biases in temperature, specific humidity, and equivalent potential temperature. Close examination of Figure 2b shows that most of these biases is associated with underestimation of midlevel atmospheric moisture. The simulation using the BMJ scheme also tends to produce a mean atmosphere for July that is cooler and drier than observed, although less pronounced than with the GR scheme. It is clear from Table 2 that using the KF scheme yields a modeled atmosphere which most resembles observations. When averaged over all measurements, the net bias when using the KF scheme is small and is significantly better than the BMJ or the GR simulations at the 95% level.

The error profiles change considerably from site to site. There is a general tendency for all schemes to underestimate lower atmospheric humidity at the northern stations (Tucson, AZ and Del Rio, TX), and there is a corresponding underestimation of equivalent potential temperature at these stations. There also appears to be a systematic underestimation of low–level moisture at MZT which, when coupled with a relative cool bias, results in marked underestimations of low–level equivalent potential temperature at this site. With some exceptions, use of the BMJ and the GR schemes results in lower than observed values of temperature at the four northernmost stations (TUS, DRT, GYM, and MCV). The midlevel atmosphere cool biases in turn yield low mid–level values of equivalent potential temperature at these sites.

Convective stability can be assessed relative to observations by examining the change in the error in equivalent potential temperature with height. Profiles of equivalent potential temperature error that become more negative with height indicate a simulated profile that is more unstable than observed, and *vice versa*. In most cases (except for TUS and MZT), the simulation using GR maintains a less-stable atmosphere than observed, which is largely due to cooler and drier air at midlevels. Longitude/height transects of equivalent potential temperature at three different latitudes (not shown) also reveal this structure. The results using the BMJ and KF schemes do not show such a consistent tendency. Possible reasons for excess instability in the GR simulation include underestimation of convective activity due to inappropriate formulation of the trigger function or its associated parameters giving an underestimation of the convective mass flux. A more detailed discussion of this is given in Section 4.

Vertical profiles of error in the u and v components of the wind (not shown) exhibit less coherence between simulations than their thermodynamic counterparts, although general tendencies do exist. All of the simulations generally underestimate the low level, v component of the wind, this being responsible for most of the northward moisture transport in the NAM region. The only systematic exceptions are at Manzanillo, where it appeared that the prevailing wind should be more northeasterly than simulated when using all three schemes. All of the simulations also exhibited difficulty in simulating the low-level u component of the wind at northern stations (TUS, DRT, and GYM). The

overestimation of low–level westerly winds at TUS and GYM and at MZT, coupled with the underestimation of the northward v component, may account for some of the underestimation of atmospheric humidity at these stations.

Verification of the model's ability to simulate the northern Gulf California Low–Level Jet (LLJ) (not shown) was facilitated by 00 UTC and 12 UTC pilot balloon measurements made at Puerto Penasco during July 1999. These (now ongoing) measurements are part of the Pan American Climate Studies Sounding Network (PACS–SONET, 2001). All root mean squared error values of the v–wind were in excess of the magnitude of the mean observed wind, thus indicating a serious deficiency in model simulation capability under the present configuration. In general, the diurnal amplitude of the wind at Puerto Penasco was greatly overestimated. Although the errors in the u–component wind were smaller than that of the v–component, each of the three models overestimates the frequency of westerly winds relative to observations.

Figure 3 shows the 925 mb mean vector wind at 12 UTC, along with the monthly mean column integrated precipitable water (PW) field for the three simulations. The fields show several clear sensitivities to the convective parameterization used. The most continuous stream of northward flow occurs over the coastal plains of western Mexico in the KF simulation. Northward flow is also present to a lesser extent in the northern half of the Gulf of California (GC) in the simulation with the BMJ scheme; however, in the simulation with the GR scheme, northward winds are limited to a small region near

Guaymas Bay and northwestern Sonora. All simulations show strong winds at 12 UTC flowing from the California desert regions from northwest to southeast. This intrusion of northwesterly winds is strongest in the simulation with the GR scheme and appears to inhibit the northward advection of moisture as revealed in the PW fields. The more continuous northward flow in the simulation with the KF scheme (and concomitant deeper penetration of high PW values into southern Arizona) suggest that, in this simulation, the regional circulation is capable of tapping deeper reservoirs of atmospheric moisture from the southern GC and the eastern tropical Pacific Ocean.

Distinct differences in the modeled PW field also occur in several other regions. Integrated moisture is generally about 5–10 mm greater in the simulation with the KF scheme than with the BMJ or the GR schemes. This result, together with the significantly lower mean biases for specific humidity at upper levels (Table 2 and Figure 2b), indicate that the simulation with the KF scheme produces a moisture atmosphere which is closer to observations than the simulations with the other two schemes. In particular, the simulations with the BMJ and GR schemes both result in marked negative biases in PW values across the northern regions of the NAM, in Arizona and New Mexico, as well as in the dry interior regions in central Mexico and southern Texas. Higher PW values are also modeled in the simulation with the KF scheme across much of the southern Pacific Ocean, although these were not verified against observations such as satellite–derived PW estimates.

Figure 4 compares the modeled July mean surface–600 mb pressure integrated streamline and divergence fields for all model output times. These fields are important because they describe aspects of regional atmospheric circulation associated with the generation and sustenance of convection. Similar general patterns of convergence occur over the North American cordillera in all three simulations, with weak divergence over the southern Great Plains, southern California, and the eastern Pacific. However, there are also distinct differences. In the KF simulation, there appears to be more extensive and weaker low–level convergence (negative divergence) over much of western Mexico that, with the BMJ and GR schemes, is largely confined to the SMO and to high terrain in Arizona and New Mexico. Perhaps the most significant feature, however, is the streamline pattern across the GC and western Mexico. It is evident that the integrated low–level wind field in the KF simulation is able to transport moisture from well south of the mouth of the GC northward into the convective regions over the SMO and onwards into southern Arizona. The BMJ simulation develops a similar flow but with a much larger westerly component than does KF. The simulation with the GR scheme develops a very different streamline pattern, which would significantly inhibit northward flow up the GC. Monthly mean profiles of the v–component wind at GYM, MZT, MAN, and GUD (discussed below and shown in Figure 5) each reveal that the magnitude of the v–wind is less in GR than in either the BMJ or KF simulation. Each simulation does, however, appear capable of producing northerly components over the far northern portion of the GC.

Although there is insufficient low–level data to verify these modeled circulation patterns,

it is relevant that the limited field observations taken during the 1990 Southwest Area Monsoon Project (Reyes et al., 1994) suggest a mean, low-level wind structure similar to that found in the simulation with the KF scheme and, to a lesser degree, with the BMJ scheme. In fact, there is a notable resemblance between the KF simulation presented here and observations presented in Douglas (1995, Figure 4a), although the northerly winds over the northern GC are further east in the simulations with the KF and BMJ schemes. Stensrud et al. (1995) also observed a similar shift in modeled wind when using an earlier version of the MM5 model running in a 12-hour assimilation/24-hour forecast mode, and a similar low-level wind structure was found in regional simulations with the NCEP regional spectral model (Anderson et al., 2000). Definitive verification and explanation of the low-level wind structure in this region awaits observations proposed in the North American Monsoon Experiment (NAME) Science Plan (NAME, 2001).

There is a perplexingly large difference between the 12 UTC 925 mb winds shown in Figure 3 and the surface-600 mb streamline fields given in Figure 4. To address the question as to why this occurs we have plotted the July mean 12 UTC, v-component winds at mandatory levels from the sounding locations of Guaymas, Mazatlan, Guadalajara, and Manzanillo against observations (see Figure 5). It is evident that, at all sites below 600 mb, the v-component wind in the GR simulation is less in magnitude than either of the other two simulations, although not universally less than observations (e.g., at Manzanillo). At some locations, such as Guaymas and Mazatlan, the GR estimated v-wind is of an opposite sign than either the BMJ or the KF estimates.

Further, the streamline fields consist of surface to 600 mb pressure integrated wind values. This means that low–level winds are weighted more heavily than are upper level winds within this layer. Thus, in regions where the low–level v–winds in GR are underestimated or of opposite sign with respect to the other simulations, one would expect this feature to persist in integrated streamline fields. This is exceptionally evident when the profile 925 mb v–winds from Mazatlan are compared.

From the v–wind profile, it is also noticed that, at both Mazatlan and Manzanillo, the magnitude of the v–wind reaches a maximum at around 700 mb. In the cases of the BM and KF simulations, the upper–level winds in the sfc–600 mb layer appear to have a significant influence on the integrated values due to the fact that the low–level winds are comparatively weak, being almost neutral. However, as the GR simulation fails to produce as intense of magnitude v–winds at upper levels anywhere in the sfc–600 mb layer, its streamlines do not possess as strong a northward component. Assuming that the mean winds at the sounding locations are at least somewhat indicative of the regional winds over the eastern Gulf of California, it is suspected that these differences are the reason for the large intersimulation differences between the 925 mb level and the sfc–600 mb integrated wind fields.

3.3 Evaluation Relative to Surface Temperatures

Table 3 gives the regionally averaged, monthly RMSE, and mean bias for the daily average temperature and dew point temperature at 2 m above ground level. Bold text

and superscripts next to mean biases indicate significantly different intersimulation biases at the 95% level, as in Table 2. There is a distinct dry bias (i.e., lower dew point) in all regions and all simulations. The underestimation in T_d in Table 3 corresponds with the general underestimation of lower atmospheric humidity noticed in the previous section. However, it is important to recognize that negative biases in surface dew point temperature can arise from elevation discrepancies between station observations and modeled values, and that smoothed model topography tends to increase the mean valley elevations of the modeled terrain where most climate stations are located (Giorgi and Shields, 1999). It is also possible that the negative bias in T_d is caused by an inaccurate representation of the planetary boundary layer (PBL) as simulated by the PBL parameterization. Poor representation of the diurnal evolution of the PBL in the northern regions of the NAMS may also contribute to negative biases in precipitation there as discussed below.

The intersimulation differences are arguably more interesting, although only the difference between the KF and GR simulations in Region 1 is statistically significant at 95%. There is a substantial negative bias in T_d in the simulation with the GR scheme as reported by Gochis et al. (2000), with rather less negative bias in the simulation with the BMJ scheme. The simulation with the KF scheme consistently has the smallest RMSE in T_d everywhere. Region 1, which covers Arizona and New Mexico, is the region with consistently highest errors. This underestimation in the northern portion of the NAM region reflects the modeled underestimation of northward transport of moisture into the

region that was suggested by large wind errors in the pilot balloon data and the v–component wind in the soundings.

The error statistics for T_{av} are similar to those for T_d, although none of the inter–simulation differences in mean biases are statistically significant at 95%. For this variable, the RMSE in Region 0 is greatest in the simulation with the BMJ scheme, followed by that with the GR, then the KF schemes. In all of the simulations, the errors are greatest in Region 2 (the southern Great Plains) followed by those in Region 1. There is less consistency in the RMSE values for T_{av} in Regions 3, 4, 5, and 6, in Mexico, than in the regions within the United States. There is a general positive bias in the maximum daily temperature (not shown) in the simulation with the GR scheme and, to a lesser extent, in the simulations with the BMJ scheme compared to that with the KF scheme. As discussed later (Section 4), this is important because it supports the hypothesis that simulations with the GR and BMJ schemes allow more instability in the model climate, possibly indicating a deficiency in adequately representing the extent of convective activity in northern regions. On the other hand, the bias in T_{max} for the simulation with the KF scheme is small in all regions, with only a slight positive bias in Regions 1 and 2.

3.4 Evaluation Relative to Observations of Precipitation

Figure 6 shows the spatial distribution of modeled precipitation from the three simulations along with a satellite–derived estimate of precipitation from the PERSIANN system (Sorooshian et al., 2000). PERSIANN–estimated rainfall has been verified

against the Stage IV merged radar/rain gauge product over two locations in Florida and in Texas, and have been shown to yield good results although some deficiencies exist as discussed by Sorooshian et al (2000). At the time of this writing, the accuracy of the PERSIANN estimates over the NAM region has yet to be verified, although preliminary analyses have shown that it captures well the diurnal cycle of deep convective activity over Mexcio and the southwestern United States. Clearly, the simulation with the KF scheme produces more extensive precipitation than with either the BMJ or GR schemes. There is a substantial difference in the magnitude and extent of the modeled rainfall over Arizona, New Mexico, Texas, Oklahoma, and central Mexico. The bias and RMSE for precipitation given in Table 3 show that errors are lowest with the KF scheme in Regions 1, 2, and 4, although this scheme slightly overestimates precipitation in these regions. Note that all intersimulation differences in regional mean biases are significant at the 95% level, as denoted by the superscripts.

Several features of the precipitation fields are worth noting. First, there appears to be substantial discrepancy in the estimation of precipitation in Region 3, the core of the monsoon region along the western slopes of the SMO. The RMSE statistics indicate a substantial error, with a significant positive bias in the simulation with the BMJ scheme and, to a lesser degree, the KF scheme. With the GR scheme, the RMSE is less than that with both BMJ and KF schemes, and its mean bias is close to zero. In the absence of reliable, high–resolution precipitation gauge data that adequately sample topography, and based on these findings, we suspect that the actual precipitation in this region is closest to

that of the GR scheme. Second, KF precipitation estimates from inland regions of Mexico and the southern Great Plains verify well against the PERSIANN data.

Third, the simulation with the KF scheme appears to suffer from a boundary condition problem along the eastern boundary of the inner domain, where a monthly total precipitation in excess of 500 mm is simulated. Such a feature is not present in the PERSIANN data, and we believe that the generation of heavy precipitation here is spurious and due to interaction between the convection scheme and the model boundary condition as found in Stensrud et al. (1995). There is inflow at this boundary, and the thermodynamic structure of the imported atmosphere is largely determined by the structure on the coarse domain that uses the BMJ convection scheme. It seems likely that the excess instability present in the BMJ scheme (suggested above) is brought into the internal domain, which is sufficient to trigger convection within the KF scheme operating in the internal domain, resulting in excessive estimates of rainfall just inside the domain boundary.

Last, there is a substantial difference in the amount of precipitation produced along the southern boundary of the internal domain and in southern Mexico in the simulations with the BMJ and KF schemes compared to GR schemes. Both the KF and the BMJ simulations appear to markedly overestimate rainfall along the southwest coast of Mexico relative to PERSIANN. This overestimation is also reflected in a substantial bias and RMSE in Region 6 with the BMJ and, to a lesser extent, the KF scheme. The exact

cause of this feature is unknown at this writing as all three simulations produce broadly similar precipitation patterns over the ITCZ on the 90–km domain. In the case of the simulation with the KF scheme, a boundary–related process similar to that described in the previous paragraph might be the cause, but this does not readily explain the (greater) overestimation of precipitation given with the BMJ scheme. This aspect of these simulations is the subject of ongoing study.

4. Discussion

The following points summarize the results of the analyses described above.

- Substantial differences in both the thermodynamic and circulation structure of the simulated July 1999 NAM atmosphere evolve when different CPS schemes are used.
- In addition to entire–domain error tendencies, subregional error tendencies are also prevalent, and many of the intersimulation differences are statistically significant.
- As reported by Gochis et al. (2000), the MM5 simulation using the GR scheme yields an atmosphere in July 1999 that is drier than observed in terms of lower and upper tropospheric moisture content and precipitation.
- MM5 simulations with both the BMJ and GR schemes give a marked underestimation of convective precipitation in the northern NAM regions, i.e., in the southwestern U.S., the southern Great Plains, and over the central Mexican Plateau. Conversely, simulations with the KF scheme show only a slight positive bias across these same regions. Over the SMO, however, and over far southern Mexico, the GR scheme appears to best simulate the observed precipitation field.

- The error in the modeled surface dew point temperature field is greater in the northern monsoon regions than in other regions, regardless of the convective scheme used. The error is greatest in these regions for the simulation with the GR scheme, followed by that with the BMJ scheme, while the error with the KF scheme is least.
- Based on profiles of equivalent potential temperature, use of the GR scheme results in more instability in the atmosphere than use of the BMJ scheme, and significantly more instability than use of the KF scheme. Similarly, use of the GR scheme results in marked underestimation of the moisture and temperature at mid–levels in the atmosphere compared to use of the other two schemes.
- As a result of the difference in the CPSs, markedly different regional circulation patterns evolve which are revealed in the integrated low–level streamline and divergence fields. The KF scheme results in a broader distribution of low–level convergence, which extends into central Mexico and into the southwestern United States. In contrast, convergence is more localized and locked primarily to the highest topographic features when both the BMJ and GR schemes are used.
- Large differences occur in the mean low–level wind structure between the three simulations. The simulation with the KF scheme maintains a continuous flow of southeasterly low–level wind across the GC that appears to transport moisture from far south of the mouth of the GC. While similar to KF, the flow in the BMJ simulation appears to have less of a northward component. Northward flow in the GR simulation is restricted only to the northern GC.
- Differences in the circulation fields result in markedly different fields of column–

integrated precipitable water. Appreciable whole–column water vapor is advected northward into Arizona and the central Mexican plateau only when the KF scheme is used in MM5.

On the basis of the results of this study, it is evident that the representation of convection in regional climate models has a marked influence not only on model–estimated precipitation, but also on the simulated circulation patterns in the NAMS. These results support the earlier findings of Stensrud (1996), who concluded that the effects modeled persistent, deep convection over the central plains of the U.S. could serve to alter the low–level circulation, generate Rossby waves, and produce upper–level perturbations that extend as far as 50° longitude from the convective region. Although a detailed discussion on the uncertainty in convective parameterization is beyond the scope of this basic sensitivity study, a brief discussion of our simulation results is provided next.

The convective trigger function is the portion of a CPS that governs when the CPS is activated. Because the GR scheme maintains a comparatively unstable atmosphere, it seems plausible to suggest that the GR CPS is not triggered as frequently as the KF CPS during simulation. The ironic feature that the GR scheme maintains more instability while producing less rainfall is supported by large differences in the July mean fields of the high–cloud fraction (not shown), which reveal that the GR simulation produces a much smaller area of high cloud than the other two simulations. Initiation of convection in a particular region can be improved by tuning CPS parameters such as lifted depth

criteria. In fact, Giorgi and Mearns (1999) recommended such tuning. However, the results may be beneficial in some regions but deleterious in others. For example, lowering the lifted–depth requirement to generate more convection in, say, Arizona may result in too much convection in southern Mexico. Perhaps this is occurring with the KF scheme, as it is overestimating precipitation in southern Mexico. It should also be noted, as discussed in Janjic (1994), that convective scheme triggering is sensitive to PBL formulation, such that different PBL formulations may either beneficially or detrimentally affect the simulation of convection.

The trigger function in the BMJ scheme also appears to inhibit convective activity in the northern NAM regions, which gives reduced precipitation and relatively cooler and drier mid level atmosphere compared with the KF simulation. This is not surprising because the convective trigger formulation used in the BMJ scheme is very similar to that used in the GR scheme, i.e., a lifted–depth criterion must be overcome by the large–scale vertical velocity. Where the BMJ scheme is activated, for example in Regions 3 and 6, there appears to be an overestimation of precipitation. This suggests that the profile adjustment procedure used in the BMJ scheme is either yielding too much column water during the relaxation of large–scale profile towards the reference profile, or that too much of the residual moisture is being converted into precipitation. It may be acceptable to tune either the reference profile parameters or the parameters in the precipitation generation equation without degrading the overall performance of the scheme. In fact, this task is simplified by the fact that the changes made by Janjic (1994) reformulated

both the reference profiles and the precipitation generation equation in terms of a "cloud efficiency" parameter. While the cloud efficiency parameter is not single–valued and can evolve, depending on the large–scale environment, it may be possible to tune the formulation of cloud efficiency to produce atmospheric structures and precipitation fields more similar to observations than at present.

The KF CPS is the most physically complex representation of the three schemes considered in this study (see Section 2 and Appendix 1). Although increased complexity does not necessarily translate into increased performance, there are attributes of the KF scheme that make it appealing when simulating convection in the NAM region. As noticed above, the KF scheme does appear to generate convective precipitation more realistically in the northern part of the NAMS than either the GR or the BMJ schemes. Moreover, the treatment of hydrometeors in the KF CPS (especially ice) ensures that exchanges of latent heat of fusion are accounted for. Ice processes are effectively neglected in the GR scheme, which may account for at least part of the observed cool bias at mid tropospheric levels. No such systematic cool bias exists in the KF simulation.

Probably most important, the KF CPS includes entraining/detraining air to and from convective clouds. Although it is difficult to diagnose the effect of the cloud model formulation in the analyses presented here, such processes are likely to become more significant in the drier convective environments of southwestern Arizona and the central plateau of Mexico. The hypothetically beneficial aspects of the KF scheme are supported

by the fact that, when it is used, mid level heat and moisture profiles have statistically significant less error than do the profiles generated when the non–entraining GR scheme is used. Detrainment of convective updrafts and downdrafts is expected to be comparatively less important in southern Sinaloa than in southwestern Arizona because the moisture profiles are deeper there. The fact that the GR scheme yields lower error estimates in southern Mexico (in Region 6) may suggest that representing cloud entrainment/detrainment may not be necessarily beneficial in tropical regions.

5. Conclusions

This study shows that MM5 simulates substantially different regional climates during the North American Monsoon when different convective schemes are used. Although there are some common features, the comparative performance of the different schemes differs across the modeled domain. This is perhaps not surprising because different CPSs have assumptions and parameter specifications that make them more appropriate in some regions than others, but it complicates the task of using regional climate models over domains of appreciable size. Running a mesoscale model over the whole NAM region presents convective parameterization challenges beyond those faced at the meso–b scale.

The simulations described above do not represent a thorough testing of the CPSs considered in this study. Nonetheless, the conclusion that there is substantial sensitivity in model–generated climate, especially with regard to the low–level circulation, to the selection of a CPS is believed to be a robust conclusion. Such sensitivity presents an

interesting challenge for long–term hydrologic prediction systems. Changes in convective parameterization can result in marked differences in the regional moisture transports into and out of a particular subregion. These circulation changes interact with changes in the local efficiency with which precipitation is released, and important feedbacks emerge that can potentially alter the modeled hydrological characteristics of a given sub region.

Acknowledgments.

Primary support for this study came from NASA grant NAG5–7554. Special thanks are extended to Robert Maddox and Steve Mullen for their critical review of this work. George Bryan for sharing his code to convert MM5 data into GrADS readable format. Wei Wang and the MM5 User Support personnel at NCAR for answering many questions regarding the model. Art Douglas for sharing his archive precipitation data from Mexico and to three anonymous reviewers whose insightful comments greatly improved the quality of this manuscript. We also thank Corrie Thies for helping with textual corrections.

Appendix A: Convective Parameterization Scheme Descriptions

A.1 Betts–Miller–Janjic Scheme

Betts (1986) and Betts and Miller (1986) proposed a convective parameterization for deep and shallow convection based on the principle of "saturation point" thermodynamics

outlined in Betts (1982). In this scheme, profiles of temperature and moisture in a column with sufficient resolved–scale vertical motion and instability are instantaneously relaxed towards observed, quasi–equilibrium structures. The method is similar to that of Kuo (1974), except that the convective column in the Kuo scheme is relaxed toward a reference that is the moist adiabatic profile. The difference is proposed because observational evidence suggests that using the moist adiabatic profile yields convective available potential energy (CAPE) in excess of observed kinetic energies. The BMJ CPS does not account for sub grid cloud and mesoscale processes such as microphysical processes or updrafts and downdrafts, although release of latent heat of fusion due to ice processes is implicit in the construction of the reference profiles. Precipitation from the deep convection scheme is calculated as the residual integrated water between the large–scale moisture profile and the reference profile. Janjic (1994) substantially modified the original Betts–Miller scheme by allowing the reference profiles to vary with the convective environment, as diagnosed by a "cloud efficiency" parameter. These modifications are included in the current version of the Betts–Miller scheme used in the MM5 modeling system.

A.2 Kain–Fritsch Scheme

The Kain–Fritsch convective parameterization scheme is a combination of the one–dimensional entraining/detraining plume model of Kain and Fritsch (1990) and the convective parameterization framework of Fritsch and Chappell (1980). The Fritsch and Chappell formulation is a mass flux scheme that governs the initiation of convection and

convective relaxation (by which instability is removed from the grid–scale convective column), while the Kain and Fritsch portion of the scheme is a cloud model, which governs the redistribution of heat and moisture, in both liquid and solid phases. The effects of moist updrafts and downdrafts and the detrainment and subsequent evaporation/sublimation of cloud condensate into the downdraft are all explicitly represented in the KF CPS. Convection is initiated when there is a net column instability and sufficient grid–resolved, upward vertical velocity to overcome any negative buoyancy in the lower atmospheric layers. The convective available potential energy (CAPE) present on the resolved scale governs the quantity of the convective mass flux required to consume the grid–resolved CAPE over an (assumed) convective time step of approximately one hour. Precipitation is formed within the cloud model as the mechanism by which excess cloud condensate is removed and occurs at a rate which is an inverse function of the mean layer vertical velocity and a direct function of a prescribed rate constant.

A.3 Grell Scheme

The Grell scheme is a one–dimensional mass flux scheme that consists of a single updraft/downdraft couplet. It is a highly simplified version of the Arakawa and Schubert (1974) cloud ensemble parameterization implemented as a single cloud member. Unlike in the KF CPS, there is no direct mixing between the updraft and downdraft and with the surrounding atmosphere, except at the top and bottom of the cloud. Thus, the convective mass fluxes are constant with height. Because all condensed water vapor in the

convective cloud is removed as potential rainwater, there is no explicit accounting of ice processes in the GR CPS. As with the KF scheme, the convective mass flux is determined by the flux required to stabilize an unstable air column, but the closure assumptions differ in implementation between the two schemes. The Grell scheme is activated using a trigger mechanism similar to that used in the KF scheme in that it is not activated until a lifting–depth criterion is met that indicates there is sufficient lift to access potential buoyant energy. Convective precipitation is calculated as a function of the convective mass flux, the amount of cloud condensate that has been removed as rainwater but not evaporated into the downdraft, and a precipitation efficiency parameter.

REFERENCES

Adams, D. K. and A. C. Comrie, 1997: The North American Monsoon. *Bull. Am. Met. Soc.*, 78, 2197–2213.

Anderson, B.T., J.O. Roads, S–C. Chen, and H–M. Juang, 2000: Regional simulation of the low–level monsoon winds over the Gulf of California and southwestern United States. *J. Geophys. Res.*, 105(D14), 17955–17969.

Arakawa, A. and W. H. Schubert, 1974: Interaction of a cumulus cloud ensemble with the large–scale environment, Part 1. *J. Atmo. Sci.*, 31, 674–701.

Barlow, M., S. Nigam and E.H. Berbery, 1998: Evolution of the North American Monsoon system. *J. Climate*, 11, 2238–2257.

Betts, A.K., 1982: Saturation point analysis of moist convective overturning. *J. Atmos. Sci.*, 39, 1484–1505.

Betts, A.K., 1986: A new convective adjustment scheme, part I: observational and theoretical basis. *Q.J.R. Met. Soc.*, 112, 677–691.

Betts, A.K. and M.J. Miller, 1986: A new convective adjustment scheme, part II: single column tests using GATE wave, BOMEX, ATEX and arctic air–mass data sets.

Q.J.R. Met. Soc., 112, 693–709.

Copeland, J.H., R.A. Pielke, and T.G.F Kittel, 1996: Potential climatic impacts of vegetation change: a regional modeling study. *J. Geophys. Res.*, 101, 7409–7418.

Dickinson, R.E., R.M. Errico, F. Giorgi, and G.T. Bates, 1989: A regional climate model for the western United States. *Clim. Change*, 15, 383–422.

Douglas, M.W., 1995: The summertime low-level jet over the Gulf of California. *Mon. Wea. Rev.* 123, 2334–2347.

Douglas, M.W., R.A. Maddox, K.W. Howard, and S. Reyes, 1993: The Mexican Monsoon. *J. Climate*, 6, 1665–1677.

Fritsch, J.M. and C.F. Chappell, 1980: Numerical prediction of convectively driven mesoscale pressure systems. part I: convective parameterization. *J. Atmos. Sci.*, 37, 1722–1732.

Giorgi, F., 1990: On the simulation of regional climate using a limited area model nested in a general circulation model. *J. Climate*, 3, 941–963.

Giorgi, F. and M.R. Marinucci, 1996: An investigation of the sensitivity of simulated precipitation to model resolution and its implications for climate studies. *Mon. Wea. Rev.* 124, 148–166.

Giorgi, F. and L.O. Mearns, 1999: Introduction to special section: regional climate modeling revisited. *J. Geophys. Res.* 104(D6), 6335–6352.

Giorgi, F. and C. Shields, 1999: Tests of precipitation parameterizations available in latest version of NCAR regional climate model (RegCM) over continental United States. *J. Geophys. Res.* 104(D6), 6353–6357.

Gochis, D.J., Z–L. Yang, W.J. Shuttleworth, and R.A. Maddox, 2000: Quantification of error in a pseudo–regional climate simulation of the North American Monsoon. Second Southwest Weather Symposium, Sept. 21–22, Tucson, AZ.

Grell, G.A., 1993: Prognostic evaluation of assumptions used by cumulus parameterizations. *Mon. Wea. Rev.*, 121, 764–787.

Grell, G.A., J. Dudhia, and D.R. Stauffer, 1994: A description of the fifth generation Penn State/NCAR mesoscale model (MM5). NCAR Tech. Note NCAR/TN–380+STR, 138 p.

Higgins, R.W., Y. Yao, and X–L. Wang, 1997: Influence of the North American Monsoon system on the U.S. summer precipitation regime. *J. Climate*. 10, 2600–2622.

Janjic, Z.I., 1994: The step–mountain eta coordinate model: further developments of the convection, viscous sublayer, and turbulence closure schemes. *Mon. Wea. Rev.*, 122, 927–945.

Kain, J.S. and M. Fritsch, 1990: A one–dimensional entraining/detraining plume model and its application in convective parameterization. *J. Atmo. Sci.*, 47, 2784–2802.

Kalnay and Coauthors, 1996: The NCEP/NCAR reanalysis project. *Bull. Am. Met. Soc.*, 77, 437–471.

Kuo, H.L. 1974: Further studies of the parameterization of the influence of cumulus convection on large–scale flow. *J. Atmos. Sci.*, 31, 1232–1240.

Molinari, J. and M. Dudek, 1992: Parameterization of convective precipitation in mesoscale numerical models: a critical review. *Mon. Wea. Review*, 120, 326–344.

NAME, 2001: North American Monsoon Experiment Science Plan. http://yao.wwb.noaa.gov/monsoon/NAME.html

PACS–SONET. 2000: Pan–American Climate Studies Sounding Network. http://www.nssl.noaa.gov/projects/pacs/

Reyes, S., M.W. Douglas and R.A. Maddox, 1994: El monzon del suroeste de Norteamerica (TRAVASON/SWAMP). *Atmosfera*, 7, 117–137.

Reynolds, R.W. and T.M. Smith, 1994: Improved global sea surface temperature analyses. *J. Climate*, 7, 929–948.

Schmitz, J.T. and S.L. Mullen, 1996: Water vapor transport associated with the summertime North American Monsoon as depicted by ECMWF analyses. *J. Climate*, 9, 1621–1634.

Seth, A. and F. Giorgi, 1998: The effects of domain choice on summer precipitation simulation and sensitivity in a regional climate model. *J. Climate*, 11, 2698–2712.

Small, E.E., 2001: The influence of soil moisture anomalies on variability of the North American monsoon system. *Geophys. Res. Let.*, 28(1), 139–142.

Sorooshian, S. K.L. Hsu, X. Gao, H.V. Gupta, B. Imam, and D. Braithwaite, 2000:

Evaluation of PERSIANN system satellite–based estimates of tropical rainfall. *Bull. Am. Met. Soc.*, 81, 2035–2046.

Stensrud, D.J., 1996: Effects of persistent, midlatitude mesoscale regions of convection on the large–scale environment during the warm season. *J. Atmo. Sci.*, 53, 3503–3527.

Stensrud, D.J., R.L. Gall, S.L. Mullen and K.W. Howard, 1995: Model climatology of the Mexican Monsoon. *J. Climate*, 8, 1775–1794.

von Storch, H. and F.W. Zwiers, 1999: Statistical Analysis In Climate Research. Cambridge University Press, 484 p.

Wang, W. and N.L Seaman, 1997: A comparison study of convective parameterization schemes in a mesoscale model. *Mon. Wea. Rev.*, 125, 252–278.

Zhang, G.J. and N.A. McFarlane, 1995: Sensitivity of climate simulations to the parameterization of cumulus convection in the Canadian Climate Centre general circulation model. *Atmos.–Ocean*, 33, 407–446.

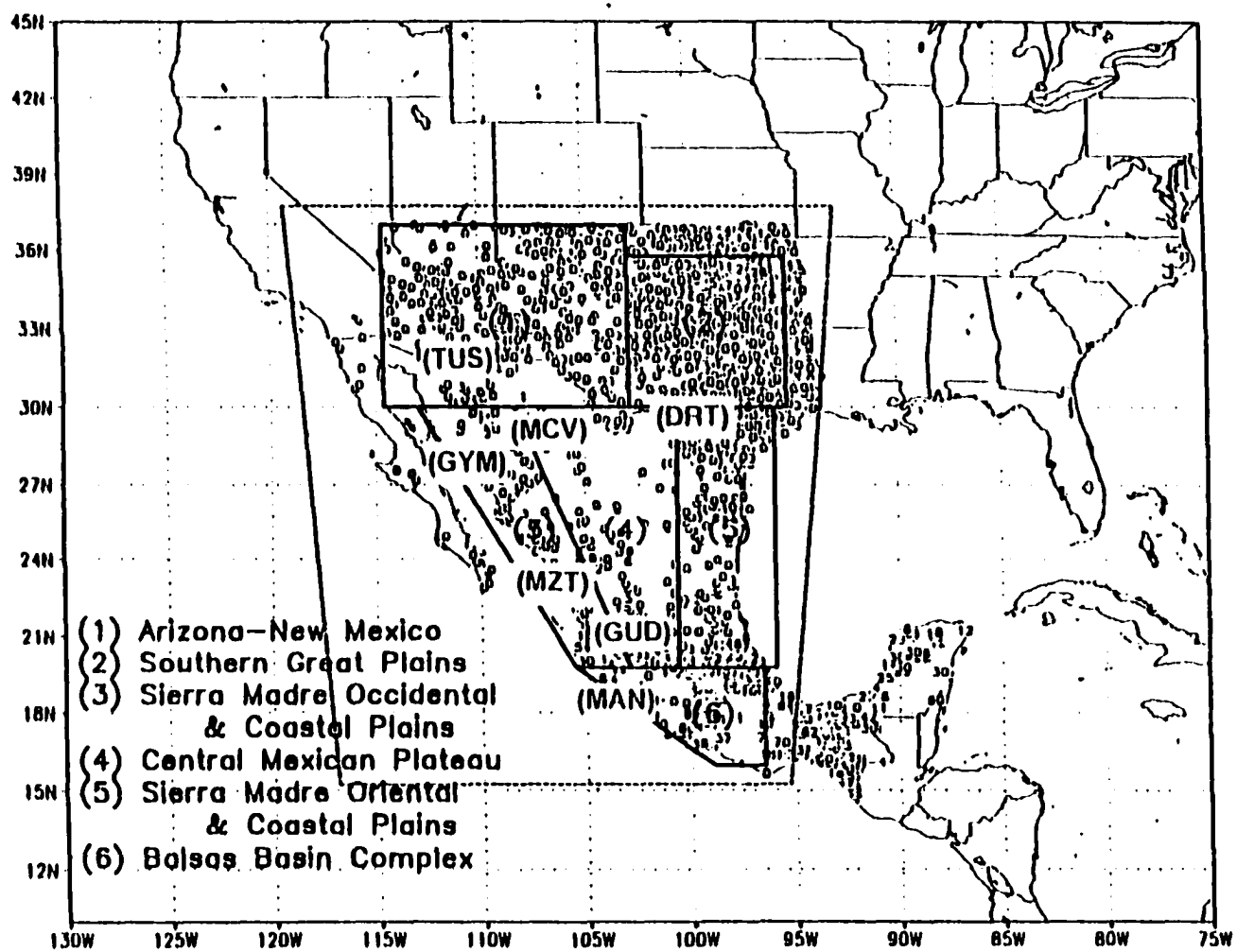

Figure A.1 Coarse (90–km, approximately map frame) and fine (30–km, dotted line) domains. Solid lines: physiographically similar areas used in the calculations of regional verification statistics. Small numbers indicate locations of daily precipitation gages. Bold letters indicate radiosonde station locations.

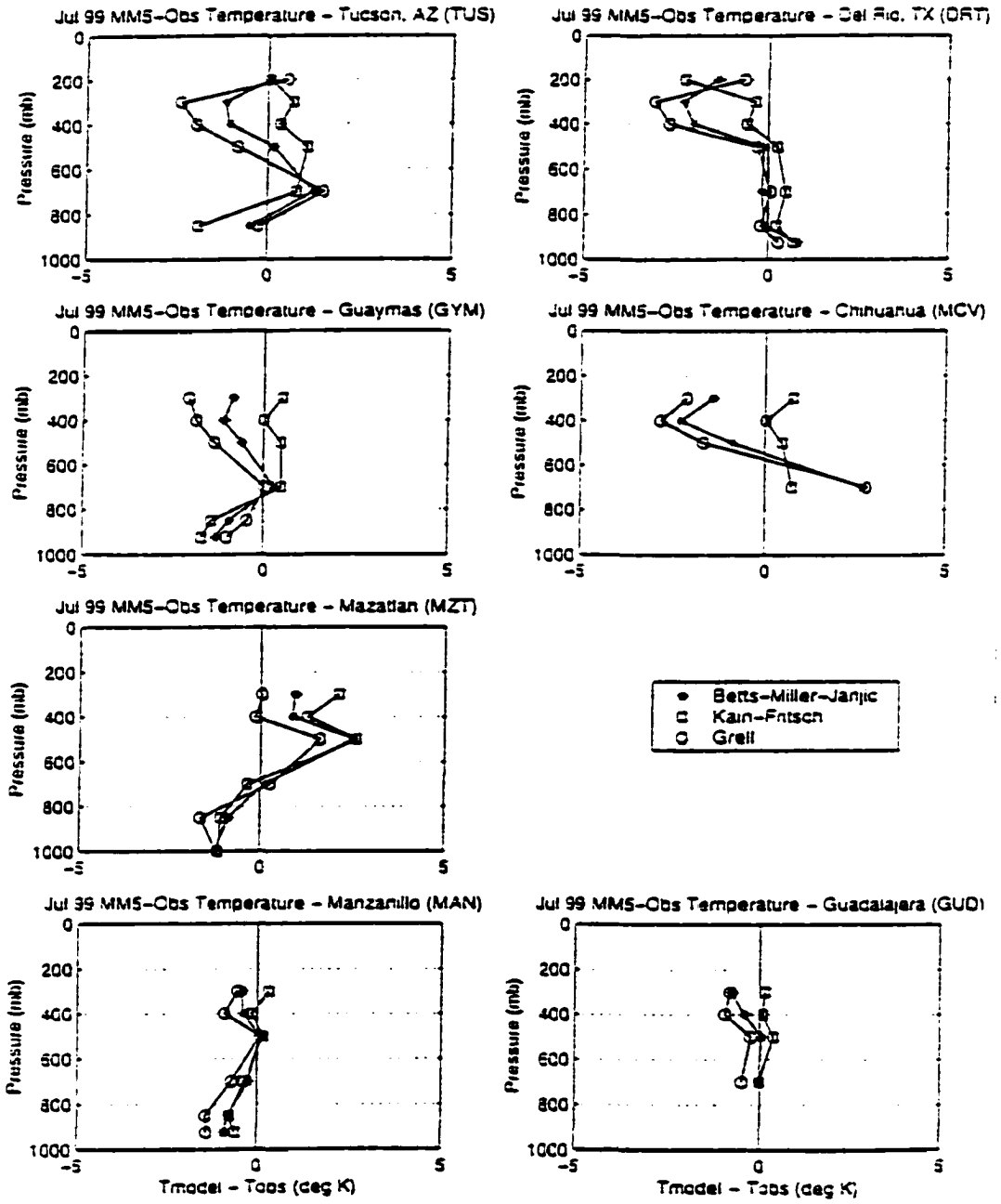

Figure A.2a Profiles of error (model–observed) of monthly mean temperature (K).

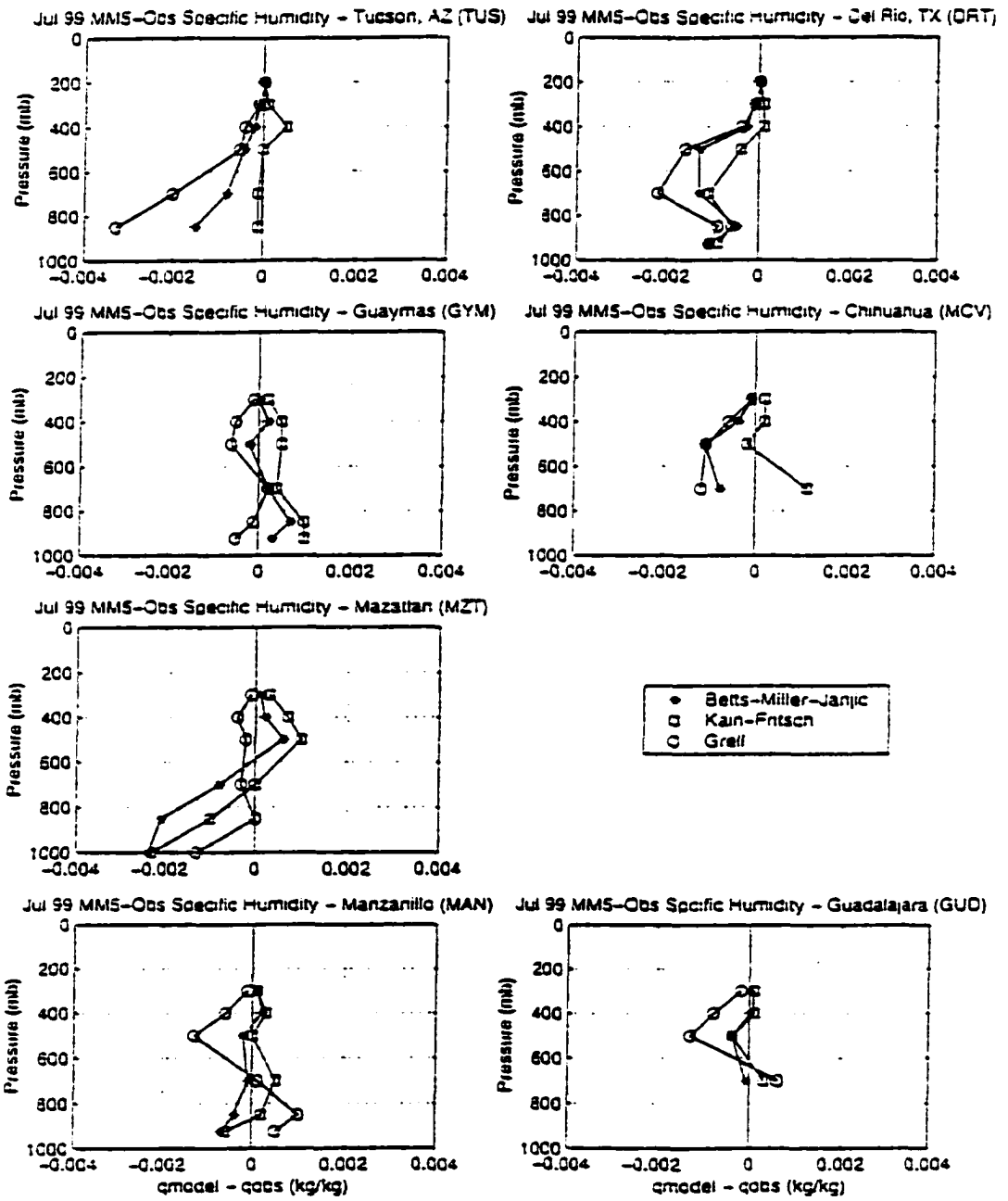

Figure A.2b Profiles of error (model–observed) of monthly mean specific humidity (kg / kg).

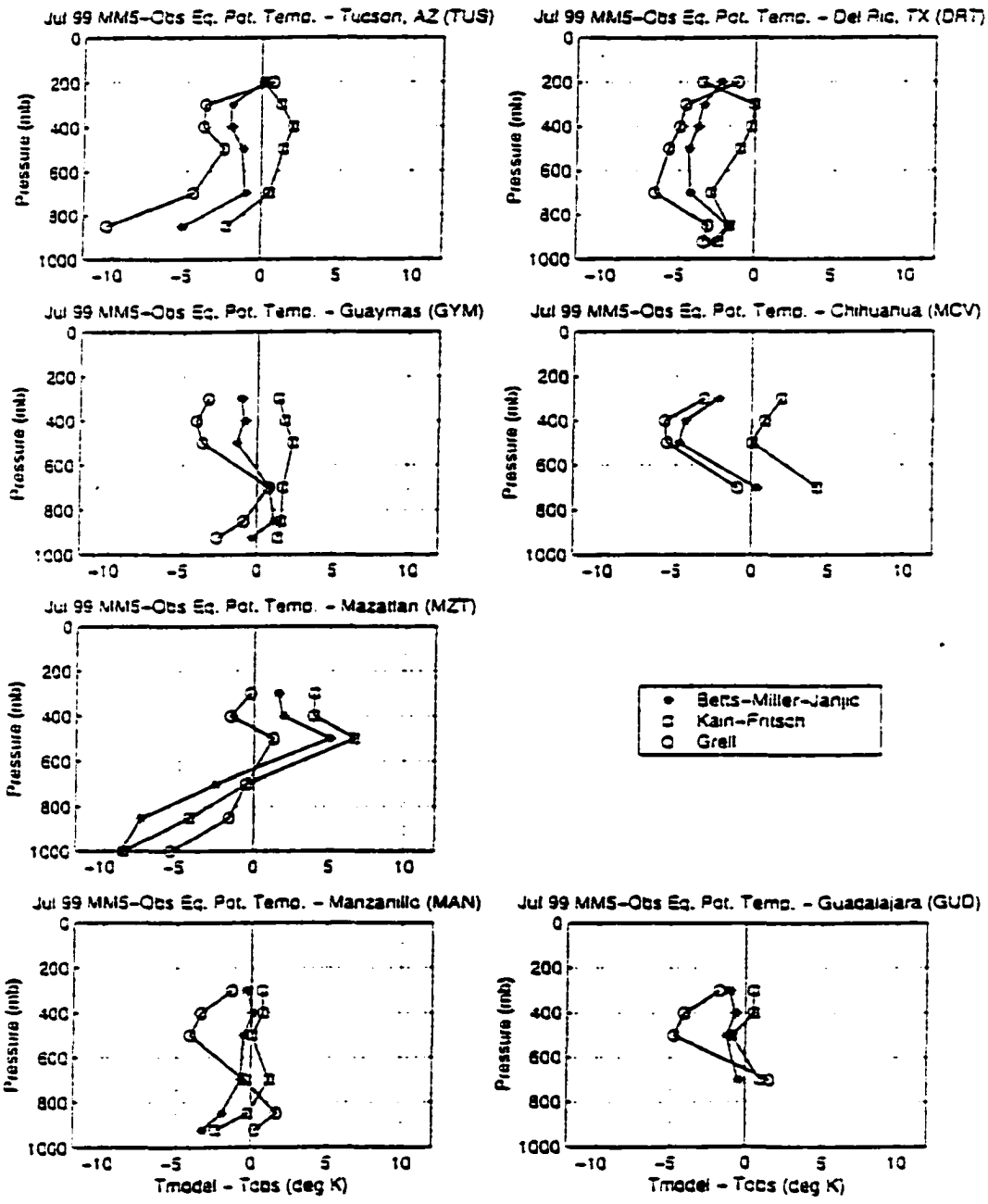

Figure A.2c Profiles of error (model–observed) of monthly mean equivalent potential temperature (K).

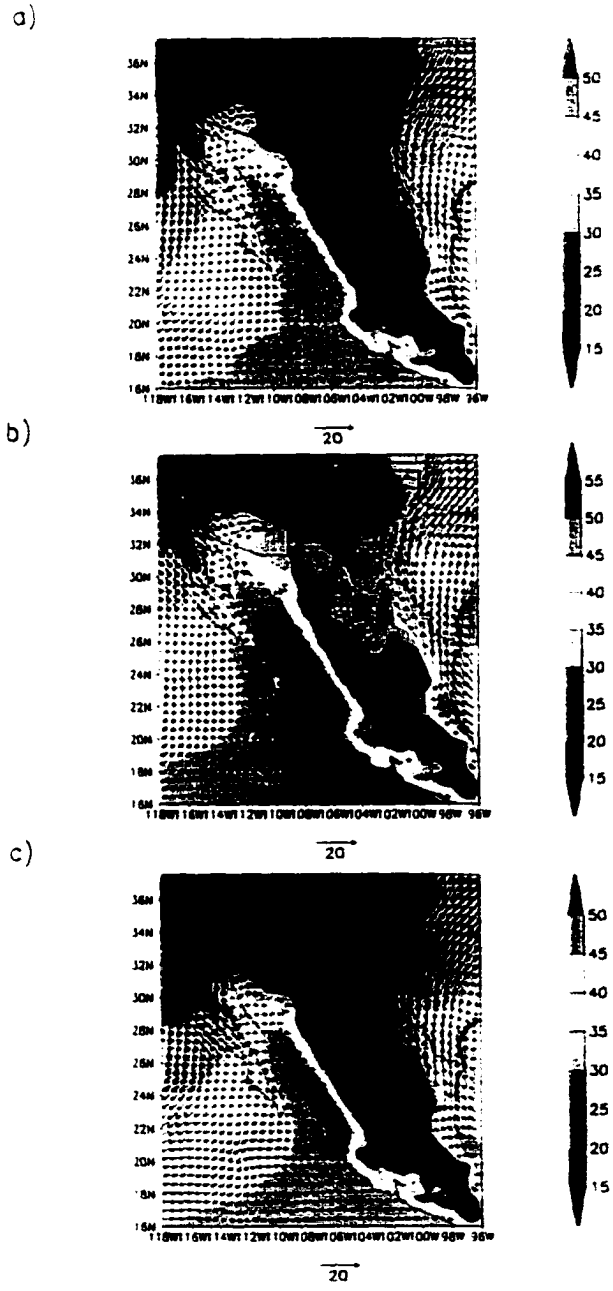

Figure A.3 **July mean column integrated precipitable water content (mm) (shaded), and mean 925 mb 12 UTC wind vectors. a) Betts–Miller–Janjic, b) Kain–Fritsch, c) Grell.**

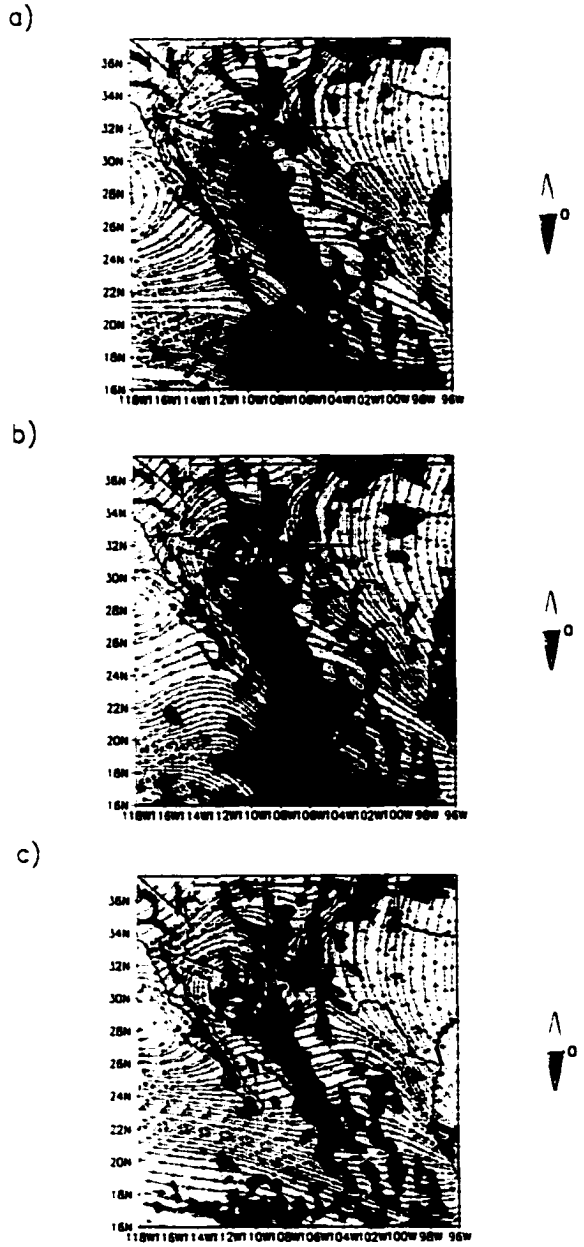

Figure A.4 July mean surface–600 mb pressure integrated divergence (s^{-1}) and mean surface–600 mb pressure integrated streamline pattern. a) Betts–Miller–Janjic, b) Kain–Fritsch, c) Grell.

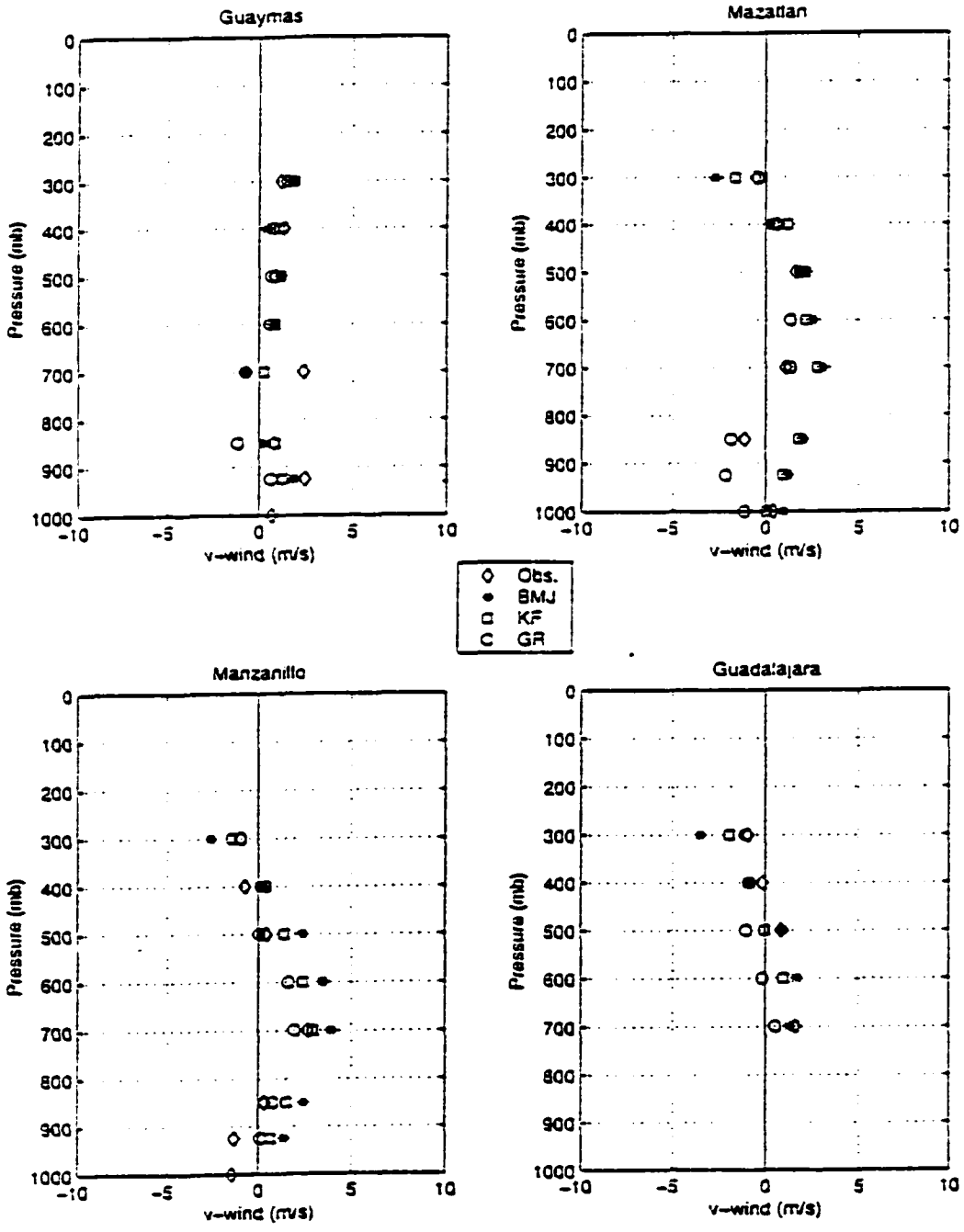

Figure A.5 Profiles of observed and model estimated 12 UTC monthly mean v–component winds (m/s) at mandatory levels.

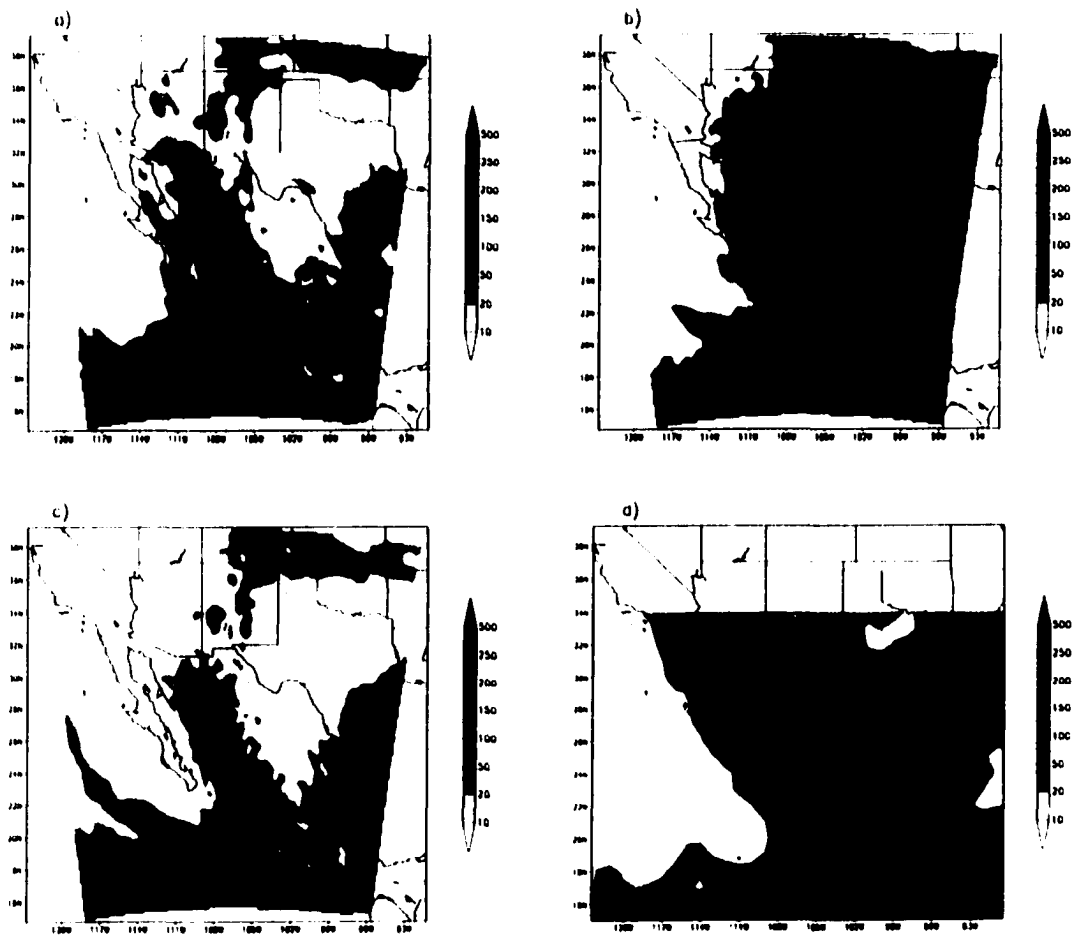

Figure A.6 July total precipitation (mm) (shaded). a) Betts–Miller–Janjic, b) Kain–Fritsch, c) Grell, d) PERSIANN.

Physics Option		Model Setup
Explicit Microphysics		Simple Ice (Grell et al., 1994)
Land-Surface Model		OSU/ETA (Chen and Dudhia, 1999)
P.B.L.		MRF (Hong and Pan, 1996)
Radiation		Cloud Rad. Scheme (Grell et al., 1994)
Cumulus	(90-km domain)	Betts-Miller-Janjic (Janjic, 1994)
	(30-km domain)	Kain-Fritsch (Kain and Fritsch, 1993)
		Grell (Grell et al., 1994)
		Betts-Miller-Janjic (Janjic, 1994)

Table A.1 Model options used in the sensitivity experiments.

	Temperature		Specific Humidity		Theta-e	
	RMSE	BIAS	RMSE	BIAS	RMSE	BIAS
	(K)	(K)	(kg kg-1)	(kg kg-1)	(K)	(K)
BMJ	1.1	-0.4 ^{KF}	0.0008	-0.004 ^{KF}	3.1	-1.8 ^{KF}
KF	1.0	0.1 ^{BMJ,GR}	0.0006	0.0000 $^{BMJ, GR}$	2.6	0.3 $^{BMJ, GR}$
GR	1.4	-0.7 ^{KF}	0.0010	-0.0006 ^{KF}	3.8	-2.8 ^{KF}

Table A.2 Root mean squared error (RMSE) and mean bias (BIAS) statistics for upper–level measurements. Error estimates are combined for the month of July from all radiosonde stations for each variable. (BMJ, KF, GR) superscripts denote simulations in which the differences in the mean bias values are significant at the 95% level.

Regionally Averaged Surface Daily Average Dew Point Statistics (deg C)

		BIAS			RMSE		
		BM	*KF*	*GR*	*BM*	*KF*	*GR*
Jul-99							
Region:	0	-3.8	-2.0	-4.5	4.6	2.7	5.6
	1	-6.8	-3.7 ^{GR}	-9.2 ^{KF}	7.0	4.4	9.5
	2	-4.3	-1.9	-4.5	4.4	2.0	4.7
	3	-2.5	-1.7	-2.3	2.8	1.9	2.3
	4	-2.5	-0.9	-2.7	3.3	1.8	3.5
	5	1.8	-1.3	-2.4	2.6	1.7	2.9
	6	-1.1	-0.7	-1.4	1.4	1.1	1.6

Regionally Averaged Surface Daily Average Temperature Statistics (deg C)

		BIAS			RMSE		
		BM	*KF*	*GR*	*BM*	*KF*	*GR*
Jul-99							
Region:	0	2.0	0.7	1.8	3.0	2.1	2.8
	1	1.9	-0.2	2.0	2.4	1.7	2.6
	2	4.1	2.2	3.6	4.2	2.4	3.7
	3	-0.4	-1.4	-0.6	0.6	1.6	0.6
	4	0.5	-0.8	0.3	1.8	1.6	1.5
	5	1.2	0.3	0.6	1.7	1.3	1.2
	6	-0.4	-0.9	-0.3	1.3	1.4	1.3

Regionally Averaged Total Precipitation Statistics (mm)

		BIAS			RMSE		
		BM	*KF*	*GR*	*BM*	*KF*	*GR*
Jul-99							
Region:	0	**17.5** $^{KF, GR}$	**27.6** $^{BM, GR}$	**-49.8** $^{BM, KF}$	112.0	72.7	76.2
	1	**-44.2** $^{KF, GR}$	**6.8** $^{BM, GR}$	**-74.6** $^{BM, KF}$	65.1	30.5	80.5
	2	**-34.5** $^{KF, GR}$	**21.1** $^{BM, GR}$	**-32.9** $^{BM, KF}$	38.3	24.5	37.4
	3	**171.3** $^{KF, GR}$	**96.3** $^{BM, GR}$	**-3.5** $^{BM, KF}$	225.5	139.3	71.8
	4	**21.6** $^{KF, GR}$	**48.8** $^{BM, GR}$	**-64.5** $^{BM, KF}$	80.9	59.3	70.6
	5	**-38.8** $^{KF, GR}$	**-5.0** $^{BM, GR}$	**-89.5** $^{BM, KF}$	65.2	67.6	111.0
	6	**169.8** $^{KF, GR}$	**52.5** $^{BM, GR}$	**-15.1** $^{BM, KF}$	200.5	97.3	63.0

Table A.3 Regionally averaged surface climate statistics (RMSE), (BIAS) for NAM subregions. Bold text and (BMJ, KF, GR) superscripts denote simulations in which the differences in the mean bias values are significant at the 95% level.

APPENDIX B.

Hydrometeorological Response of the Modeled North American Monsoon to Convective Parameterization

David J. Gochis[1], W. James Shuttleworth[1,2], Zong-Liang Yang[1]

Submitted to *Journal of Hydrometeorology*, November 15, 2001

[1]Department of Hydrology and Water Resources, University of Arizona, Tucson, AZ 85721, USA
[2]Department of Atmospheric Sciences, University of Arizona, Tucson, AZ 85721, USA

Subject: Re: Permission to use article in Thesis
Date: Mon, 28 Jan 2002 07:57:56 -0500
From: Melissa Weston <mweston@ametsoc.org>
To: Dave Gochis <gochis@hwr.arizona.edu> (by way of Tara Partlow <tpartlow@ametsoc.org>)

Dear Dave:

Through this e-mail, the American Meteorological Society grants you permission to reprint the following articles as described in your request.

Ref: MWR 2337 "Sensitivity of the Modeled North American
Monsoon Regional Climate to Convective Parameterization"
Gochis, Shuttleworth, Yang

Ref: 083-01-JHM " Hydrometeorological Response of the Modeled
North American Monsoon to Convective Parameterization"
Gochis, Shuttleworth, Yang

Full acknowledgments to AMS as the copyright holder and bibliographical details of the publication should be cited.

Best regards,
Melissa Weston

Hydrometeorological Response of the Modeled North American Monsoon to Convective Parameterization

Abstract

The convective parameterization schemes of Betts–Miller–Janjic, Kain–Fritsch and Grell were tested using version 3.4 of the PSU/NCAR MM5 meso–scale model running in a pseudo–climate mode. Model results for the initial phase of the 1999 NAM are compared. Substantial differences in both the stationary and transient components of the moisture flux fields were found between the simulations. Differences in the moisture flux result appear to in differences in moisture convergence patterns, precipitation and surface evapotranspiration. Basin–average calculations of hydrologic variables indicate that in nearly all the basins, the magnitude of the surface moisture source/sink differs substantially between the simulations and, in some cases, the sign of the source/sink changes. Further, there are substantial differences in rainfall–runoff processes as evidenced by basin averaged rainfall intensity, convective fractions and runoff coefficients between simulations. The results indicate that in regions of sustained, deep convection selection of a sub–grid convective parameterization in high–resolution atmospheric models can have hydrometeorological impacts similar or greater in magnitude than those attributed to land–surface forcing on regional analyses.

1. Introduction

This paper represents the second part of a two–part study seeking to document the sensitivity of the simulated North American Monsoon (NAM) circulation to different representations of convection. Impetus for developing and testing seasonal hydrometeorological prediction systems for regions under the NAM system (NAMS) influence is provided by the fact that water resources in many such regions are highly stressed. Contemporary communities in the southwestern U.S. and northern Mexico also directly or indirectly rely on rains attributed to the NAMS for their social well being and economic livelihood. (See, for example: Morehouse et al., 2000; or Liverman, 1996) Seasonal hydrological cycling in the NAM region is critical to plant productivity. For a site in southern Arizona, Scott et al. (2000) showed that while winter precipitation controls woody plant (e.g. mesquite) growth, summer rains drive annual grass production which are critical to the livestock industry. The relative importance of summer precipitation on regional streamflows is evident in Figure B.1 which shows the monthly percentage of mean annual discharge for 7 river systems in the NAM region. (U.S. streamflow data in Figure B.1 comes from the USGS online historic streamflow records; USGS, 2001 and Mexican data comes from the BANDAS archive; BANDAS, 1998) It is clear that summer precipitation generates a greater portion of the annual streamflow than winter precipitation or snowmelt at the lower latitudes of Mexico.

An earlier component of this study (Gochis et al., 2001, hereafter referred to as G1) focused on elucidating the sensitivity of precipitation, column–integrated precipitable

water, surface air and dewpoint temperatures, and atmospheric stability to three different representations of sub–grid convection. The PSU/NCAR MM5 model was run three times in a nested–domain, pseudo–regional climate mode, the only difference between the runs being that the representation of sub–grid convection in the internal, 30 km domain was made using each the Betts–Miller–Janic (BMJ), Kain–Fritsch (KF) and the Grell (GR) schemes, respectively. The main conclusions from G1 were:

- Substantial differences in both the time–integrated thermodynamic and circulation structures of the simulated July 1999 NAM atmosphere evolve when different convective parameterization schemes (CPSs) are used. Markedly different regional circulation patterns evolve, which are revealed in the vertical velocity and low–level divergence fields.
- Differences in the circulation fields contribute to markedly different fields of July average column–integrated precipitable water. Errors in the modeled surface dewpoint temperature field is greater in the northern monsoon regions than in other regions, regardless of the convective scheme used.
- All simulations were capable of reproducing the maximum of precipitation along the western slope of the Sierra Madre Occidental. However, root mean squared errors and model biases in precipitation and surface climate variables were substantial, and showed strong regional dependencies between each of the simulations.

The present study extends the previous research by examining the difference in the hydrological response to the three climate simulations generated by using different CPSs.

Several authors have examined the atmospheric branch of the NAMS using different datasets. Schmitz and Mullen, 1996, Higgins et al., 1997, Berbery, 2001, Anderson and Roads, 2001 and Anderson et al., 2000a, for example, have each undertaken diagnostic moisture flux analyses for the NAM region. Using several years of analyzed or re–analyzed data, each of these studies has incrementally contributed towards increased understanding of the regional moisture flux patterns and moisture budgets that evolve with the NAM circulation. In particular, Schmitz and Mullen (1996), using ECMWF re–analysis data at T106 spectral resolution, showed that moisture flux into the core NAM region of western Mexico and the southwestern U.S. was attributable to low–level stationary components proceeding northward over the Gulf of California (GoC). While the larger scale circulation around the summertime, continental anticyclone over the southeastern U.S. was subsequently responsible for transporting the moisture from mid–tropospheric levels (associated with deep convection over the Sierra Madre Occidental) northward into the southwestern U.S. The transient component of the moisture flux, though comparatively small, comprises a significant portion of the total moisture flux emanating from the northern GoC. Regionalized estimates of moisture convergence also revealed a tendency for land regions to act as moisture sinks, and the open waters of the Gulf of California, the eastern Pacific, and the Gulf of Mexico to act as moisture sources.

Using analyses and short–term forecasts from the operational Eta Data Assimilation System (EDAS) at 40 km resolution, Berbery (2001) also found large and persistent

divergence of moisture over the northern GoC, along with an increased transient moisture flux out of this region. However, there were substantial differences in the direction of the integrated moisture flux over most of the GoC, between the analyses of Schmitz and Mullen (1996) and Berbery (2001). According to Berbery, the differences in the flux fields, are due to differences in the 'mesoscale nature' of the analysis products and are attributable to the higher resolution topography used in the EDAS model. Such mesoscale features appear to be well captured in recent modeling studies by Anderson et al., (2000a, 2000b) who documented the diurnal behavior of the GoC low-level jet as well as the occurrence of gulf surges.

Determining the underlying causes for differences between the above analyses is difficult due to the fact they were made for different time periods, different spatial resolutions and with markedly different modeling systems. In the present study, we seek to isolate one of the potential differences in these and other such comparisons by making identical simulations, apart from the representation of sub-grid convection. One important difference between the work presented here and the earlier studies of Berbery (2001) and Schmitz and Mullen (1996) is that, during the present convective sensitivity study the MM5 model is applied in free-running regional climate mode, as opposed to assimilation mode (Note: see G1 for the working definition of regional climate modeling). In the present simulations, the forcing is provided via lateral boundary conditions and the sea surface temperature field. This allows the model to evolve a climate within the modeled domain that is a non-linear function of the boundary

conditions and model physics parameterizations (Giorgi and Mearns, 1999).

Research focusing hydrological aspects of the NAM, such as runoff and evapotranspiration are few compared to those focusing on precipitation and circulation aspects. Precipitation climatologies using infra–red satellite imagery (Douglas et al., 1993; Negri et al., 1994; and Vazquez, 1999), surface rain gauge networks (e.g. Higgins et al., 1996; Comrie and Glenn, 1998) and, more recently, merged precipitation products (e.g., Xie and Arkin, 1996) have documented the mean annual and mean monthly features of the warm season precipitation regime over North America. It has been shown that the "core" monsoon region, the region which that possesses the strongest monsoon signal, is along the western slope of the Sierra Madre Occidental (Douglas et al., 1993; Higgins et al., 1999) in western Mexico. A principal components analysis of precipitation regimes by Comrie and Glenn (1998) also determined a similar (but larger) region as the leading mode in the southwestern North American precipitation field, while a sub–regional analysis of this same study indicated that the region encompassing the Sierra Madre Occidental in central Mexico possess the strongest monsoon signal. It is in this same region where the largest percentages, in excess of 70%, of the annual average rainfall occur during the warm season months of July, August and September. The temporal structure of convective precipitation remains largely undocumented by ground–based observing networks. Remotely sensed precipitation products reveal a diurnal cycle of convection which possesses a strong maximum in the evening and a minimum near local sunrise. (Negri et al., 1994; Vazquez, 1999) Definitive verification of the intensity

and duration of convective precipitation over the core monsoon region, currently awaits the implementation of an enhanced surface observing network such as that proposed by Shuttleworth et al. (2001) under the auspices of the North American Monsoon Experiment. (NAME. 2002)

As part of a global streamflow analysis, Dettinger and Diaz (2000) estimated that the NAM region has among the highest variability in both precipitation and streamflow in the world. They found that the peak in runoff over the NAM region occurred during the months of September and October and possessed a time lag of approximately two months behind the seasonal precipitation maximum. In excess of 50% of the annual streamflow occurred during the peak month in the core monsoon region while peripheral regions showed progressively less of a monsoon signal. Runoff per unit area values were small compared to other regions around the world, on the order of a few tens of millimeters per year, exemplifying significant losses of precipitation to either evaporation or deep percolation. Correspondingly, runoff efficiency values, defined as streamflow divided by precipitation, in the core NAM region ranged between 20% and 50%. It was also found that interannual variation in annual streamflow exceeds the variation in annual precipitation over much of the NAM region by factors of eight or more. Reasons for this were not given in detail but highlight the non–linear relationship between precipitation and runoff.

As previously stated, this study extends G1 by focusing on the impact of differences in

simulated regional circulation on fields of hydrologic importance. In particular, we examine how changes in the regional moisture transport affect moisture convergence patterns, net surface moisture flux, precipitation characteristics, and surface runoff. The structure of the paper is as follows; Section 2 overviews model setup and describes the analysis methods used. Section 3 gives the results, which are then discussed in section 4. Section 5 provides concluding remarks.

2. Model and Analysis Methods

2.1 Model Setup

A brief synopsis of the model setup is provided below but the reader is referred to G1 for greater details. We made three very similar simulations using the PSU/NCAR MM5 mesoscale model version 3.4 (Grell et al., 1994). Each simulation had a two-domain configuration: the coarse domain resolution was 90 km and the fine domain resolution was 30 km (see Figure 1 in G1). The model was integrated from 00Z May 16 through 00Z August 2nd 1999 with lateral boundary conditions on the coarse domain provided by 6-hr analyses taken from the NCEP/NCAR re-analysis dataset (Kalnay et al., 1996). In all three simulations, subgrid convection on the coarse model domain was represented using the Betts-Miller-Janic CPS. Thus, the only difference between the three simulations was the representation of subgrid convection on the internal, 30 km domain where each the Betts-Miller-Janjic (Betts 1986; Betts and Miller, 1986; Janjic, 1994), Kain-Fritsch (Kain and Fritsch, 1990) and Grell (1993; Grell et al., 1994) CPSs, respectively.

In this study the land surface parameterization (LSP) used in the MM5 modeling system is of critical importance because it represents the hydrologic and energy exchange processes at the land–atmosphere interface. The LSP used in the simulations was the OSU/NCEP land surface scheme, adapted for application within MM5. Details of the LSP (e.g. the way it calculates evaptranspiration, soil moisture flux, and surface runoff generation) are given in Chen and Dudhia (2001a, 2001b) along with verification analyses. Readers are referred to these papers for a detailed description. Where essential, brief descriptions of specific processes are included.

2.2 Hydrometeorological Analyses

In G1, a suite of analysis products were presented that compared several different simulated surface and tropospheric variables with observations. Such comparisons established relative model error with respect to observations and elucidated differences in state variables and accumulated precipitation values between models. Here we present a suite of hydrometeorologically focused analyses that explore how differences in the summertime circulation pattern with alternative convective representations alter the surface hydrologic response.

A primary difference between this study and G1 is that analyses here are performed over macroscale hydrologic basins as defined by the USGS 1:250k hydrologic unit coverages (HUC) for North America (USGS, 2001). This basin definition was regridded to 30 km

resolution and reprojected to the Lambert–Conformal coordinate grid to match the model grid used in the MM5 simulations. Figure 2 shows the six Level 2 basins used in this study. All basin–relevant statistical calculations were performed within the ARC/INFO Geographical Information System (ESRI, 2000). The basins selected (Figure 2), namely the Colorado, Rio Bravo (Rio Grande), Sierra Madre Occidental (SMO), Aguanaval, and Lerma–Santiago (L–S), represent major hydrologic regions which are under the influence of the NAM. The box shown in Figure 2 delineates the MM5 internal (30 km) domain. All basin–average quantities, including derived quantities such as the convective fraction and the runoff coefficient, are calculated first for each grid cell and then spatially averaged.

The northern portion of the Colorado River basin lies outside of the MM5 model domain (Figure 2). Omission of part of this basin will clearly affect any comparison between basin–averaged calculations and observations but it does not greatly affect the results of the present sensitivity study. It is also worth noting that the Sierra Madre Occidental basin does not represent a single watershed *per se*, but rather an amalgamation of several basins along the crest of the Sierra Madre cordillera.

2.2a Precipitable Water

The precipitable water (PW) analyses given in G1 were extended in the present study to include the change in PW content from June to July of 1999. In 1999, the onset of the monsoon occurred on June 26th in Tucson, AZ (according to the National Weather

Service, Tucson, AZ; NWS, 2002). Consequently, June and July results roughly correspond to pre– and post–onset values over most of the northern NAM region.

2.2b Vertically Integrated Moisture Flux

Total column integrated moisture flux $\vec{q}$ can be calculated (Piexoto and Oort, 1992) from:

$$\vec{q}=\frac{1}{g}\int q\vec{v}\,dp \qquad (1)$$

where q is specific humidity, $\vec{v}$ is the horizontal wind vector, g is gravity, dp is a pressure layer and bounds on the integrals can be changed to limit the integration to specific levels in the atmosphere. In this study, we chose the limits to be between the land surface and the top model layer so the value represents the total modeled column integrated moisture flux. Following Rasmussen (1967), the total water vapor flux at a given level can be partitioned into its time–mean and transient components by:

$$\overline{q\vec{v}}=\overline{q}\,\overline{\vec{v}}+\overline{q'\vec{v}'} \qquad (2a)$$

which, using Eq. 1 has the form:

$$\vec{q}=\frac{1}{g}\left(\int \overline{q}\,\overline{\vec{v}}\,dp+\int \overline{q'\vec{v}'}\,dp\right) \qquad (2b)$$

The left hand side of Eq. (2b) is the total mean moisture flux, the first term on the right hand side is the stationary, time–average component while the second term is the component due to transient eddies. In Section 3.3, both the stationary and transient components of the integrated moisture flux for each convective scheme are compared.

2.2c Precipitation Characteristics

In G1, it was shown that there were marked differences in monthly total rainfall between the simulations with the three different CPSs. Here, differences in precipitation are further examined by partitioning the total monthly precipitation into its convective and non–convective components. The convective portion is that which is calculated when the respective CPS is triggered due to environmental conditions. (An overview of each parameterization was provided in G1 and interested readers are referred to G1 and the original references listed in Section 2.1 for details.) Non–convective precipitation occurs when gridpoint saturation occurs within the model (Grell 1994). The micro–physical parameterization of Dudhia (1989) was used to implicitly simulate sub–grid microphysical processes occurring within grid–resolved clouds. The relative contribution of convective and non–convective processes to precipitation for a watershed can be assessed from these components using the convective fraction (CFX), which is calculated here by:

$$CFX = \frac{rc}{(rc + rn + \varepsilon)} \qquad (4)$$

where, rc and rn are the monthly total convective and non–convective rainfall amounts, respectively, and ε (=0.001) is a term that ensures that Eq. (4) is defined when there is no rainfall.

The core region of the NAM is characterized by a subject strong diurnal variation in precipitation (Douglas 1995, Negri 1994, Berbery 2001). In this study, the impact of CPSs on the diurnal cycle of precipitation was examined by calculating the monthly–mean precipitation intensity at each gridpoint at three–hour intervals (i.e. at 00, 03, 06, ... 21UTC), and then importing the values into ARC/INFO to calculate the basin–average intensity.

2.2d Surface Runoff

Surface runoff is calculated by the land surface model in the MM5 modeling system. The formulation adopted by Chen and Dudhia (2001a) is the Simple Water Budget method, first proposed by Schaake (1996). In the LSP, surface runoff is the portion of precipitation reaching the ground surface, that falls at a rate in excess of the maximum infiltration rate (I_{max}) for the soil (i.e. *Hortonian* runoff). I_{max} is not a static value, but is a function of the saturated hydraulic conductivity (K_{sat}) of the soil and the available infiltration capacity and is given by:

$$I_{max} = MIN(I'_{max}, K_{sat}) \qquad (5)$$

where, I'_{max} in Eq. 5 is the maximum rate of infiltration that can occur on a model time step which depletes all of the available storage capacity. Thus, infiltration is a function of soil type through K_{sat} and the soil's saturated volumetric water content. Infiltration is also a function of the time evolving soil moisture content such that as the soil becomes

saturated, excess precipitation is converted into runoff as opposed to infiltrating. (Note: Interested readers should refer to Schaake et al. (1996) for details of the model infiltration parameterization.)

The relationship between precipitation and runoff was explored by estimating the runoff coefficient (QFX) which is the portion of total precipitation which ultimately becomes surface runoff and is calculated by:

$$QFX = \frac{Q}{P} \qquad (6)$$

where, Q is the surface runoff calculated by the LSP for each grid cell and P is the total precipitation for each grid cell which is the sum of the convective and non-convective portions of precipitation.

3. Results

3.1 Precipitable Water

In G1, it was suggested that differences in the modeled low-level wind fields over western Mexico and the Gulf of California were largely responsible for the differences in the July 1999 mean column-integrated precipitable water (PW) fields (see: Figure 3 from G1). This hypothesis is explored further by examining the elements of the atmospheric water balance, specifically the modeled evolution of precipitable water, surface inputs, as well as the decomposed moisture flux. Figures 3a, 3c and 3e show the

change in PW content from July 1 to August 1 for the BMJ, KF and GR simulations, respectively. All three of the simulations show similar mean PW fields for June 1999 (not shown) indicating that the differences in the mean fields for July are largely due to processes that occur in July when regional convection is a dominant feature. As discussed in G1, integrated moisture is generally about 5–10 mm greater for interior regions in the simulation made with the KF scheme than those made with the BMJ and the GR schemes. In particular, simulations with the BMJ and GR schemes both result in lower PW values across the northern regions of the NAM, in Arizona and New Mexico, and drier interior regions in central Mexico and southern Texas when compared to the KF simulation.

The change in PW in July (Figures 3a, 3c and 3e), reveals a widespread moistening of the atmosphere in the eastern Pacific region in all three simulations. However, there are large differences between the simulations in the Gulf of California region and over surrounding land areas. The KF simulation shows the most dramatic moistening, with increases of PW of over 25 mm in the east central Gulf of California. Widespread increases in PW (over 10 mm) extend over much of Arizona and the western portion of New Mexico, while more moderate increases, between 5–10 mm, are found over the central Mexican plateau. The simulation with the BMJ scheme, although producing fairly similar spatial distributions of PW, calculates increases that are generally about 5 mm less than with the KF scheme, except in eastern portions of the interior domain. The simulation using the GR scheme exhibits the smallest change in PW. With the GR

scheme, PW changes in excess of 15 mm are limited to regions south of the U.S.–Mexican boarder, mainly west of the Sierra Madre Occidental in western Mexico.

Basin average changes in PW ($dPW=PW_{Jul\ 31} - PW_{Jul\ 1}$) for July 1999 are given in Table 1. The KF scheme gives the most atmospheric moistening for all basins except for the Lerma–Santiago (L–S) in southern Mexico. Inter–simulation differences in dPW in excess of 50% occur within the Colorado, Rio Bravo, Aguanaval and L–S basins. Basin–average increases in dPW are lowest for the simulation with the GR scheme for all basins except the L–S.

3.2 Regional Source/Sink Analyses

Figures 3b, d, f show the average value of E–P for July 1999. In general the surface tends to act as a sink of moisture over the high rainfall areas of the SMO and across much of southern Mexico in all simulations. However, in some regions there are distinct differences in the magnitudes of the sink between the simulations. For example, in the simulation with the BMJ scheme there is a very large sink (corresponding to heavy rainfall) over the SMO. In G1, it was noted that the BMJ and, to a lesser degree, the KF simulations both overestimate rainfall relative to observations in this region and also in far southern Mexico. The wider spatial extent of rainfall given in the KF simulation results in more widespread surface sink values in compared with the BMJ and GR simulations. The differences sometimes have opposite sign, notably in the case of the GR simulation in the southwest U.S. and central Mexico. Conversely, while all three

simulations calculate positive (source) estimates over the Gulf of California, the GR simulation locates the strongest source signal there. This is likely because the simulation with the GR scheme calculates lower atmospheric humidity levels in the northern Gulf of California.

There are also changes in sign in the basin–average values of surface moisture source/sink given in Table 1. The KF simulation calculates a negative value (sink) for all the basin–average estimates while the BMJ simulation only calculates a source (positive) for the Rio Bravo Basin. However, the GR simulation simulates the inland basins of the Colorado, Rio Bravo, and the Aguanaval as sources for atmospheric moisture. The sign of the source–sink is the same for the SMO and L–S basins in all simulations, but there are large differences in magnitudes which highlight the sensitivity of simulated land–surface hydrologic exchanges to convective parameterization.

3.3 Moisture Flux Components

To better explain the differing evolutions of the PW field, the decomposed moisture fluxes were examined. Stationary and transient eddy, vertically integrated moisture flux fields are shown in Figure 4. The stationary component (BMJ–4a, KF–4c, GR–4e) indicates that the dominant feature is the Great Plains low level jet in this region in all three simulations. Moisture flux values are on the order of 300 kg–m s^{-1}. Moisture fluxes over the central Mexican plateau have a westward component and are typically less than 90 kg–m s^{-1}, indicating that comparatively small component of the moisture

flux emanating from the Gulf of Mexico crossed the plateau during July 1999. (Note: This has also been found in the recent analyses by Berbery, 2001, Anderson and Rhodes, 2001, and is implied in Stensrud et al., 1995.) The largest differences between simulations occur along the coast of western Mexico. Both the KF and the BMJ simulations yield southeasterly fluxes up the axis of the Gulf of California that originate well south of the mouth of the Gulf. This result compares well with field measurements taken during the Southwest Area Monsoon Project in 1990 (Douglas, 1995) and the modeling study by Anderson et al. (2000b). These flux field points northward into the low deserts of Arizona and northwestern Mexico. However, the simulation using the GR scheme produces a markedly different flux field in this region, in which moisture is transported with a much stronger westward component towards the Pacific Ocean from the west coast of Mexico. When the integrated flux was separated into low-level (surface–700mb) and upper-level (700mb–400mb) components (not shown), it was found that most of the northward component of the integrated flux over the Gulf of California was at low levels while the much of westward component was at high levels. In the GR simulation mean fluxes across the Gulf of California are quite small and show little directional coherence. [Note: taking monthly average moisture flux fields may mask some of the true behavior in this region because of diurnal variability (Berbery, 2001)].

As found in the short climatology of Berbery (2001), transient moisture flux fields (BMJ–3b, KF–3d, GR–3f) are generally a full order of magnitude less than their

stationary counterparts in most regions. However, this is not the case over the Gulf of California and the eastern Pacific. In eastern Pacific region the transient flux is an important portion of the total flux regardless of the CPS used. However, notable differences in the modeled transient flux fields are found due to differences in the way transient features are represented. In this region, tropical storms, easterly propagating waves, and, to a lesser degree, mid–latitude shortwaves all likely contribute to the mean transient flux (Schmitz and Mullen, 1996, Anderson et al., 2000a), and the differing simulations reflect differences in the representation of such features with alternative convective schemes. Over the Gulf of California, the direction of the transient flux component is northwest in all three schemes, indicating that transient features tend to advect moisture away from the core monsoon region over the Sierra Madre Occidental. Transient fluxes are negligible across most of central Mexico with all convective schemes, and have a northeastward component out of northeastern Mexico, indicating that it is unlikely significant moisture is transported westward by transients from the Gulf of Mexico into the core monsoon region. However, in all the simulations, especially in the KF simulation, transient moisture fluxes over Arizona have a marked westward component from New Mexico suggesting transient activity may transport moisture into Arizona which possibly originates from the Gulf of Mexico. Further analyses that include diagnostic or prognostic tracer routines are needed to test this hypothesis.

3.4 Precipitation Characteristics

July total precipitation and the July convective fraction (*CFX*) are shown in Figures 5a–f. Regional and sub–regional errors in the total precipitation fields were discussed at length in G1. Here we focus on regional dependency of the convective fraction to investigate where and to what extent convective processes participate in the generation of modeled precipitation. From Figures 5b. d. f. it is evident that convective processes are influential in modeled precipitation across much of the domain in all of the simulations. However. there are marked sub–regional differences which potentially have important consequences for hydrologic response.

Basin–average values of total. convective and non–convective precipitation and *CFX* are given in Table 2. Over the Colorado River basin *CFX* ranges from 0.53 for the BMJ simulation to 0.82 for the GR simulation. Although generating the highest convective fraction use of the GR scheme gives the lowest total precipitation (both convective and non–convective) on a basin–average basis. 10% of that simulated by KF and less than 20% of that simulated by BMJ. The marked underestimation of precipitation by both the GR and BMJ schemes was noted in G1. The very low convective rainfall. indicates that the GR convective scheme is not being triggered as frequently as either the BMJ or KF scheme in this northernmost region. Similar behavior is observed over the Rio Bravo basin. although the KF scheme produced much more convective and hence total precipitation than either BMJ or GR.

In the core monsoon region (the SMO) large quantities of basin–average convective

precipitation occurred in all schemes. As noted in G1, both the BMJ and KF schemes overestimated precipitation in this region compared with observations, while the GR scheme only shows a modest underestimation. It is interesting to note that the spatial gradients in total precipitation along the high topography of the SMO are quite large when the BMJ and GR schemes are used but are less when the KF scheme is used. This feature is likely to have an important effect on basin–averaged rainfall–runoff processes, as discussed later. In general, convective fraction is quite high throughout the SMO basin indicating frequent and sustained convective activity for the KF and BMJ schemes, while the GR scheme generates decreasing values of *CFX* proceeding southward along the coast (Figure 5f).

The GR simulation (Figure 5f) shows comparatively low values of *CFX* over much of southern Mexico, and this contributes to the low basin–average value (0.53) for the L–S basin. Non–convective precipitation over the L–S basin is higher when using the GR scheme, while the BMJ and, to a lesser degree, the KF schemes maintain comparatively high values of *CFX* across southern and south–central Mexico. Although using the KF scheme generates the most precipitation and highest value of *CFX* in the Aguanaval basin, using the BMJ scheme generates the highest basin–averaged values in the L–S basin. This points to a tendency for the GR scheme to allow more resolved precipitation than the other two parameterizations.

In summary, use of the KF scheme generates the most widespread rainfall, most of which

is convective in nature. When active, the BMJ scheme tends to produce excessive amounts of convective rainfall compared to the other schemes (and compared to observations, as detailed in G1), while very little non–convective rainfall is generated by this scheme. The GR simulation produces comparatively less precipitation in the northern and inland regions of the NAMS. Although the modeled convective fraction given by the GR scheme may be high in these regions this scheme does not generate sufficient basin–average convective rainfall when compared to other schemes and observations. In regions where substantial precipitation is generated by using the GR scheme there is a concomitant increase in non–convective precipitation indicating that these environments are persistently moist and are likely regions with enough moisture convergence to support both convective and non–convective precipitation.

The diurnal cycle of basin–average total precipitation intensity from each simulation is shown in Fig. 6. Some of the basin–to–basin differences in peak intensity times may be related to differences in local solar time though these differences would be only on the order of one hour. There are several features that indicate a clear sensitivity of the timing and intensity to convective parameterization. The northernmost basins, the Colorado and Rio Bravo rivers, and the inland basin of the Agaunaval, all show a depressed diurnal cycles relative to that of the SMO and L–S basins. Table 3 shows that using the KF CPS generates the highest mean intensity and the maximum rainfall intensity in northern and inland regions. Because convective rainfall in these northern regions is substantially greater than non–convective rainfall, this supports the hypothesis

(posed in G1) that the KF scheme triggers more frequently than the BMJ or GR schemes. Similarly, in all regions, the KF simulation generates rainfall earlier in the day, indicating that its convective trigger is activated at a comparatively lower threshold.

In the core region of the monsoon (the SMO) and the L–S basin, there are marked increases in modeled precipitation intensity during afternoon hours with all the schemes. In each region, peak intensity occurs 3–6 hours earlier in KF than it is in either BMJ or GR. Although the KF simulation generates intense precipitation earlier in the day than the other two schemes, the BMJ scheme generates the highest intensity, 0.60 and 0.66 mm/hr for the SMO and L–S basins, respectively. This again supports the hypothesis that the BMJ scheme tends to markedly overpredict rainfall in these regions.

The diurnal cycle with the GR scheme is notably depressed in amplitude compared with that of KF or BMJ schemes. Maximum intensities are approximately 30% of those for the KF and BM simulations in the river basins most affected by the monsoon (SMO and L–S). This is the result of two factors. First, a larger portion of the precipitation falling in these basins is non–convective, as described above. Convective fractions for the SMO and L–S basins when using the GR CPS were 0.83 and 0.53, respectively compared to 0.86 and 0.84, respectively for the KF CPS and 0.92 and 0.97, respectively for the BMJ CPS. Second, the strong spatial gradients in total precipitation calculated with the GR scheme when compared to the KF scheme means that in basin–average calculations, regions with widespread areas of low precipitation will significantly smooth the

maximum precipitation intensity signal which is localized along the western slope of the SMO. Similar compensation likely occurs in the case of the BMJ simulation, but the extreme magnitudes of SMO rainfall in the BMJ simulation dominate the basin–average values. Differing characteristics in precipitation amounts, timing and intensities impact the generation of runoff from these basins, as discussed below.

While basin–average calculations are informative in defining the sensitivity of the regional hydroclimatology to model parameterization, aspects of the hydrologic cycle may not be adequately captured due to the spatial averaging procedure. As shown in the next section, the spatial gradients in precipitation have an important influence on basin–average statistics and runoff generation processes. These are masked when precipitation amount and intensity are averaged across sufficiently large regions. Temporal averaging also smoothes precipitation intensity values. None of the rainfall intensities given in Figure 6 and in Table 3 are, for instance, likely to generate appreciable amounts of surface runoff. These problems are at the core of hydrologic scaling issues, as discussed theoretically by Wood et al. (1988), and are the subject of ongoing research.

3.5 Surface Runoff

Basin–average and maximum total precipitation and surface runoff are tabulated in Table 4, along with basin–average values of the runoff coefficient, *QFX*. Values of *QFX* are quite low (1%–3%) for all schemes and in all basins, except for the SMO indicating that, as a spatial average, precipitation rate rarely exceeds the local infiltration rate. However,

on a local (or gridpoint) basis, this may not be the case. The simulation with the BMJ scheme generates the highest runoff coefficients in the Rio Bravo and Aguanaval basins, and matches *QFX* values for the KF and GR schemes in the Colorado and L–S basins, respectively. On the other hand, the GR scheme generates the highest values of runoff in the SMO. Combining all basins, using the BMJ scheme gives the highest average surface runoff coefficient (0.03), followed by the GR scheme (0.02), and the KF scheme having the lowest value (0.01). These relative rankings are perplexing at first sight due to the fact that the BMJ and KF schemes generate substantially greater basin–average peak precipitation intensity than the GR scheme. In terms of total surface runoff, the BMJ scheme yields the most runoff in the Colorado, SMO, Aguanaval, and the L–S basins, while the KF simulation produces the greatest surface runoff in the Rio Bravo. Additionally, GR scheme produces more runoff in the SMO and L–S basins than the KF scheme but less total and less convective rainfall. These results are counterintuitive as one might expect the greatest runoff to be generated from those basins with the greatest basin–averaged precipitation or the highest basin–averaged rainfall intensity.

To examine this issue further, consider the spatial patterns of runoff in Figures 7a, c, e and *QFX* in Figures 7b, d, f. Consistent with surface runoff values in Table 4, local surface runoff with the KF scheme is shown to be much less than with either the BMJ or GR schemes in the core monsoon region (the SMO). This is interesting because the KF scheme produces not only more total and convective basin–averaged rainfall than the GR scheme but it also exhibits a markedly higher basin–average rainfall intensity as shown

in Figure 6. However, surface runoff is generated in the model only when the local rainfall rate exceeds the local maximum infiltration rate, and the GR simulation has locally greater precipitation which is falling at very high rates compared to the KF simulation. This feature is evident along the southern coast of Mexico as well as along the SMO.

There is evidence of this in Table 4. In every basin the BMJ scheme yields the highest maximum values of both precipitation and surface runoff. As suggested in Section 3.5 and G1, when the BMJ scheme does generate convective rainfall it does so at rates well in excess of observations and the other two schemes. Much of the precipitation given by the BMJ scheme also falls at comparatively intense rates, as suggested by the intensity plots for the SMO and L–S basins (Figure 6). In other basins with the BMJ scheme, the basin– average rainfall intensity and basin–average total precipitation are moderated by the spatial averaging process by including large regions with no rainfall. Although the GR scheme produces greater maximum rainfall in the SMO basin than the KF scheme, the difference in surface runoff is not proportional. Similarly, more surface runoff is produced in the L–S basin with the GR scheme than the KF scheme, even though the local maximum precipitation is lower.

All of the above features draw attention to the fact that the generation of surface runoff is more closely correlated to discrete precipitation events of substantial intensity than to total monthly precipitation or the monthly mean precipitation intensity at a particular

time on the diurnal cycle. To illustrate this point, consider the cumulative mass curves for the two gridcells with the largest surface runoff in the SMO basin from the KF and GR simulations (Figures 8a, b, respectively). (Note: These are not at the same location in the two simulations and with the KF scheme the location with the maximum surface runoff is not where monthly total maximum precipitation occurs, as it does in the GR scheme.) In Figure 8, in both cases large increases in surface runoff are correlated with large precipitation events. In the case of the GR simulation (Figure 8a) there are three large events, each lasting more than 3 hours with local rainfall rates greater than or equal to 15 mm/hr, and several other smaller events of shorter duration but near equal intensity which also contributed to the cumulative surface runoff. In the simulation with the KF scheme (Figure 8b), while there is an equally persistent occurrence of precipitation, at this location, only one event had sufficiently intense precipitation (~13 mm/hr) to generate surface runoff. This example illustrates the general point that local precipitation intensity in discrete storms plays a more important role in the generation of local (and subsequently basin–average) surface runoff than does basin–average accumulations or basin–average rainfall intensity.

4. Discussion and Conclusions

This study extends the sensitivity analyses in G1 to investigate regional and sub–regional sensitivities of hydrometeorological and hydrological responses to the convective parameterization used in a regional climate simulation of the North American Monsoon. The main conclusions from this study can be summarized as follows:

- Differing evolutions of the July precipitable water fields between model simulations are associated with differences in both the column–integrated moisture flux fields and the strength of the surface source or sink.
- There are substantial differences in the magnitude of the surface source or sink between simulations in specific basins. In some cases, the sign of the source/sink is reversed. Because the KF scheme generates extensive rainfall coverage, it consistently predicts a surface sink of moisture in all regions. Conversely use of the GR scheme results in a basin–averaged moisture source for all the basins except the SMO and the L–S.
- The simulations give markedly different patterns in terms of convective and non–convective precipitation components.
- As suggested in G1, the KF scheme produces more widespread convective rainfall than do the BMJ or GR schemes the latter two giving precipitation which is largely locked to the topography of the SMO and into southern Mexico. When triggered, the BMJ scheme produces comparatively high rates of convective rainfall while producing comparatively low amounts of non–convective precipitation. The GR scheme consistently produces the lowest amount of convective precipitation of the three CPSs.
- The KF scheme yields the highest basin–average rainfall intensity in the northern and inland basins of the Colorado, Rio Bravo and the Aguanaval, while the BMJ scheme produces the highest basin average values for the SMO and the L–S. The GR scheme shows a suppressed diurnal cycle of basin–average precipitation intensity compared to the other two CPSs, due, in part, to strong spatial gradients in precipitation resulting

in extensive regions with low precipitation.

- There are large differences in the monthly–total surface runoff between simulations that appear to be more closely related to differences in local. precipitation intensity than to time–average or basin–average intensity. With all schemes the generation of surface runoff is more dependent on local precipitation rates in individual events than on monthly total basin–averaged precipitation .

This study shows that regional climate sensitivity induced by convective representation propagates through the hydrologic system in both intuitive and counter–intuitive ways. The strong dependence of the modeled regional climate on the convective parameterization used complicates hydrological analysis and prediction based on data sets generated by atmospheric models and it hampers understanding of the role of land–surface feedbacks within the regional climate system during the NAM. The sensitivity found in this study is greater than that found in a similar study by Small (2001) which investigated the effect of artificial soil moisture anomalies on tropospheric ridge structure and regional precipitation patterns during the NAM. Small reported changes in regional precipitation patterns on the order of 20%. but differences in precipitation in the present study vary by up to several hundred percent in some basins. Because land–surface forcing can affect the triggering of convective events through partitioning of the surface energy balance it is likely that the results of land–surface sensitivity studies will be strongly influenced by selection of the CPS used in the model.

Based on the results of this study and of G1, it is apparent that hydrometeorological analyses with similar physically–based models will have substantial uncertainty associated with the representation of sub–grid convective processes. This uncertainty extends to not only to the total precipitation generated by the model but also to the magnitude and distribution of latent heating generated by the moist convection itself an important influence on the regional circulation (Barlow et al., 1998). The character of the precipitation, its convective apportionment, its frequency of occurrence, and, of particular importance to hydrological investigations, the intensity of individual storms events will also be in question.

A major shortcoming of the present study is that no calibration of the parameters in the CPSs or in the LSP was attempted. Several major obstacles inhibit the task of model calibration, and some pertaining to CPSs were discussed in G1. With regard to the LSP, calibration studies could be conducted to determine more appropriate values for parameters, such as those involved in the computation of soil infiltration capacity, but extensive surface data are required, which is currently lacking over much of the NAM domain.

Notwithstanding these shortcomings, it is clear from the present study that hydrological fluxes in the semi–arid region of the NAM show marked seasonality, with activity highest during the summer months of June–September increasing southwards into Mexico. The climatic variations and their hydrologic responses, that generate floods and

challenge water resource managers in the region of southwest North America, are not well understood due to the lack of a sufficiently dense, long–term instrumentation network in this sparsely populated region (Magana and Conde, 2000). Lack of high quality data also complicates the problem of model assessment, verification, and calibration. Hence, while models can currently estimate the range of hydrological responses to variability in the NAM climate, increased understanding through quantitative assessment, and increased predictability awaits implementation of an enhanced regional observation network such as that proposed for the North American Monsoon Experiment (NAME, 2001).

Acknowledgments

Primary support for this study was received from NASA grant NAG5–7554. Special thanks go to Dr. Robert A. Maddox and Prof. Steven Mullen whose critical evaluation of this work greatly improved its quality.

REFERENCES

Anderson B.T., Roads J.O., 2001: Summertime moisture divergence over The southwestern US and northwestern Mexico. *Geophys. Res. Let.*, 28 (10), 1973–1976. MAY 15, 2001.

Anderson B.T., Roads J.O., Chen S.C., 2000a: Large–scale forcing of summertime monsoon surges over the Gulf of California and the southwestern United States *J. Geophys. Res.*, 105 (D19), 24455–24467.

Anderson, B.T., J.O. Roads, S–C. Chen, and H–M. Juang, 2000b: Regional simulation of the low–level monsoon winds over the Gulf of California and southwestern United States. *J. Geophys. Res.*, 105(D14), 17955–17969.

BANDAS, 1998: CDROM–Bancos Nacional de Datos de Aguas Superficiales. Comission Nacional del Agua (can) y Instituto Mexicano de Tecnologia del Agua (IMTA).

Barlow, M., S. Nigam and E.H. Berbery, 1998: Evolution of the North American Monsoon system. *J. Climate*, 11, 2238–2257.

Berbery, E.H., 2001: Mesoscale Moisture Analysis of the North American Monsoon.

Journal of Climate., Vol. 14, No. 2, 121–137.

Betts, A.K., 1986: A new convective adjustment scheme. part I: observational and theoretical basis. *Q.J.R. Met. Soc.*, 112, 677–691.

Betts, A.K. and M.J. Miller, 1986: A new convective adjustment scheme. part II: single column tests using GATE wave, BOMEX, ATEX and arctic air–mass data sets. *Q.J.R. Met. Soc.*, 112, 693–709.

Chen F. and Dudhia J., 2001a: Coupling an advanced land surface–hydrology model with the Penn State–NCAR MM5 modeling system. Part I: Model implementation and sensitivity. *Mon. Wea. Rev.*, 129(4), 569–585.

Chen F. Dudhia J., 2001b: Coupling an advanced land surface–hydrology model with the Penn State–NCAR MM5 modeling system. Part II: Preliminary model validation. *Mon. Wea. Rev.*, 129 (4), 587–604.

Copeland, J.H., R.A. Pielke, and T.G.F Kittel, 1996: Potential climatic impacts of vegetation change: a regional modeling study. *J. Geophys. Res.*, 101, 7409–7418.

ESRI, 2000: ARC/INFO version 8.0. Environmental Systems Research Institute, Incorporated.

Douglas, M.W., 1995: The summertime low–level jet over the Gulf of California. *Mon. Wea. Rev.* 123, 2334–2347.

Giorgi, F. and L.O. Mearns, 1999: Introduction to special section: regional climate modeling revisited. *J. Geophys. Res.* 104(D6), 6335–6352.

Gochis, D.J., Z–L. Yang, W.J. Shuttleworth, 2001: Sensitivity of the modeled North American Monsoon regional climate to convective parameterization. Accepted: *Mon. Wea. Review.*

Grell, G.A., 1993: Prognostic evaluation of assumptions used by cumulus parameterizations. *Mon. Wea. Rev.*, 121, 764–787.

Grell, G.A., J. Dudhia, and D.R. Stauffer, 1994: A description of the fifth generation Penn State/NCAR mesoscale model (MM5). NCAR Tech. Note NCAR/TN–380+STR, 138 p.

Higgins, R. W., J. E. Janowiak, and Y. Yao, 1996: A Gridded Hourly Precipitation Data Base for the United States (1963–1993). NCEP/Climate Prediction Center Atlas 1, 47 pp.

Higgins, R.W., Y. Yao, and X–L. Wang, 1997: Influence of the North American Monsoon system on the U.S. summer precipitation regime. *J. Climate*, 10, 2600–2622.

Janjic, Z.I., 1994: The step–mountain eta coordinate model: further developments of the convection, viscous sublayer, and turbulence closure schemes. *Mon. Wea. Rev.*, 122, 927–945.

Kain, J.S. and M. Fritsch, 1990: A one–dimensional entraining/detraining plume model and its application in convective parameterization. *J. Atmo. Sci.*, 47, 2784–2802.

Kalnay and Coauthors, 1996: The NCEP/NCAR reanalysis project. *Bull. Am. Met. Soc.*, 77, 437–471.

Magana, V.O. and C. Conde, 2000: Climate and freshwater resources in northern Mexico: Sonora, a case study. *Environmental Monitoring and Assessment*, 61(1), 167–185.

Morehouse, B.J., R.H. Carter and T.W. Sprouse, 2000: The implications of sustained drought for transboundary water management in Nogales, Arizona and Nogales, Sonora. *Nat. Res. Journal.*, 40, 783–817.

NAME, cited–2001: North American Monsoon Experiment Science Plan. [Available online: http://vao.wwb.noaa.gov/monsoon/NAME.html].

Negri, A.J., R.F. Adler, E.J. Nelkin and G.J. Huffman, 1994: Regional rainfall climatologies derived from special sensor microwave imager (SSM/I) data. *Bull. Am. Met. Soc.*, 75, 1165–1182.

(NWS) National Weather Service, Tucson Weather Forecast Office Website, cited–March, 2002. [Available online: http://www.wrh.noaa.gov/tucson/monsoon/monsoon_stats.html].

Peixoto, J.P. and A.H. Oort, 1992: Physics of Climate. American Institute of Physics, 520 pages.

Rasmusson, E.M.: Atmospheric water vapor transport and the water balance of North America, 1. Characteristics of the water vapor flux field. *Mon. Wea. Rev.*, 95, 403–426.

Schaake J.C., V.I. Koren, Q.Y. Duan, K. Mitchell, and F. Chen, 1996: Simple water balance model for estimating runoff at different spatial and temporal scales. *J. Geophys. Res.* 101 (D3), 7461–7475.

Schmitz, J.T. and S.L. Mullen, 1996: Water vapor transport associated with the summertime North American Monsoon as depicted by ECMWF analyses. *J. Climate*, 9, 1621–1634.

Small, E.E., 2001: The influence of soil moisture anomalies on variability of the North American monsoon system. *Geophys. Res. Let.*, 28(1), 139–142.

Stensrud, D.J., R.L. Gall, S.L. Mullen and K.W. Howard, 1995: Model climatology of the Mexican Monsoon. *J. Climate*, 8, 1775–1794.

USGS, cited–2001: Digital coverage archive [Available online: http://water.usgs.gov/GIS/metadata/usgswrd/huc250k.html].

Vazquez, M.C., 1999: Marcha annual de la actividad convectiva en Mexico. *Atmosfera*, 12, 101–110.

Wood, E.F. M. Sivapalan, K. Beven and L. Band, 1988: Effects of spatial variability and scale with implications to hydrologic modeling. *J. Hydrology*, 102, 29–47.

Xie, P. and P. Arkin, 1996: Analysis of global monthly precipitation using gage observations, satellite estimates, and numerical model predictions. *J. Climate*, 9, 840–858.

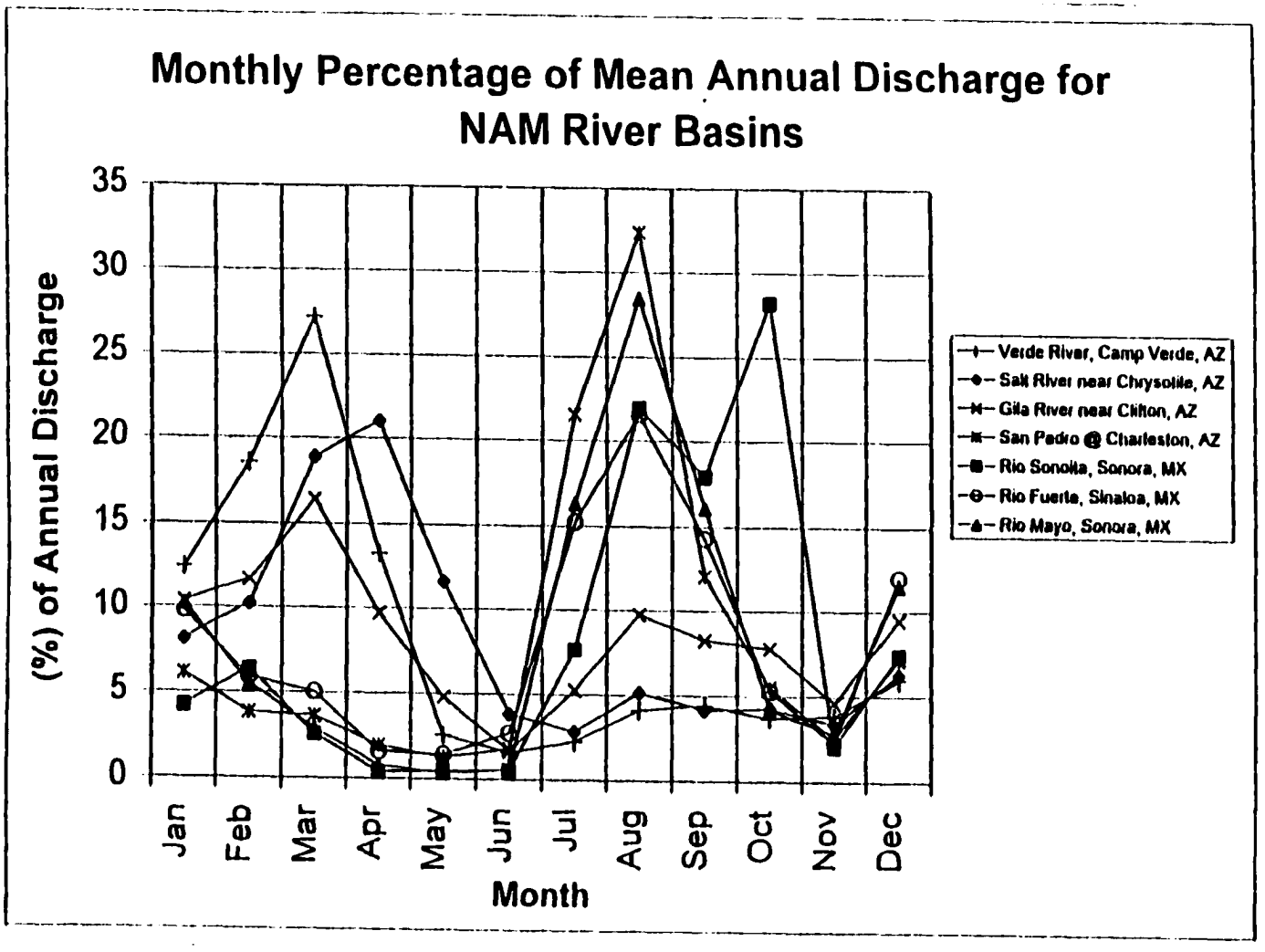

Figure B.1 Monthly percent of mean annual discharge volume for selected basins in the southwest U.S. and northwest Mexico.

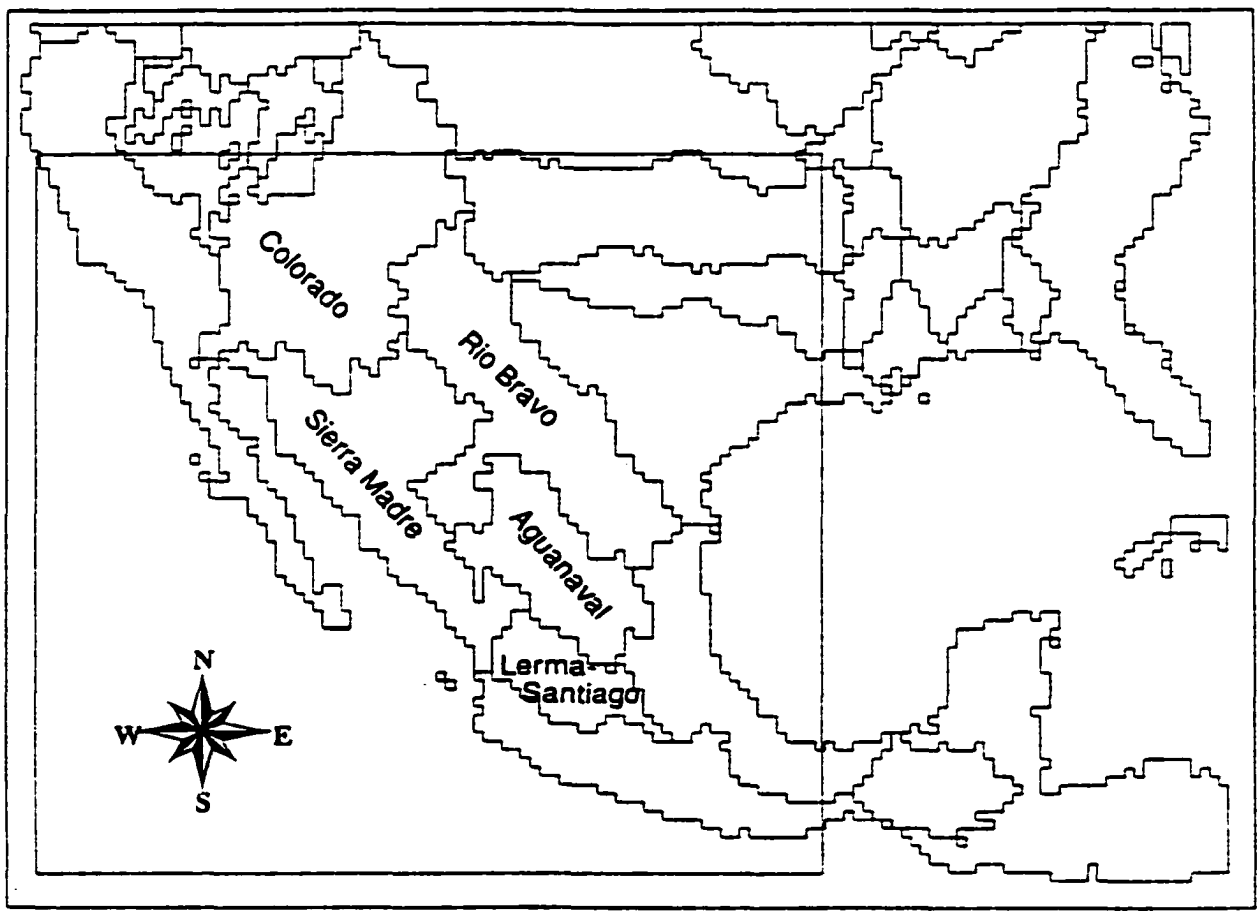

Figure B.2 Basin coverages for basin–average calculations used in this study. Coverages regridded to 30 km resolution. Box denotes the approximate extent of the internal (30 km) MM5 domain.

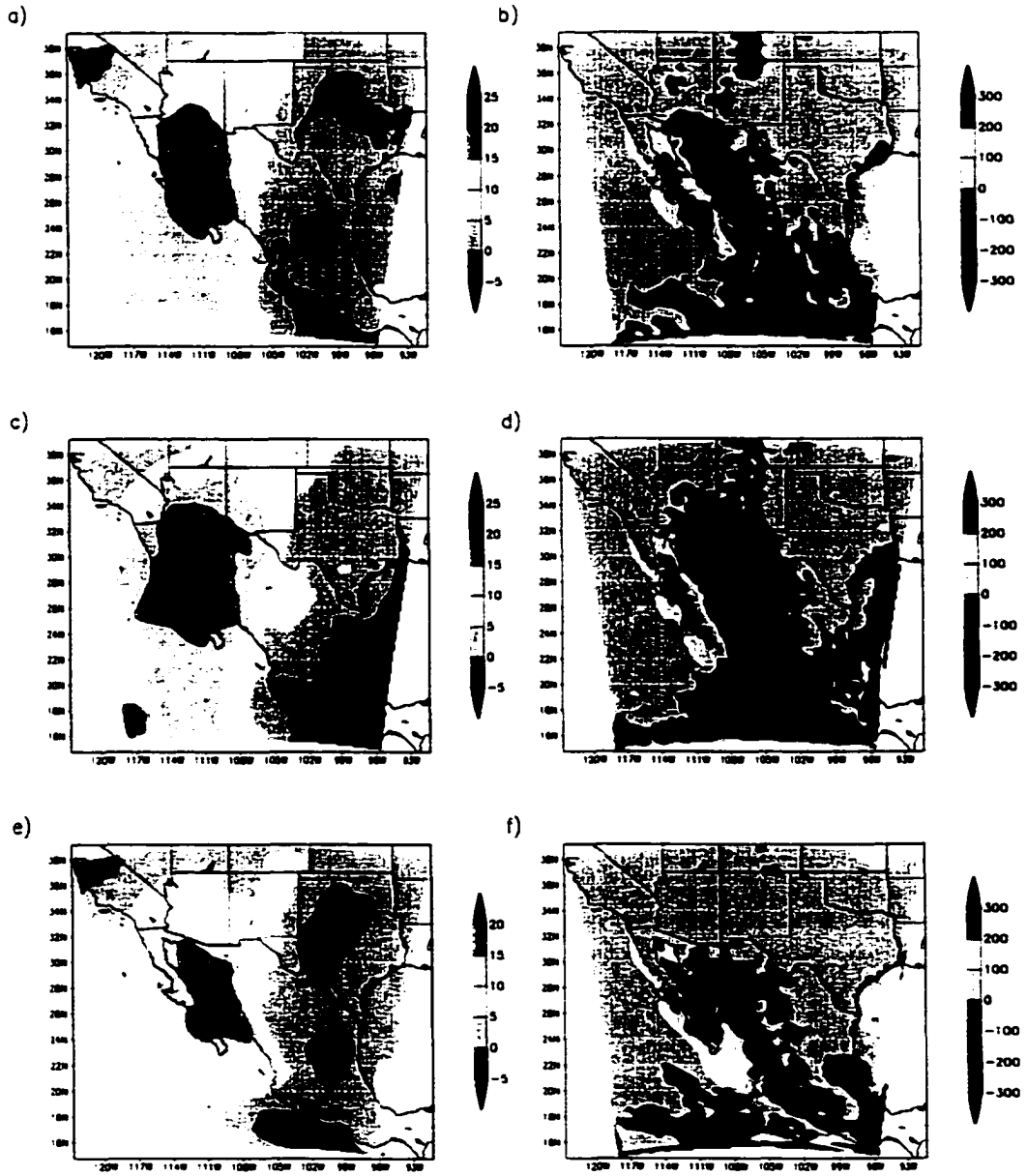

Figure B.3 Change in monthly mean, column–integrated precipitable water content (a–BMG, c–KF, e–GR) and the net source/sink (+/–) calculated as monthly total precipitation minus monthly total evapotranspiration (b–BMG, d–KF, f–GR). All units are in (mm).

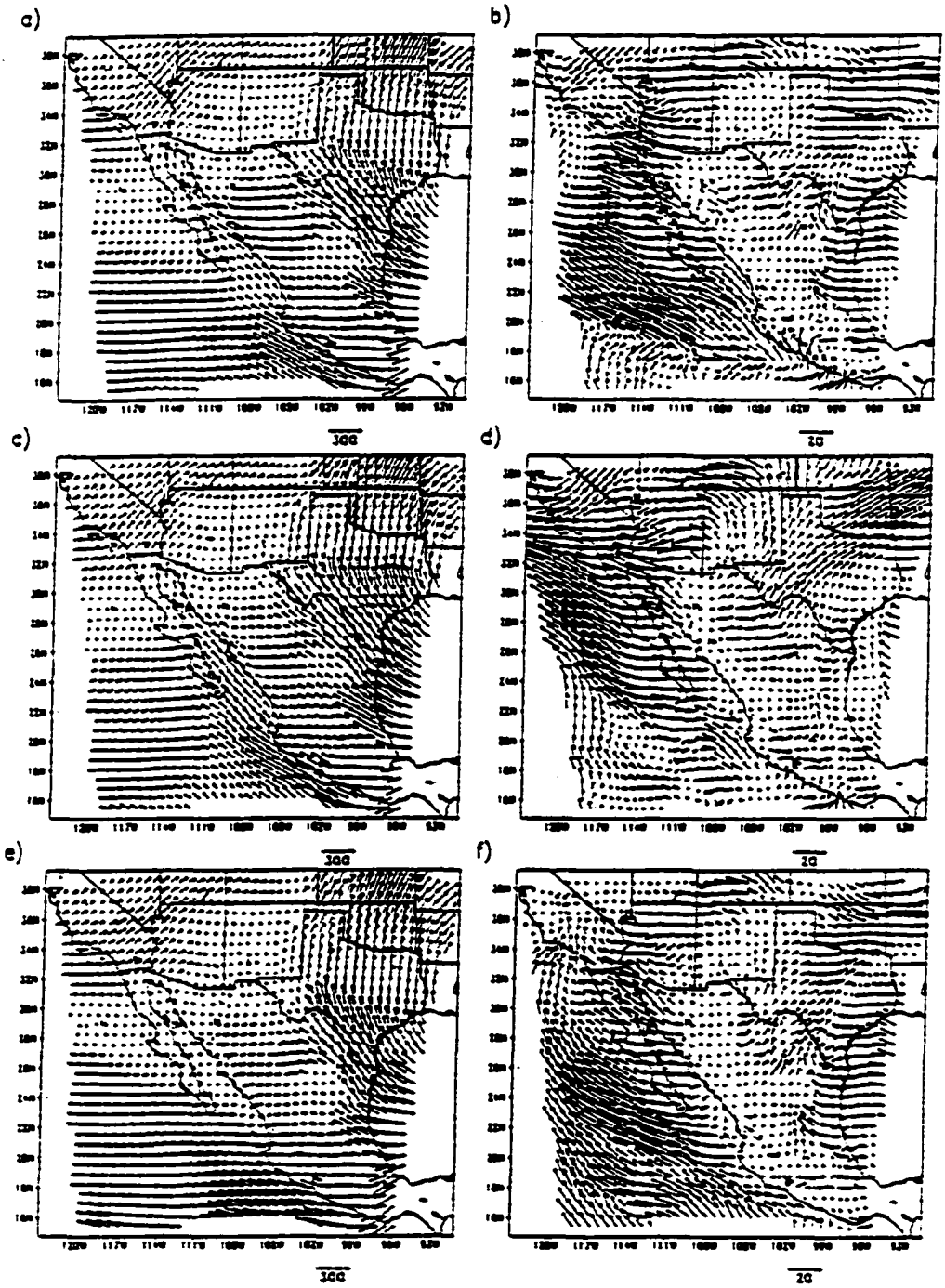

Figure B.4 July stationary component (a–BMG, c–KF, e–GR) and transient component of the column–integrated moisture flux (b–BMG, d–KF, f–GR). Units in (kg–m / s).

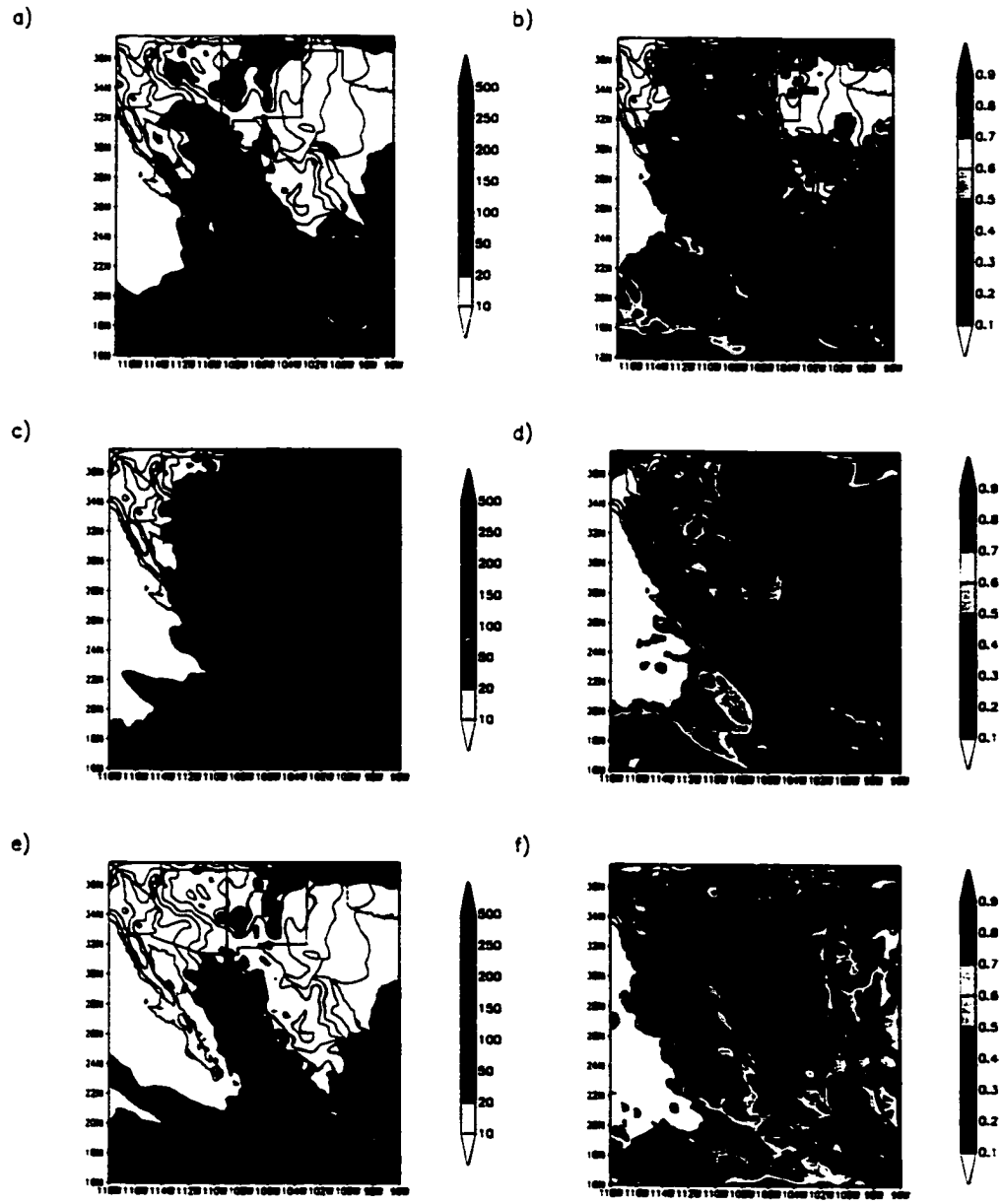

Figure B.5 July total precipitation (a–BMG, c–KF, e–GR; units in mm) and total convective fraction (b–BMG, d–KF, f–GR; dimensionless).

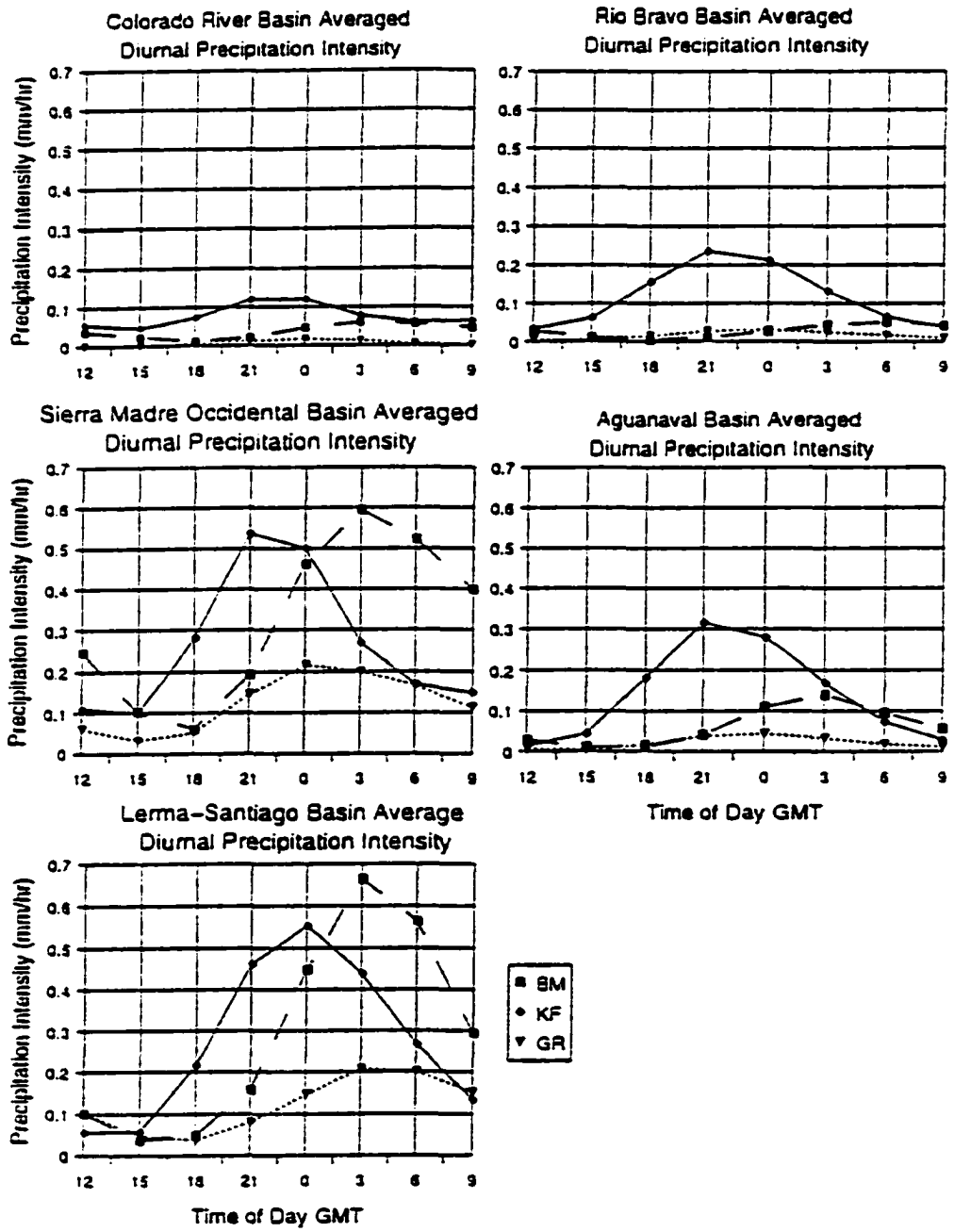

Figure B.6 Basin–averaged, July mean diurnal precipitation intensity. Units in (mm/hr).

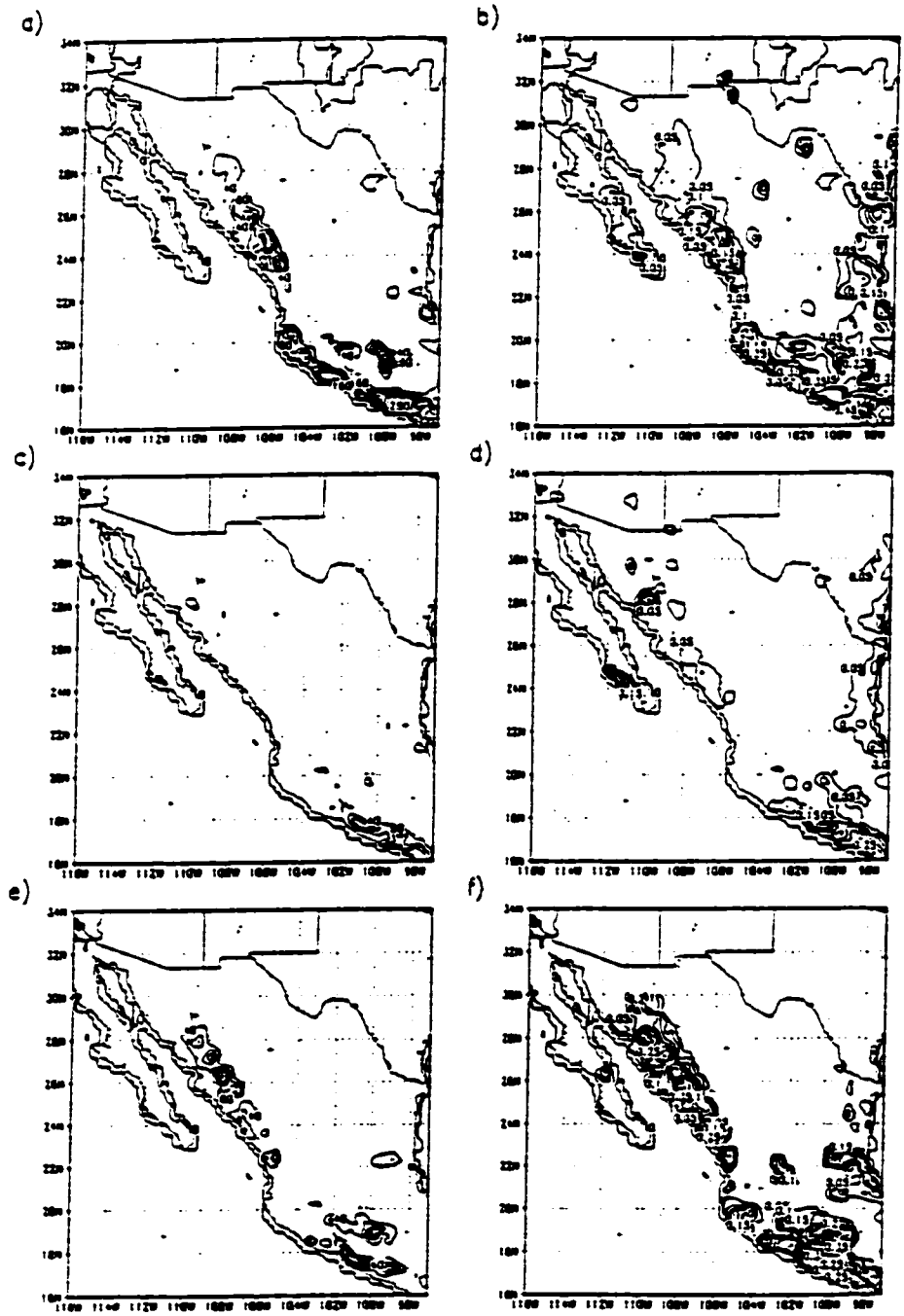

Figure B.7 July total surface runoff (a–BMG, c–KF, e–GR; units in mm) and runoff coefficient (b–BMG, d–KF, f–GR; dimensionless). Contour interval for Figs. 7a, 7c and 7e are 40 mm. Contour interval for Figs. 7b, 7d and 7f are 0.05.

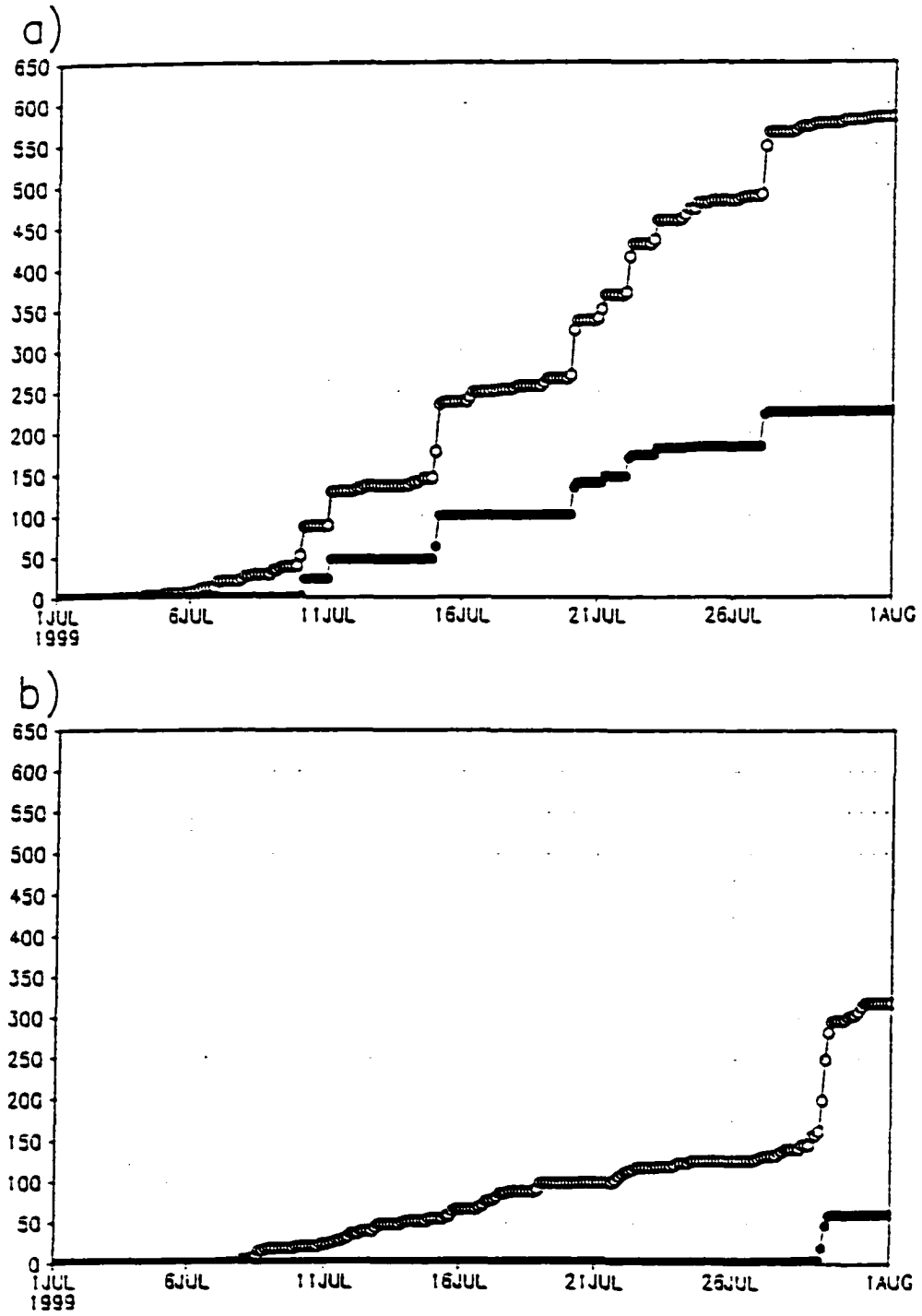

Figure B.8 Cumulative mass curve for precipitation (open circles) and surface runoff (closed circles) at the location of maximum surface runoff in the SMO basin for GR–8a and KF–8b. Units are in (mm).

Table 1. Atmospheric mass balance for NAM macroscale basins

Basin / CPS	dPW (mm)	E–P (mm)
Colorado River		
BM	10.84	–1.92
KF	12.39	–13.08
GR	6.66	11.07
Sierra Madre Occidental		
BM	12.91	–155.32
KF	15.44	–105.11
GR	11.84	–43.08
Rio Bravo		
BM	3.41	5.09
KF	6.11	–12.52
GR	2.74	10.58
Central Mexico – Aguanaval		
BM	0.61	–10.6
KF	3.89	–25.8
GR	0.82	2.77
Lerma–Santiago		
BM	0.33	–111.74
KF	0.89	–96.03
GR	1.19	–35.59

Table B.1 Basin–average atmospheric mass balance terms for NAM macroscale basins. All values represent basin average estimates calculated over the regions labeled in Figure 2. All units in (mm).

Table 2. Precipitation characteristics for NAM macroscale basins

Basin / CPS	Total Precipitation (mm)	Convective Precipitation (mm)	Non-Conv. Precipitation (mm)	Convective Fraction
Colorado River				
BM	27.91	24.68	3.23	0.53
KF	56.16	41.25	14.91	0.67
GR	5.61	4.85	0.76	0.82
Sierra Madre Occidental				
BM	239.75	236.05	3.71	0.92
KF	196.12	163.67	32.45	0.86
GR	90.99	61.4	29.60	0.83
Rio Bravo				
BM	19.85	17.67	2.17	0.58
KF	87.1	80.83	6.28	0.96
GR	11.84	10.67	1.17	0.88
Central Mexico – Aguanaval				
BM	46.38	43.18	3.2	0.84
KF	103.67	97.42	6.25	0.95
GR	16.48	11.34	5.14	0.82
Lerma–Santiago				
BM	214.63	207.73	6.9	0.97
KF	203.13	168.12	35.01	0.84
GR	90.63	41.63	49.00	0.53

Table B.2 Basin–average precipitation characteristics for NAM macroscale basins shown in Figure 2. See text for detailed explanation of terms.

Table 3 Diurnal Precipitation Intensity (mm/hr)

	BM		KF		GR	
	MEAN	MAX	MEAN	MAX	MEAN	MAX
Basin						
Colorado	0.04	0.06	**0.08**	**0.12**	0.01	0.02
Rio Bravo	0.03	0.05	**0.12**	**0.24**	0.02	0.03
Sierra Madre Occidental	**0.32**	**0.60**	0.26	0.54	0.12	0.22
Aguanaval	0.06	0.14	**0.14**	**0.31**	0.02	0.04
Lerma-Santiago	**0.29**	**0.66**	**0.27**	0.55	0.12	0.21

Ranges (All Schemes): MEAN: 0.01 – 0.32 MAX: 0.02 – 0.66

Table B.3 Basin–average, monthly mean diurnal precipitation intensity (mm/hr) for NAM macroscale basins. Bold text indicates maximum value of the three simulations.

Table 4. Runoff characterstics for NAM macroscale basins

Basin / CPS	Total Precipitation (mm)	MAX Total (mm)	Surface Runoff (mm)	MAX Sfc Runoff (mm)	Deep Drainage (mm)	Runoff Ratio SFC/Total (mm)
Colorado River						
BM	27.91	493.19	0.93	33.96	3.92	0.01
KF	56.16	274.53	0.80	17.72	2.97	0.01
GR	5.61	81.49	0.03	1.31	2.88	0.00
Sierra Madre Occidental						
BM	239.75	971.97	21.5	278.64	10.42	0.05
KF	196.12	531.33	6.44	60.44	0.26	0.03
GR	90.99	583.56	15.89	225.61	0.23	0.08
Rio Bravo						
BM	19.85	359.99	0.71	21.99	0.74	0.02
KF	87.10	332.69	1.20	7.66	0.32	0.01
GR	11.84	126.60	0.07	1.91	0.28	0.00
Central Mexico – Aguanaval						
BM	46.38	440.06	1.45	25.41	0.38	0.02
KF	103.67	228.88	1.01	7.82	0.01	0.01
GR	16.48	117.43	0.20	20.18	0.00	0.01
Lerma-Santiago						
BM	214.63	1172.70	10.95	308.7	19.76	0.03
KF	203.13	435.00	2.55	33.01	3.10	0.01
GR	90.63	402.75	3.80	49.38	1.15	0.03

Table B.4 Basin–average rainfall–runoff characteristics for NAM macroscale basins shown in Figure 2. 'MAX' columns indicate gridpoint maximum values for the respective basin and simulation. See text for detailed explanation of terms.

APPENDIX C.

Evaluation of the Simulations of the North American Monsoon in the NCAR CCM3

Zong-Liang Yang[1], David J. Gochis[1], W. James Shuttleworth[1,2]

Geophysical Research Letters, Vol. 28, No.7, Pages 1211-1214, April 1, 2001

Department of Hydrology and Water Resources, University of Arizona, Tucson, AZ 85721, USA
Department of Atmospheric Sciences, University of Arizona, Tucson, AZ 85721, USA

2000 Florida Avenue, NW
Washington, D.C. 20009 U.S.A.
Tel: +1-202-462-6900
Fax: +1-202-328-0566
URL: www.agu.org

17 January 2002

David J. Gochis
Department of Hydrology and Water Resources
University of Arizona
Tucson, Arizona 85721

Dear Mr. Gochis:

AGU grants permission for you to reproduce the following article in your thesis:

> "Evaluation of the Simulations of the North American Monsoon in the NCAR CCM3" Zong-Liang Yang, David J. Gochis, W. James Shuttleworth Geophysical Research Letters, Vol. 28, No.7, Pages 1211-1214, April 1, 2001

Permission is restricted to the use stipulated. The original publication must be appropriately cited. The credit line should read: "authors, journal or book title, volume number, page numbers, year, and the phrase "Copyright by the American Geophysical Union." Substitute the last phrase with "Published by the American Geophysical Union if the paper is not subject to U.S. copyright -- see the copyright line on the first page of the published paper for such classification. Further distribution or reproduction is prohibited.

Sincerely,

Andrea Wieting
Executive Assistant,
Publications Directorate

GEOPHYSICAL RESEARCH LETTERS, VOL. 28, NO. 7, PAGES 1211-1214, APRIL 1, 2001

Evaluation of the simulations of the North American monsoon in the NCAR CCM3

Zong-Liang Yang, Dave Gochis, and William James Shuttleworth

Department of Hydrology and Water Resources, University of Arizona, Tucson, Arizona

Abstract. The six-year average of a ten-year integration of the National Center for Atmospheric Research (NCAR) Community Climate Model version 3 (CCM3), forced with prescribed, climatological sea surface temperatures, was compared with the Legates-Willmott precipitation climatology and the National Centers for Environmental Prediction (NCEP)-NCAR reanalysis product. Summertime precipitation associated with the North American Monsoon (NAM) circulation is largely underrepresented in simulations using the CCM3. The CCM3 simulates excessive amounts of tropical eastern Pacific and Caribbean precipitation, depressed precipitation over Mexico and the southwestern United States, and largely misrepresents the summertime circulation pattern over North America as compared to the reanalysis climatology fields. Basic diagnostic analyses suggest that excessive convection over tropical waters in the eastern Pacific and the Caribbean alters the summertime circulation pattern which produces excess subsidence over much of Northern Mexico and the southwestern U.S. and prohibits the northward transport of atmospheric moisture into the NAM region. The vertically integrated moisture flux and precipitable water estimated by the CCM3 are significantly different in amount and direction (in the case of fluxes) than those observed in the reanalysis data. Introducing anomalously wet land-surface conditions over the NAM region at model initialization yields minimal improvement. Suspected causes for the erroneous simulation of the summertime circulation in the CCM3 are discussed.

Introduction

The North American monsoon (NAM) is an important hydroclimatologic phenomenon which is prone to intraseasonal-to-interannual variability and which can bring severe thunderstorms and related phenomena that pose a serious hazard for residents in the southwestern United States and northwestern Mexico [*Douglas et al.*, 1993]. As a water resource the summer rains associated with the NAM are also responsible for over 60% of the average annual rainfall over much of western Mexico [*Higgins et al.*, 1999]. Therefore, it would be of great social and economic benefit to understand the characteristics associated with the average summer rainfall and mean monsoon circulation.

Despite the huge effort that has been made to characterize the salient features of the NAM system, no mechanistic understanding of how the NAM is developed, sustained, and dissipated has yet been offered [*Douglas et al., 1993; Stensrud et al., 1995; Adams and Comrie, 1997; Higgins et al.*, 1997]. One useful way to study the mechanisms of the NAM system is to employ an atmospheric general circulation model and to document its capabilities in simulating the NAM circulation pattern and rainfall by making comparisons with observations. This is a prerequisite to downscaling the GCM-calculated variables using a fine-resolution regional scale climate model.

Paper number 2000GL011733.
0094-8276/01/2000GL011733$05.00

Model and methodology

This study uses the latest version of the National Center for Atmospheric Research (NCAR) Community Climate Model version 3 (CCM3) [*Kiehl et al.*, 1998]. The NCAR CCM3 is a global spectral model with a horizontal T42 resolution (approximately 2.8° × 2.8° transform grid). It has 18 atmospheric layers in the vertical, with the model top at 2.9 mb, and it includes a diurnal cycle with shortwave and longwave radiative fluxes and the radiative effects of clouds calculated every hour. The model time step for this resolution is 20 minutes. Moist convection is represented using the deep cumulus formalism of *Zhang and McFarlane* [1995] in conjunction with the shallow convection scheme developed by *Hack* [1994]. A detailed global assessment of the dynamical simulation of CCM3 is given in *Hurrell et al.* [1998].

The standard land-surface model in the NCAR CCM3 is LSM [*Bonan*, 1996]. The NCAR CCM3 also was coupled to an alternative land model, the Biosphere-Atmosphere Transfer Scheme (BATS) [*Dickinson et al.*, 1993]. A summary of the simulations of the land climate in the coupled CCM3 and BATS is given in *Hahmann and Dickinson* [2000], while *Yang et al.* [1999] focused on snow simulations.

In this study, the coupled CCM3-land surface models were integrated for 11 years using monthly climatological sea surface temperature (SST) fields. The results from the time-average of the last 10-year integration are essentially similar to the averages from the last 6 years. The time-average modeled climates for the last six years were assessed relative to the data of *Legates and Willmott* [1990] to assess rainfall, and relative to the National Centers for Environmental Prediction (NCEP)-NCAR global reanalysis data [*Kalnay et al.*, 1996] to assess the atmospheric circulation and moisture fields.

Results

Irrespective of the land surface model used in CCM, the model underestimates zonal mean warm season (July-September) rainfall fields relative to observations [*Legates and Willmott*, 1990] in Arizona and New Mexico (30-35°N) by a factor of eight or greater (Figure 1). To the south and north of this latitudinal band, the model also overestimates rainfall during the warm season. The above statement holds true qualitatively when using precipitation data

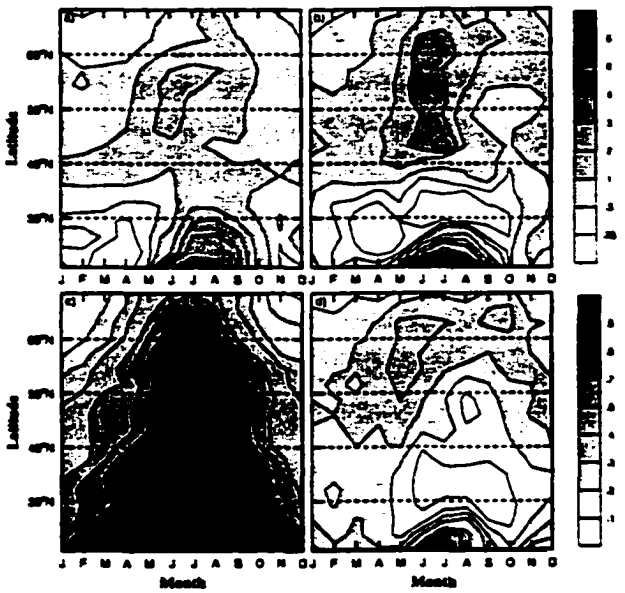

Figure 1. Latitude-month plots of (a) observed precipitation, (b) simulated precipitation from CCM3 coupled with BATS (i.e., CCM3-BATS), (c) ratio of convective to total precipitation in CCM3-BATS, and (d) vertically integrated, random overlap, high cloud amount (400 mb - 50 mb) in CCM3-BATS. The results are shown as zonal averages over land points between 114°W and 104°W.

of *Xie and Arkin* [1996]. The severeness of the summer rainfall underestimation is apparently an artifact due to use of the yearly-repeating climatological SST. With the yearly-varying AMIP SST, the CCM3 produces a much improved simulation of the monsoon rainfall in New Mexico. While the vertically integrated horizontal water vapor transport across the boundaries of the monsoon region (20-40°N, 114-104°W) appear similar during the pre-monsoon months, there are marked differences during the peak monsoon months of July-August (Figure 2). The NCEP-NCAR reanalysis [*Kalnay et al.*, 1996] shows a strong southerly flux across the southern boundary, while the CCM3 simulates a northerly flux. The model also shows a much stronger easterly flux across the eastern boundary compared to the analysis. These results are consistent with the low-level (900 mb) wind vector patterns indicating that lower levels are responsible for greater portions of the overall moisture advection. At the 200 mb level, the reanalysis data indicate that the anticyclonic system is meridionally oriented with a center over western Mexico, but the model shows an eastward displacement of the anticyclonic system which has a zonal orientation (not shown). In addition, there is an overestimation of the moisture convergence over the Gulf of Mexico and tropical oceans that coincides with the overprediction of precipitation in this region. It is realized that the NCEP-NCAR reanalysis may not be perfect, however, the differences seen between the NCEP-NCAR reanalysis and the CCM3 simulations are larger than the differences between the NCEP-NCAR reanalysis and the reanalysis from the European Centre for Medium-range Weather Forecasts (ECMWF) [*Barlow et al.*, 1998].

The underestimated monsoon rainfall in Arizona and New Mexico is consistent with the underrepresentation of deep convective activities. This is evident (Figure 1) from the low values of high cloud between 400 mb-50 mb produced during these simulations when compared with previous studies of deep convection in the NAM [*Douglas et al.*, 1993]. Figure 3 shows that the precipitable water over Mexico and southwest U.S. is less in the model than the analysis by a small factor. This is much smaller than the difference in the modeled precipitation (Figure 1), indicating that the model converts a reduced proportion of precipitable water into precipitation. In the reanalysis, the high values of precipitable water are oriented along the Gulf of California and over the U.S. central plains, while the model displays maximum precipitable water over the tropical eastern Pacific and the Gulf of Mexico. 162

The core upward motion in the reanalysis data overlies the Sierra Madre Occidental in Mexico, and the southern continental divide and northeastern Great Basin in the U.S. (Figure 3). The stronger upward motions in CCM3 near 15°N over the tropical eastern Pacific, the Caribbean, and the Gulf of Mexico are consistent with an overestimation of the precipitable water and precipitation in these areas, and there is weaker upward motion over Arizona and New Mexico. As shown in the meridional streamfunction plots (Figure 4), CCM3 simulates an overly intense rising branch of the Hadley Cell around 15°N throughout the depth of the troposphere. In addition, the model produces a wide, subsiding branch between 30-40°N. In contrast, the analysis data indicate a weak and shallow rising branch of the Hadley

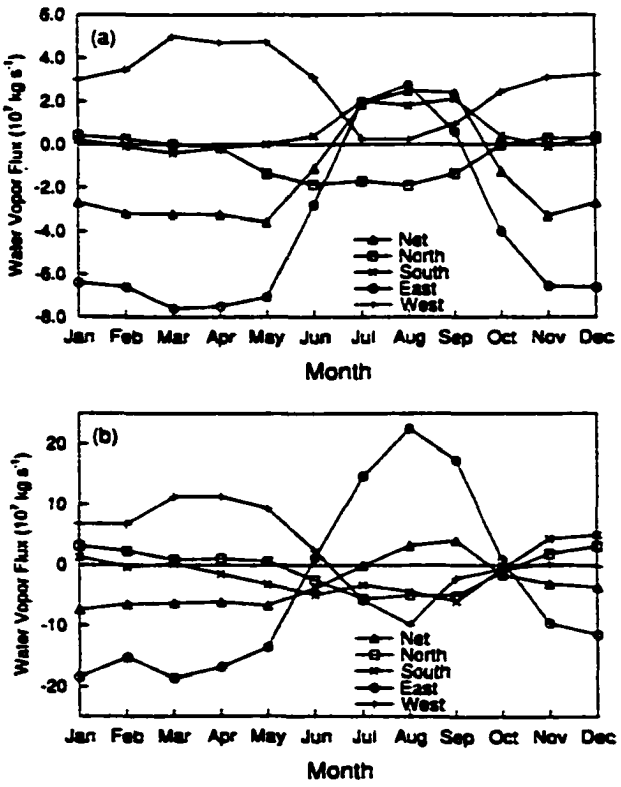

Figure 2. Comparison of vertically integrated vapor fluxes across 20-40°N, 114-104°W from (a) observations and (b) CCM3-BATS.

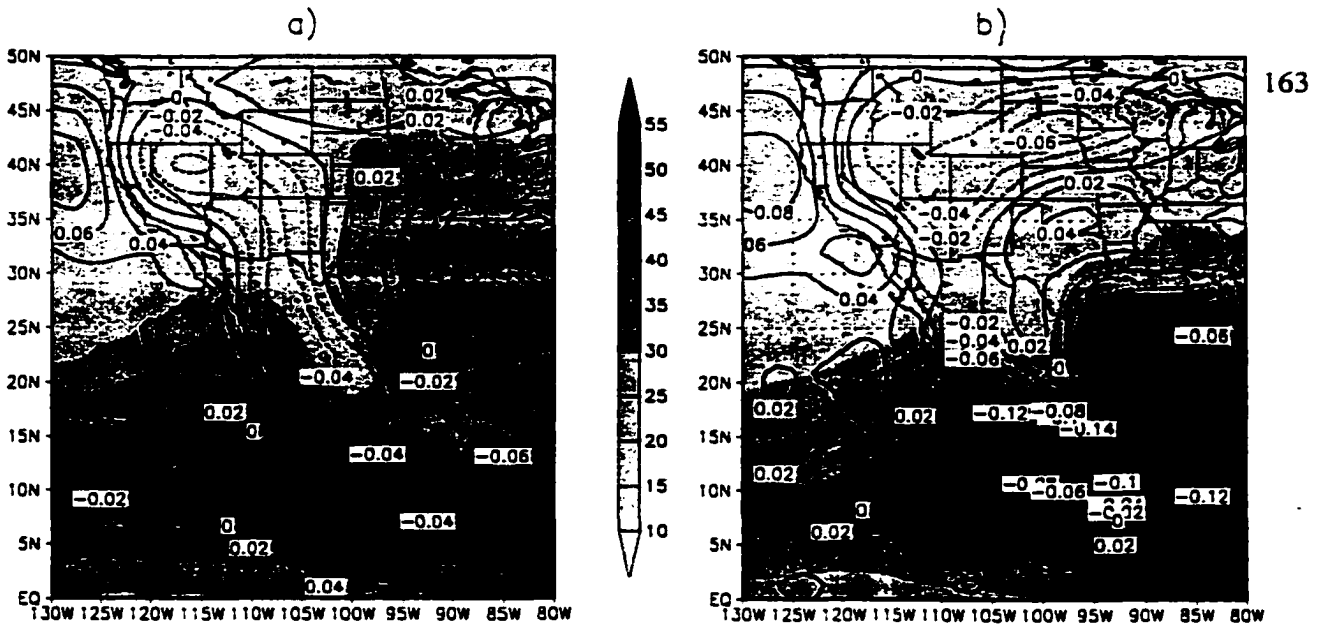

Figure 3. Comparison of July-August-September 600 mb vertical velocity (mb s^{-1}) (contoured) and column integrated precipitable water (mm) (shaded) from (a) NCEP-NCAR reanalysis and (b) CCM3-BATS.

Cell that is confined below 700 mb but which extends from 10°N to 30°N, where the upward motion is found throughout the depth of the troposphere.

Discussion

There are several factors which may be responsible for the above-described distortion of the summertime monsoon circulation and under-representation of rainfall over the southwestern United States. One possibility is that the model simulates overly dry soils over this region. To test this, six integrations were made in which extreme soil-moisture anomalies (i.e., saturated soils) were introduced into the area corresponding to Mexico, Arizona, and New Mexico on May 31 of the last six years of the control run. In each case, the model was then allowed to evolve naturally from June 1 through September 30. The July-August-September (JAS) average precipitation for these six runs was compared to the JAS precipitation average for the (unperturbed) last six years in the control run (Figure 5). The monsoon rainfall is marginally enhanced compared to the control run by introducing this anomalous soil moisture but the model still under-represents precipitation in the southwestern U.S.

The underrepresentation of monsoon rainfall can be significantly reduced by using the yearly-varying AMIP SST during 1979-1988, suggesting the transient SSTs in the extreme years play an important role in contributing to the monsoon precipitation climatology. The simulations of the circulation patterns, however, show little changes compared to the runs from using the yearly-repeating SSTs.

Several other candidate causes are likely also influential in shaping the poorly modeled monsoon circulation. One possible deficiency is the convection scheme used in CCM3. In addition, the T42 resolution used in this study does not resolve the coastlines (e.g., the Gulf of California) and terrain features in the Sierra Madre Occidental Mountains. *Dirmeyer* [1998] showed that the variations in the meridional extent of land in the tropics and subtropics affect the strength of the Hadley Cell and climate over land. These topics are the subject of ongoing investigation.

Summary

The performance of the NCAR CCM3 in simulating the North American monsoon was evaluated by comparing it with the Legates and Willmott precipitation climatology and the NCEP-NCAR reanalysis fields. The model is unable to simulate regional patterns of the monsoon circulation

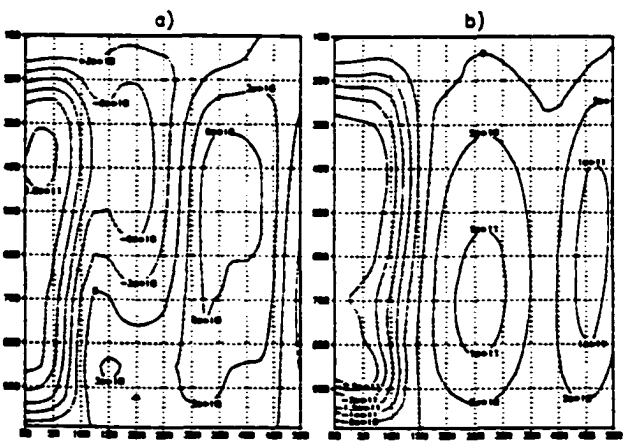

Figure 4. Comparison of July-August-September zonally averaged (130-80°W) meridional streamfunction (kg s^{-1}) from (a) NCEP-NCAR reanalysis and (b) CCM3-BATS.

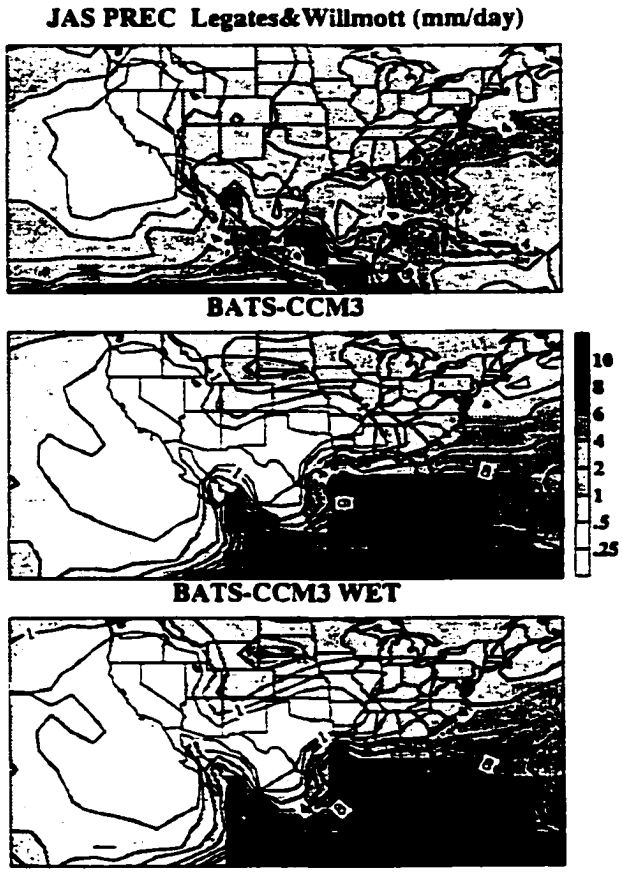

Figure 5. Comparison of mean precipitation in July-August-September (JAS) (mm/day) from (a) observations, (b) the control simulation from the CCM3-BATS, and (c) the wet soil-moisture anomaly simulation with the CCM3-BATS in which the soil moisture was initialized as saturated values over Mexico, Arizona, and New Mexico on May 31. An ensemble run of six members was used to produce the results shown in (c).

and rainfall. The modeled rainfall over the southwest U.S. and Mexico is much too low, while there is overestimation of tropical precipitation in the tropical eastern Pacific and in the Caribbean. Correspondingly, there seems to be an intensification of the Hadley Cell circulation in the model compared to the reanalysis data. The underrepresentation of deep convection in the monsoon region is suggested by the relatively low values of randomly overlapped high cloud, and there are large differences in the vertical motion and precipitable water fields between the model and the reanalysis. The modeled upper level ridge is displaced eastward relative to the reanalysis data in August, and CCM3 simulates a stronger anticyclone at 25-35°N. A sensitivity study that introduced wet soil-moisture anomalies suggests that regional land-surface forcing may play only a marginal role on the large-scale atmospheric circulation. Clearly, further work is needed to define the factors that are shaping the monsoon circulation.

Acknowledgments. This study was supported by the NASA Earth Science Enterprise Land Surface Hydrology Program under contract NAS5-7554. The editorial services provided by Corrie Thies are greatly valued.

References

Adams, D. K. and A. C. Comrie, The North American monsoon, *Bull. Amer. Meteor. Soc., 78*, 2197-2213, 1997.

Barlow, M., S. Nigam, and E. H. Berbery, Evolution of the North American monsoon system, *J. Climate, 11*, 2238-2257, 1998.

Bonan, G. B., A Land Surface Model (LSM version 1.0) for ecological, hydrological, and atmospheric studies: technical description and user's guide, *Tech. Note NCAR/TN-417+STR*, 150 pp., National Center for Atmospheric Research, Boulder, CO, 1996.

Dickinson, R. E., A. Henderson-Sellers, and P. J. Kennedy, Biosphere-Atmosphere Transfer Scheme (BATS) version 1e for NCAR Community Climate Model, *Tech. Note NCAR/TN-387+STR*, 72 pp., National Center for Atmospheric Research, Boulder, CO, 1993.

Dirmeyer, P. A., Land-sea geometry and its effect on monsoon circulations, *J. Geophys. Res., 103*, 11555-11572, 1998.

Douglas, M. W., R. A. Maddox, K. Howard, and S. Reyes, The Mexican monsoon, *J. Climate, 6*, 1665-1667, 1993.

Hack, J. J., Parameterization of moist convection in the National Center for Atmospheric Research Community Climate Model (CCM2), *J. Geophys. Res., 99*, 5551-5568, 1994.

Hahmann, A. N. and R. E. Dickinson, A fine-mesh land approach for general circulation models and its impact on regional climate, *J. Climate*, in press, 2000.

Higgins, R. W., Y. Yao, and X. L. Wang, Influence of the North American monsoon system on the U.S. summer precipitation regime, *J. Climate, 10*, 2600-2622, 1997.

Higgins, R. W., Y. Chen, and A. V. Douglas, Interannual Variability of the North American Warm Season Precipitation Regime, *J. Climate, 12*, 653-680, 1999.

Hurrell, J. W., J. J. Hack, B. A. Boville, D. L. Williamson, and J. T. Kiehl, The dynamical simulation of the NCAR Community Climate Model version 3 (CCM3), *J. Climate, 11*, 1207-1236, 1998.

Kalnay, E. and Coauthors, The NCEP/NCAR 40-year reanalysis project, *Bull. Amer. Meteor. Soc., 77*, 437-471, 1996.

Kiehl, J. T., J. J. Hack, G. B. Bonan, B. A. Boville, D. L. Williamson, and P. J. Rasch, The National Center for Atmospheric Research Community Climate Model: CCM3, *J. Climate, 11*, 1131-1149, 1998.

Legates, D. R. and C. J. Willmott, Mean seasonal and spatial variability in gauge-corrected global precipitation, *Int. J. of Climatology, 10*, 111-127, 1990.

Stensrud, D. J., R. Gall, S. L. Mullen, and K. Howard, Model climatology of the Mexican monsoon, *J. Climate, 8*, 1775-1794, 1995.

Xie, P., P. Arkin, Analysis of global monthly precipitation using gauge observations, satellite estimates, and numerical model predictions, *J. Climate, 9*, 840-858, 1996.

Yang, Z.-L., R. E. Dickinson, A. N. Hahmann, G.-Y. Niu, M. Shaikh, X. Gao, R. C. Bales, S. Sorooshian, and J. M. Jin, Simulation of snow mass and extent in global climate models, *Hydrological Processes, 13 (12-13)*, 2097-2113, 1999.

Zhang, G. J. and N. A. McFarlane, Sensitivity of climate simulations to the parameterization of cumulus convection in the Canadian Climate Centre general circulation model, *Atmos.-Ocean, 33*, 407-446, 1995.

Zong-Liang Yang, Dave Gochis, and William James Shuttleworth, Department of Hydrology and Water Resources, University of Arizona, Tucson, AZ 85721. (e-mail: liang@hwr.arizona.edu; gochis@hwr.arizona.edu; shuttle@hwr.arizona.edu)

(Received April 21, 2000; revised November 10, 2000; accepted December 28, 2000.)

APPENDIX D.

The Impact of Sea Surface Temperature on the North American Monsoon: A GCM Study

Zong-Liang Yang[1], David J. Gochis[1], W. James Shuttleworth[1,2]

Submitted to *Geophysical Research Letters*, 2001

[1] Department of Hydrology and Water Resources, University of Arizona, Tucson, AZ 85721, USA
[2] Department of Atmospheric Sciences, University of Arizona, Tucson, AZ 85721, USA

The impact of sea surface temperature on the North American monsoon: A GCM study

Zong-Liang Yang, Dave Gochis, William James Shuttleworth, and Guo-Yue Niu

Abstract. We have examined the capability of several configurations of Version 3 of the National Center for Atmospheric Research (NCAR) Community Climate Model (CCM3), operating at T42 resolution, when simulating the circulation and rainfall patterns of the North American monsoon system (NAMS). When forced with repeated identical annual cycles of climatological average sea surface temperatures (SSTs), the CCM3 significantly under-represents monsoon rainfall in the southwest United States while simulating excessive precipitation in the tropical eastern Pacific Ocean and the Caribbean Sea. However, when forced with the observed monthly average SSTs from 1979 to 1997, the CCM3 produces an improved simulation of monsoon rainfall in the southwestern U.S., as well as in the eastern tropical Pacific Ocean and the Caribbean Sea. Using the SSTs for 1983 in the Pacific and climatological SSTs elsewhere, the modeled circulation and rainfall distribution resembles that given with observed monthly average SSTs. The simulations are sensitive to the size of the domains over which the Pacific SST anomalies are imposed. Overall, these results suggest that the magnitude and size of wintertime Pacific SST anomalies have a significant influence on summertime rainfall in the southwest U.S., and that these SSTs contribute to the NAMS precipitation climatology in extreme years more than in less extreme years.

Introduction

The North American Monsoon System (NAMS) provides an important water resource to the arid/semi-arid southwest United States, and understanding the cause of variations in the strength of the NAMS potentially has profound social and economic implications [*Douglas et al.*, 1993; *Adams and Comrie*, 1997]. Recent observational studies have suggested that tropical and north Pacific sea surface temperatures (SSTs) correlate with the NAMS circulation and rainfall at the seasonal-to-interannual time scales [*Higgins et al.*, 1999; *Castro et al.*, 2001]. Potentially, because General Circulation Models (GCMs) are important tools for understanding the physical mechanisms controlling the NAMS, it is important to test whether GCMs can reproduce these

observed relationships.

Yang et al. [2001] showed that, when forced with the identical annual cycles of climatologically average SSTs, Version 3 of the National Center for Atmospheric Research (NCAR) Community Climate Model (CCM3) significantly underestimates warm season precipitation in Arizona and New Mexico (between 30°N and 35°N). This indicates that using climatologically average SSTs in the GCM may underestimate the strength of the influence of SSTs in the Pacific Ocean. In this paper, we first assess the performance of the CCM3 when forced with observed monthly SSTs relative to that when forced with climatological SSTs. In addition, to further explain the difference between these simulations, a series of sensitivity experiments are reported which investigate the importance of the magnitude and extent of the Pacific SST anomalies on the ability of CCM3 to simulate NAMS.

Models

In this study, the NCAR CCM3 [*Kiehl et al.*, 1998] was used with resolution and physical parameterizations identical to those used in *Yang et al.* [2001]. Specifically, we used a 20-minute time step, T42 resolution (i.e., approximately 2.8° × 2.8° transform grid) in the horizontal, and 18 atmospheric layers in the vertical, with the model top at 2.9 hPa. However, in the present study, we used two versions of the CCM3: CCM3.2 and CCM3.6, while *Yang et al.* [2001] used only CCM3.2. These two versions have identical physical parameterizations, but CCM3.6 differs in coding structure and includes bug fixes. Climate applications using both versions of CCM3 have appeared in the literature, but documentation of their performance when simulating monsoons is rare. This paper focuses on assessing their ability to model the circulation and rainfall pattern of the NAMS.

The Land Surface Model (LSM) [*Bonan*, 1996] is the standard land-surface model used in the NCAR CCM3. In this study, the NCAR CCM3.2 was also coupled to an alternative land model, namely the Biosphere-Atmosphere Transfer Scheme (BATS) [*Dickinson et al.*, 1993].

Experiments

Eight model experiments were made using two versions of CCM3, two different land-surface models, and different SST specifications (Table 1). In Experiments A, B, and G, the CCM3 was driven with identical annual cycles of climatological SSTs. Results from Ex-

periments A and B were previously described in *Yang et al.* [2001]. In Experiment H, the CCM3 was forced with observed monthly SSTs as used in the Atmospheric Models Intercomparison Project (AMIP) [*Gates*, 1992] for the period 1979-1997.

The remaining experiments (C, D, E, and F) examine the sensitivity of NAMS circulation and rainfall patterns as simulated in the CCM3 to the size and magnitude of the SST anomalies in the Pacific Ocean. The observed SSTs in the Nino-3 region show a strong positive anomaly (up to 3.6°C) during the period 1982-1983 (Figure 1). In the same period, the SST anomalies in the central north Pacific (CNP) and eastern north Pacific (ENP) are negative. The major differences between SSTs in 1982 and 1983 are that tropical SST anomalies increase approximately linearly from zero in January to about 3.6°C in December in 1982, while this is reversed in 1983 (Figure 1). It is of interest to see how the CCM3 responds to these differences.

Experiments A, B, and G all have the same initial conditions. Only results from the last six years in these experiments were used for analysis (in fact, the results from the last six years are essentially identical to those from the last 10 years). Experiments C, D, E, and F were all initialized from the modeled status on December 31 of the 5th year in Experiment B and integrated for six years to allow the results to be readily compared with those from Experiment B (as well as the other experiments). Results from the run with AMIP SSTs were averaged for a period corresponding to the observed precipitation data.

Time-average modeled precipitation data were evaluated relative to the data of *Legates and Willmott* [1990] (hereafter called LW) and *Xie and Arkin* [1996] (here after called XA), these being two data sets commonly used by the climate modeling community to assess modeled rainfall. The National Centers for Environmental Prediction (NCEP)-NCAR global reanalysis data [*Kalnay et al.*, 1996] were used to assess the atmospheric circulation and moisture fields.

Results

Precipitation

Figure 2 shows that the CCM3 model run with the AMIP SSTs simulates the spatial distribution of precipitation more accurately than with the climatologically averaged SSTs, especially over Arizona, New Mexico, northwestern Mexico, and the tropical oceans. However, both experiments underpredict precipitation in the southwest United States and overpredict precipita-

tion in Colorado, Kansas, the tropical eastern Pacific, the Caribbean, and the Gulf of Mexico.

Figure 3 compares observed (LW and XA) monthly precipitation zonally averaged over land between 114°W and 104°W with that calculated by the CCM3 experiments using different specifications of SSTs. While both observations (Figures 3a-b) differ considerably in the tropics (0-30°N), and the LW data show a stronger monsoon rainfall, the observational data agree reasonably well elsewhere. *Yang et al.* [2001] reported that the CCM3 experiment with climatological SSTs underestimates the NAMS rainfall. This underestimation is reduced in the CCM3 when forced with the AMIP SSTs between 1979 and 1997 (Figure 3c). Arguably, the comparison between the run with AMIP SSTs and the XA climatology (Figure 3a) is better than with the LW climatology (Figure 3b) because, in the former case, both observations and data refer to the same averaging period (1979-1997). Relative to both observed data sets, the model with the AMIP SSTs tends to underestimate rainfall during the warm season in the southwest USA (30-35°N) and overestimates rainfalls south and north of this latitudinal band. In addition, the modeled monsoon peaks in June/July are one or two months earlier than the observed peaks.

In the study of *Yang et al.* [2001], an old version of the model (version CCM3.2) was used, while the model data presented in Figure 2 and Figures 3c-d were calculated with a more recent version (CCM3.6). It is of interest to document the differences between these two versions when depicting the NAMS. Figure 3e (calculated with CCM3.2) can be compared directly with Figure 3d (calculated with CCM3.6) because both use climatological SSTs and the LSM model. The run with CCM3.6 yields a slightly more accurate simulation of the warm season rainfall in the southwest U.S. (30-35°N) than the CCM3.2, but other features are similar. Moreover, the simulation using CCM3.2 with BATS (Figure 3f) is similar to that with LSM (Figure 3e). Therefore, sensitivity experiments to investigate the effect of SSTs were conducted using the CCM3.2 coupled with BATS.

When the Pacific SSTs in the climatological run are replaced by the observed SSTs in 1982, the modeled results (Figure 3g) are essentially similar to those of the control run (Figure 3f). However, significant differences occur when the 1983 SSTs are used repeatedly. Specifically, enhanced warm season rainfall is generated between 30°N and 35°N (Figure 3h). These simulations together suggest that the magnitude of wintertime SST anomalies in the Pacific, especially in the eastern trop-

ical Pacific, is important to the development and intensity of subsequent summertime rainfall in the southwest United States. A strong positive SST anomaly is associated with a modeled increase in rainfall over the southwest United States, a result consistent with that suggested by observations [*Higgins et al.*, 1999; *Castro et al.*, 2001].

Circulation

Consistent with the results given by *Yang et al.* [2001] the newer version of CCM3 forced with the AMIP SSTs simulates circulation patterns (Figure 4) that are broadly similar to the NCEP-NCAR reanalysis [*Kalnay et al.*, 1996]. However, the low-level (900 hPa) wind vectors in the model again show a stronger-than-observed convergence in the eastern tropical Pacific Ocean, the Caribbean Sea, and the Great Plains. These correspond with areas where the model overestimates precipitable water, precipitation, and rising motion. At the 200-hPa level, the reanalysis data indicate that the anticyclonic system is meridionally oriented with a center over western Mexico, but the model still shows an anticyclonic system that is displaced eastwards relative to reanalysis and has zonal orientation.

In the experiments with the imposed anomalies in the Pacific SSTs, the size of the domain where these anomalies are imposed is important. If the size is as small as that used by *Castro et al.* [2001] to define their NAMS index, both the circulation and rainfall patterns (Figure 5a,c) show little difference with respect to each other and the control run. When the domain size over which the anomaly is imposed is increased to cover the most of the Pacific Ocean, the most noticeable change is decreased rainfall in the Caribbean and the Gulf of Mexico (Figures 5b,d). As a result, the precipitation pattern resembles better that obtained using the AMIP SSTs between 1979-1997. The run with the 1983 SSTs imposed across the Pacific produces rainfall enhancement in New Mexico (Figure 5d). At the 200-hPa level, the anticyclonic system over the southern tier of the Gulf of California appears to be strengthened, while the other center over the Gulf of Mexico tends to be weakened. These changes compare favorably with observations.

Summary

This study shows that the simulations of the NAMS circulation and rainfall in the NCAR CCM3 are related to the way in which the Pacific SSTs are prescribed in model studies. Using identical annual cycles of the long-term mean climatological SSTs underestimates the

mean NAMS rainfall, while using the SSTs that include interannual variations improves the model simulations. These results indicate that the influence of the SSTs on the strength of the NAMS rainfall is a nonlinear process. Presumably, the long-term mean SSTs filter out the year-to-year transient features that may be important to the development of the NAMS while, on the other hand, these features in extreme years (e.g., ENSO) can lead to a nonlinearly strong response in the NAMS. This result is well illustrated by the sensitivity studies in which the observed 1983 SST is imposed in the Pacific Ocean while retaining climatological SSTs elsewhere. The resulting rainfall patterns in the southwest United States, the Caribbean Sea, and the Gulf of Mexico closely resemble those obtained using the AMIP SSTs. The improved simulation from the 1983 SSTs anomaly experiment implies that the magnitude and size of wintertime SST anomalies are important factors influencing the summertime rainfall in the southwest United States. Further, this sensitivity study indicates that, in the extreme conditions, transient (as opposed to the long-term mean) SSTs influence monsoon precipitation climatology more than the mean SSTs.

Acknowledgments.
This study was supported by NASA grants under contracts NAG5-7554 and NAG8-1520. We thank Corrie Thies for helping with textual corrections.

References

Adams, D. K. and A. C. Comrie, The North American monsoon, *Bull. Amer. Meteor. Soc. 78*, 2197-2213, 1997.

Bonan, G. B., A Land Surface Model (LSM version 1.0) for ecological, hydrological, and atmospheric studies: technical description and user's guide, *Tech. Note NCAR/TN-417+STR*, 150 pp., National Center for Atmospheric Research, Boulder, CO, 1996.

Castro, C. L., T. B. McKee, and R. A. Pielke, Sr., The relationship of the North American monsoon to tropical and north Pacific sea surface temperatures as revealed by observational analysis, *J. Clim.*, in press, 2001.

Dickinson, R. E., A. Henderson-Sellers, and P. J. Kennedy, Biosphere-Atmosphere Transfer Scheme (BATS) version 1e for NCAR Community Climate Model, *Tech. Note NCAR/TN-387+STR*, 72 pp., National Center for Atmospheric Research, Boulder, CO, 1993.

Douglas, M. W., R. A. Maddox, K. Howard, and S. Reyes, The Mexican monsoon, *J. Clim. 6*, 1665-1667, 1993.

Gates, W. L., AMIP - The Atmospheric Model Intercomparison Project, *Bull. Amer. Meteor. Soc. 73*, 1962-1970, 1992.

Higgins, R. W., Y. Chen, and A. V. Douglas, Interannual Variability of the North American Warm Season Precipitation Regime, *J. Clim. 12*, 653-680, 1999.

Kalnay, E. and Coauthors, The NCEP/NCAR 40-year re-

analysis project, *Bull. Amer. Meteor. Soc.* 77, 437-471, 1996.

Kiehl, J. T., J. J. Hack, G. B. Bonan, B. A. Boville, D. L. Williamson, and P. J. Rasch, The National Center for Atmospheric Research Community Climate Model: CCM3, *J. Clim. 11*, 1131-1149, 1998.

Legates, D. R. and C. J. Willmott, Mean seasonal and spatial variability in gauge-corrected global precipitation, *Int. J. of Climatology 10*, 111-127, 1990.

Xie, P., P. Arkin, Analysis of global monthly precipitation using gauge observations, satellite estimates, and numerical model predictions, *J. Clim. 9*, 840-858, 1996.

Yang, Z.-L., D. Gochis, and W.J. Shuttleworth, Evaluation of the simulations of the North American monsoon in the NCAR CCM3, *Geophys. Res. Lett.* , in press, 2001.

Zong-
Liang Yang, Dave Gochis, William James Shuttleworth, and Guo-Yue Niu, Department of Hydrology and Water Resources, University of Arizona, Tucson, AZ 85721. (e-mail: liang@hwr.arizona.edu; gochis@hwr.arizona.edu; shuttle@hwr.arizona.edu; niu@hwr.arizona.edu)

(Received _____)

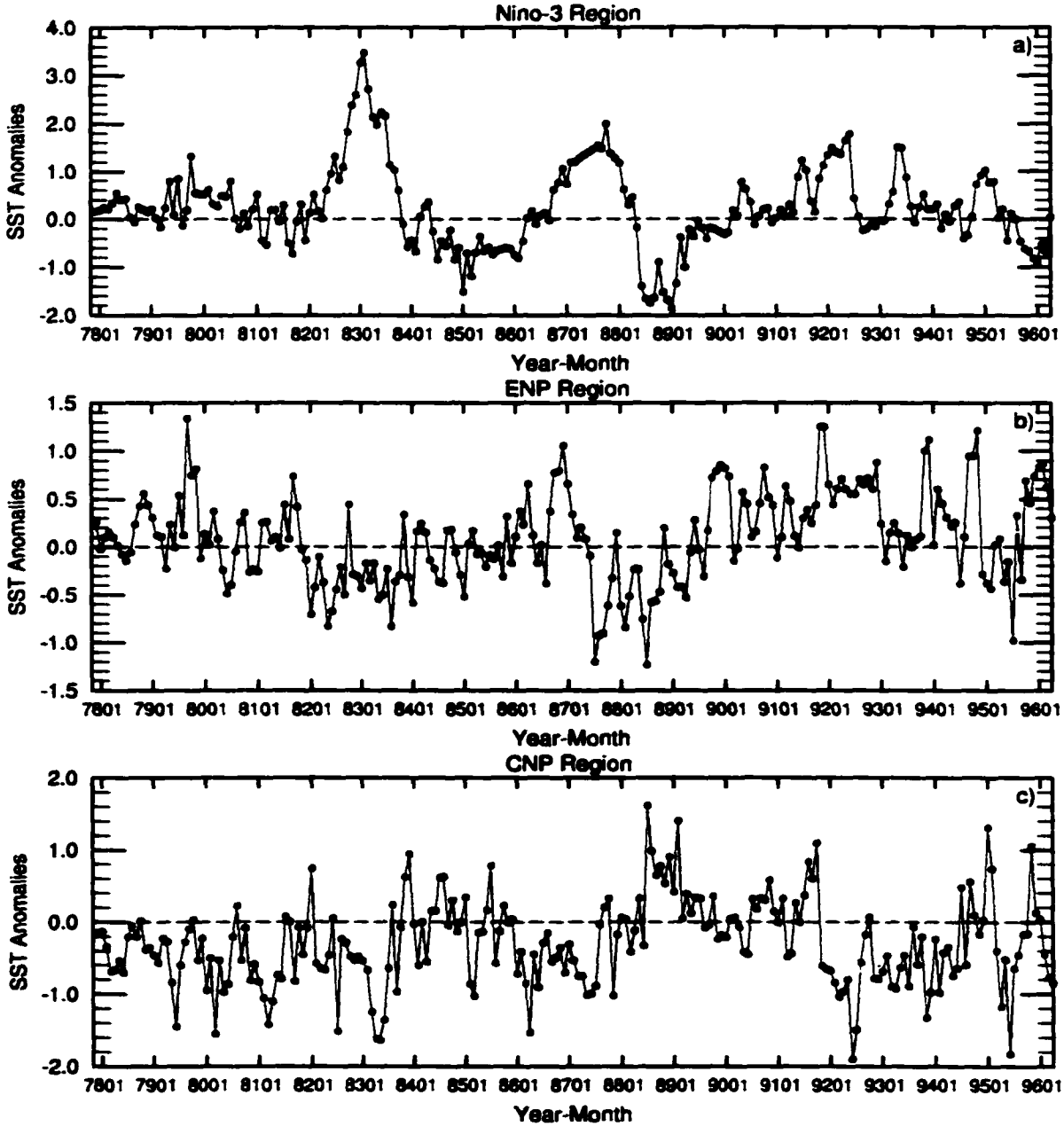

Figure D.1 Time series of observed SST anomalies used in some of the CCM experiments.

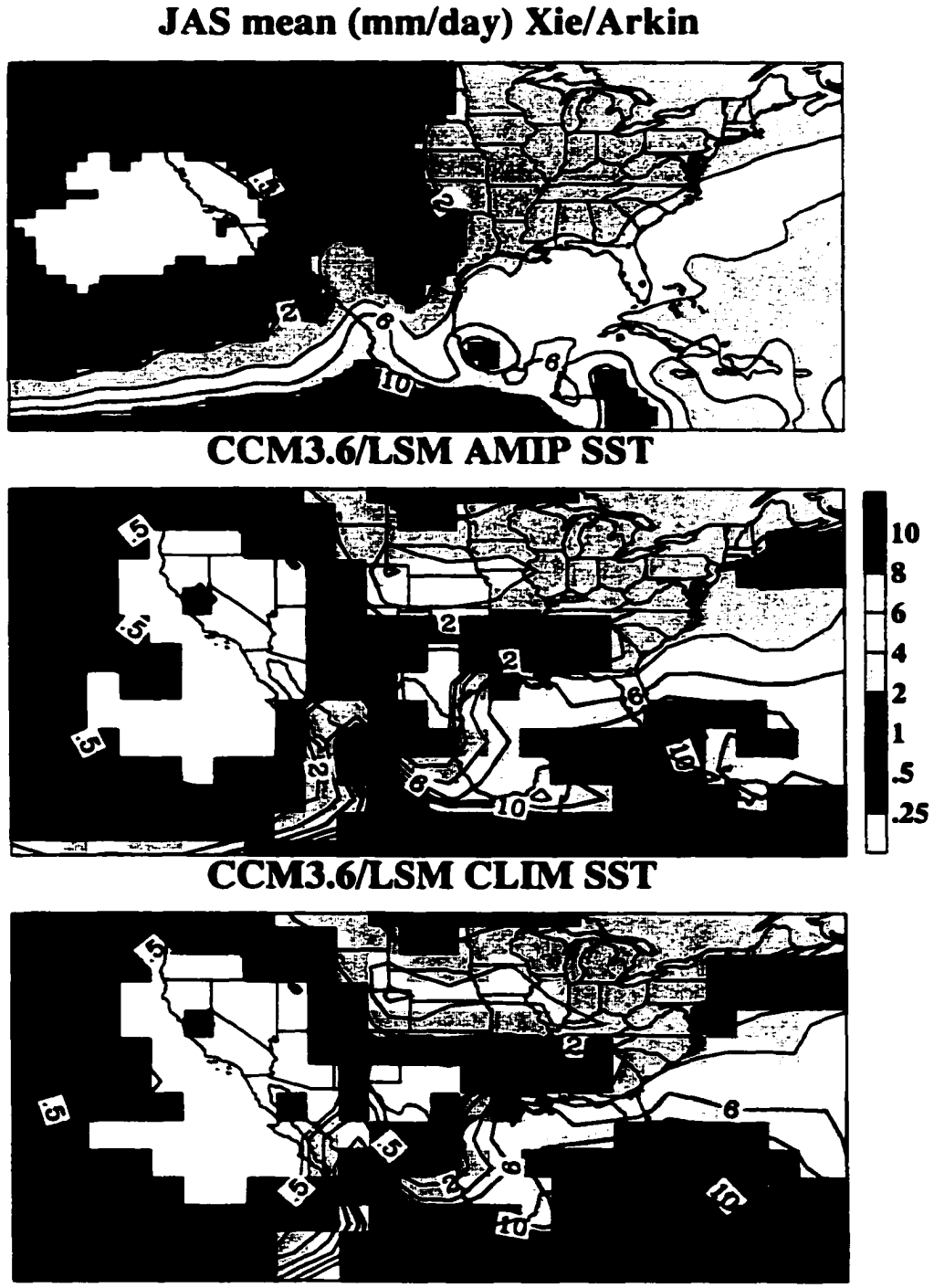

Figure D.2 Comparison of mean precipitation in July–August–September (JAS) (mm/day) from (a) Xie and Arkin [1996], (b) CCM3.6/LSM using AMIP SSTs, and (c) CCM3.6/LSM using climatological SSTs.

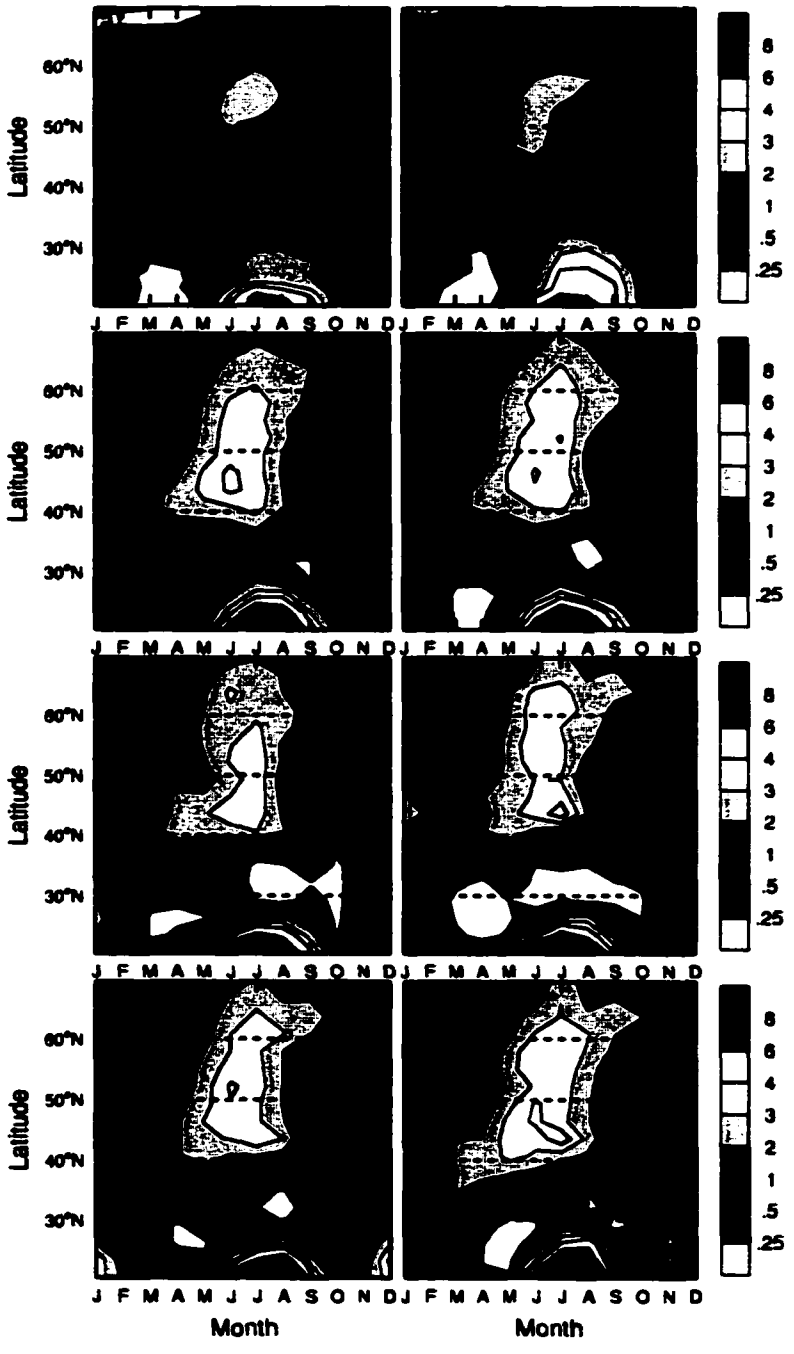

Figure D.3 Latitude–month comparison of precipitation averaged over land between 114 W and 104 W from (a) Xie and Arkin [1996], (b) Legates and Willmott [1990], (c) CCM3.6/LSM using AMIP SSTs, (d) CCM3.6/LSM using climatological SSTs, (e) CCM3.2/LSM using climatological SSTs, (f) CCM3.2/BATS using climatological SSTs, (g) same as (f) but using observed 1982 SSTs in most of the Pacific, and (h) same as (f) but using observed 1983 SSTs in most of the Pacific.

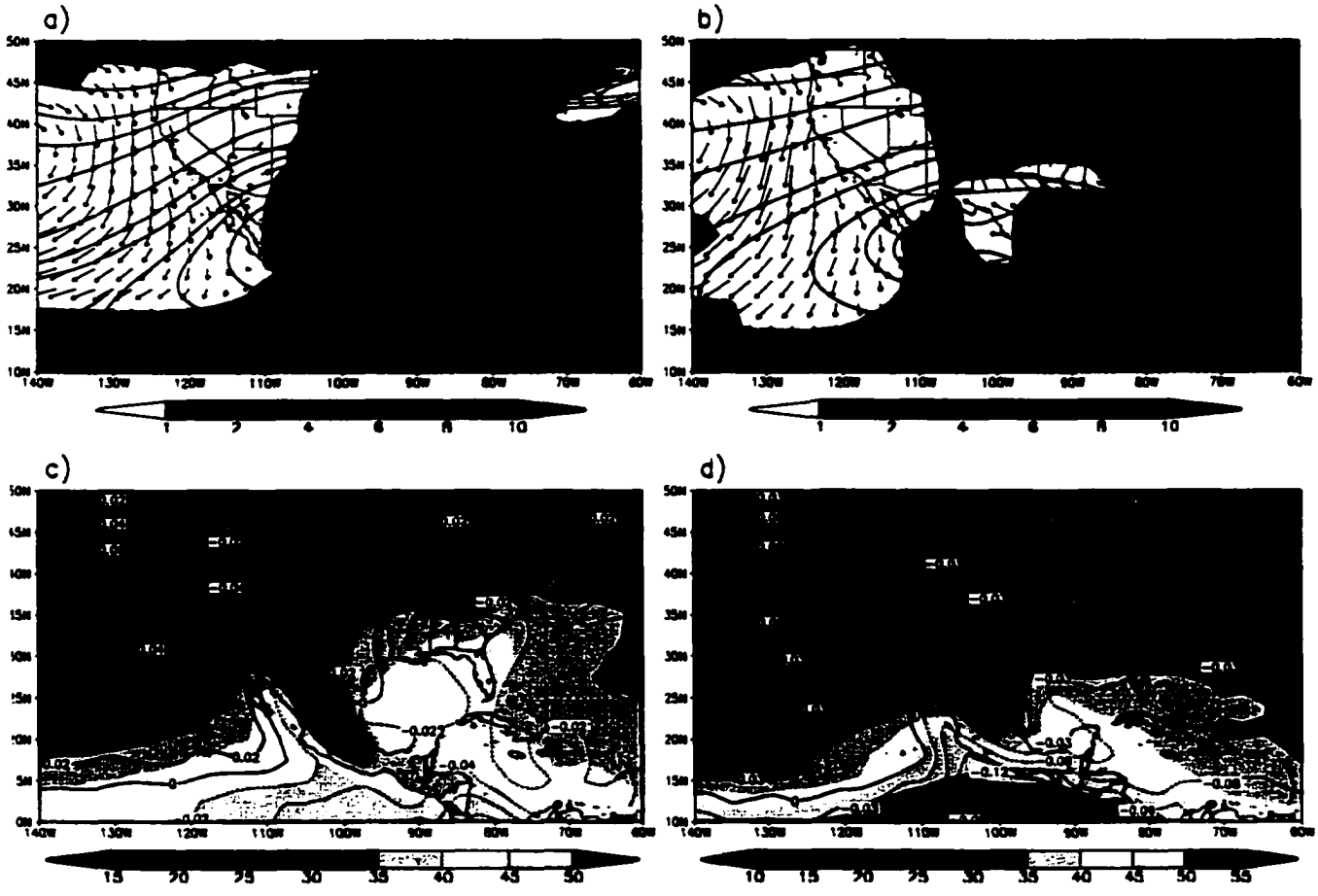

Figure D.4 Mean (July–September) 925–hPa vector wind, 200–hPa streamlines, and precipitation (mm/day) (shaded) from (a) the NCEP–NCAR reanalysis [Kalnay et al., 1996] and (b) CCM3.6/LSM using AMIP SSTs. Mean (July–September) 600–hPa vertical velocity (hPa/s) (contoured) and column–integrated precipitable water (mm) (shaded) from (c) the NCEP–NCAR reanalysis and (d) CCM3.6/LSM using AMIP SSTs.

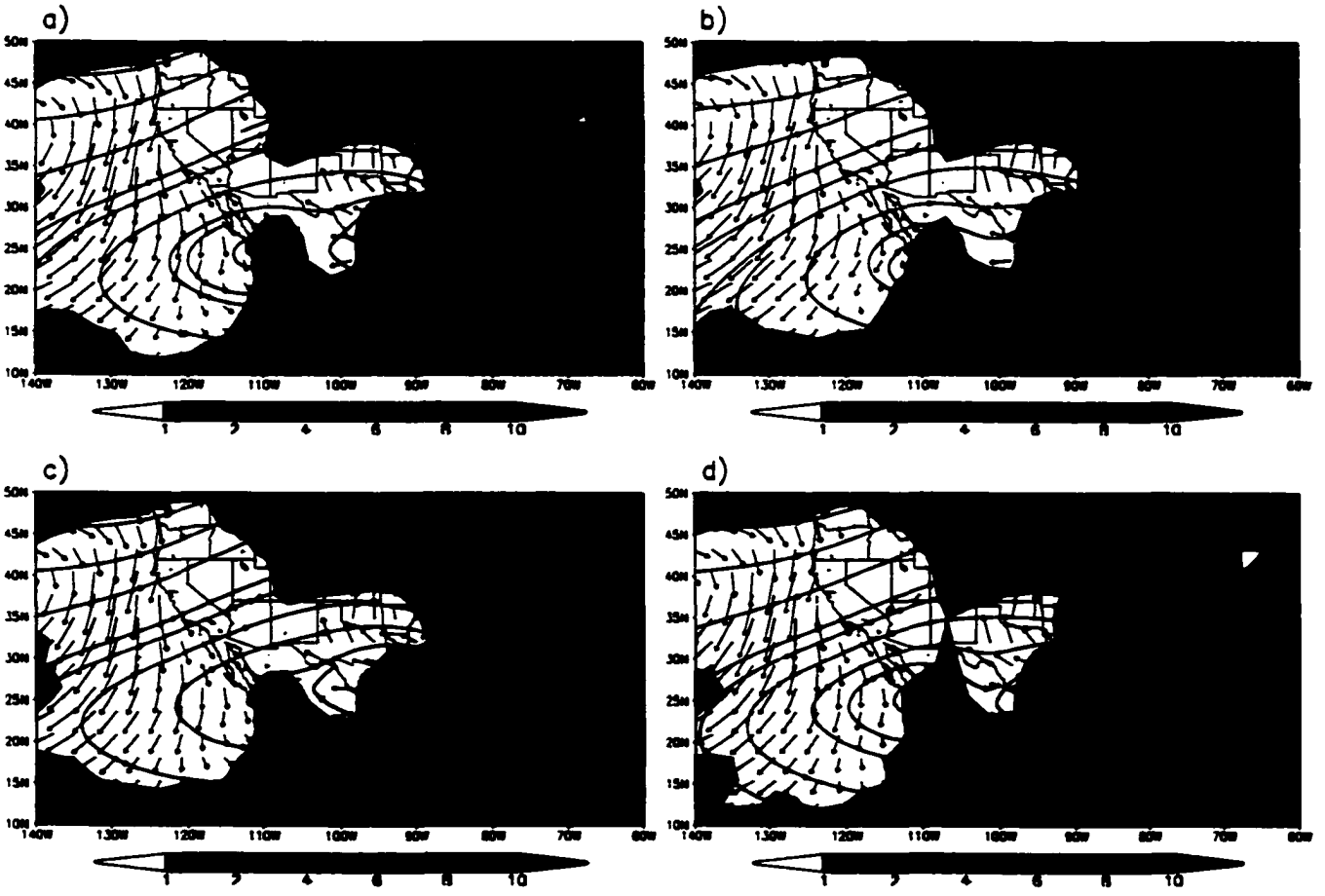

Figure D.5 Mean (July–September) 925–hPa vector wind, 200–hPa streamlines, and precipitation (mm/day) (shaded) from (a) CCM3.2/BATS with climatological SSTs except 1982 SSTs are used in three small Pacific areas (Table 1), (b) CCM3.2/BATS with climatological SSTs except 1982 SSTs are used in most of the Pacific (Table 1), (c) the same as in (a) except for SSTs for 1983 are used, and (d) the same as in (b) except for SSTs for 1983 are used.

Table 1. Model and sea surface temperature specification and integration time used in the CCM3 experiments.

Experiment	Version of CCM3	Land-surface model	SST specification	Integration (Years)
A	CCM3.2	LSM	Climatological	11
B	CCM3.2	BATS	Climatological	11
C	CCM3.2	BATS	1982 SST (small areas)	6
D	CCM3.2	BATS	1982 SST (most of the Pacific)	6
E	CCM3.2	BATS	1983 SST (small areas)	6
F	CCM3.2	BATS	1983 SST (most of the Pacific)	6
G	CCM3.6	LSM	Climatological	11
H	CCM3.6	LSM	AMIP SST	19 (1979-1997)

Note: In runs C and E, the SSTs observed in 1982 or 1983 are used in three small areas in the Pacific Ocean (Nino3: 150°W-90°W, 5°S-5°N; Central North Pacific: 177°E-164°W, 26°-36°N; Eastern North Pacific: 150°W-125°W, 35°N-50°N), while climatological SSTs are used elsewhere. In runs D and F, the SSTs observed in 1982 or 1983 are used in most of the Pacific (120°E-90°W, 20°S-50°N), while climatological SSTs are used elsewhere.

Table D.1 Model and sea surface temperature specification and integration time used in the CCM3 experiments